

PARTNERS FOR ADVANCED TRANSPORTATION TECHNOLOGY  
INSTITUTE OF TRANSPORTATION STUDIES  
UNIVERSITY OF CALIFORNIA, BERKELEY

# Multi-Modal Intelligent Traffic Signal System (MMITSS) Phase III Extension for Additional Enhancements

## Final Report

California PATH

August 3rd, 2023



Partners for Advanced Transportation Technology works with researchers, practitioners, and industry to implement transportation research and innovation, including products and services that improve the efficiency, safety, and security of the transportation system.

## **DISCLAIMER STATEMENT**

This document is disseminated in the interest of information exchange. The contents of this report reflect the views of the authors who are responsible for the facts and accuracy of the data presented herein. The contents do not necessarily reflect the official views or policies of the State of California or the Federal Highway Administration. This publication does not constitute a standard, specification or regulation. This report does not constitute an endorsement by the Department of any product described herein.

For individuals with sensory disabilities, this document is available in alternate formats. For information, call (916) 654-8899, TTY 711, or write to California Department of Transportation, Division of Research, Innovation and System Information, MS-83, P.O. Box 942873, Sacramento, CA 94273-0001.

## Primary Authors

### **Dr. Kun Zhou (PI)**

Associate Research Engineer

California PATH

University of California, Berkeley

[kzhou@berkeley.edu](mailto:kzhou@berkeley.edu)

### **Dr. Qijian Gan**

Computational Data Science Research Specialist

California PATH

University of California, Berkeley

[qgan@berkeley.edu](mailto:qgan@berkeley.edu)

This page left blank  
intentionally

## REVISION HISTORY

Date	Sections	Change Description
04/10/2023	All	Draft document by PATH
08/03/2023	All	Incorporated with Caltrans Review Comments
08/03/2023	Final Version	

This page left blank  
intentionally

## Table of Contents

Executive Summary .....	13
<b>1. Introduction .....</b>	<b>16</b>
<b>2. Enhancements to Intersection Safety and Transit Signal Priority Performance .....</b>	<b>22</b>
<b>2.1 Enhancements to the MAP Engine Library .....</b>	<b>23</b>
<b>2.1.1 Functions to identify downstream intersections and estimate the corresponding distances and travel times .....</b>	<b>23</b>
<b>2.1.2 Functions to determine lane-of-travel for vulnerable road users .....</b>	<b>24</b>
<b>2.1.3 Functions to track road user movements inside an intersection conflict area .....</b>	<b>24</b>
<b>2.2 New schemes in constructing MAP and SPaT messages for HAWK signals .....</b>	<b>25</b>
<b>2.2.1 One MAP/SPaT message per signal .....</b>	<b>25</b>
<b>2.2.2 Two MAP/SPaT per signal .....</b>	<b>25</b>
<b>2.3 Discussion .....</b>	<b>26</b>
<b>3. Enhancements to the Deployability of MMITSS Vehicle-Resident Applications .....</b>	<b>29</b>
<b>3.1 Needs for an interface specification on exchange of SAE J2735 V2X messages between an OBU and a local device .....</b>	<b>29</b>
<b>3.2 Interface Specification on Exchange of SAE J2735 Messages between an OBU and a Local Device 31</b>	
<b>3.3 Implementation of API Functions .....</b>	<b>32</b>
<b>3.4 Testing of Implemented API Functions .....</b>	<b>32</b>
<b>4. Development of an Arterial Performance Measurement System (A-PeMS) .....</b>	<b>36</b>
<b>4.1 Architecture design .....</b>	<b>36</b>
<b>4.2 Methodologies and algorithms .....</b>	<b>38</b>
<b>4.2.1 Detector data Aggregation .....</b>	<b>38</b>
<b>4.2.2 Detector Health Analysis .....</b>	<b>41</b>
<b>4.2.3 Detector data Filtering .....</b>	<b>42</b>
<b>4.2.4 Signal phase data aggregation .....</b>	<b>43</b>
<b>4.2.5 Arterial traffic state estimation .....</b>	<b>46</b>
<b>4.3 Performance measurement functions .....</b>	<b>49</b>
<b>4.3.1 Data availability .....</b>	<b>49</b>
<b>4.3.1.1 Real-time detector data availability .....</b>	<b>49</b>
<b>4.3.1.2 Real-time traffic signal status .....</b>	<b>50</b>
<b>4.3.2 Detector data analysis .....</b>	<b>51</b>
<b>4.3.2.1 Detector layout and inventory .....</b>	<b>52</b>

4.3.2.2	Detector aggregated data .....	53
4.3.2.3	Detector filtered data.....	55
4.3.2.4	Detector-level health analysis .....	56
4.3.2.5	Intersection-level health analysis.....	58
4.3.3	Signal phase data analysis.....	59
4.3.3.1	Signal timing inventory .....	59
4.3.3.2	Phase duration statistics.....	60
4.3.3.3	Phase gap-out/max-out statistics .....	62
4.3.3.4	Pedestrian phase duration statistics.....	64
4.3.4	Traffic performance .....	65
4.3.4.1	Coordination analysis.....	65
4.3.4.2	Traffic estimation .....	68
4.4	Assessment of arterial traffic performance through A-PeMS .....	70
4.4.1	Identifying traffic bottlenecks .....	70
4.4.2	Identifying insufficient signal settings .....	71
4.4.3	Identification of traffic congestion .....	73
4.4.4	Overall assessment and potential solutions .....	74
5.	Development of an Active Control Strategy for Dynamic Offsets.....	76
5.1	Algorithm to change offsets in Aimsun.....	76
5.2	Algorithm of the active control strategy for dynamic offsets.....	77
5.2.1	Traffic state representation in the flow-occupancy plot.....	77
5.2.2	State transition diagram in the active control strategy .....	78
5.2.3	Determination of offset changes in Path B.....	79
5.2.4	Determination of offset changes in Path C.....	80
5.3	Calibration of a microsimulation model for the California CV Testbed .....	82
5.3.1	The California CV Testbed model in Aimsun.....	82
5.3.2	Calibration method and criteria .....	83
5.3.3	Calibration results.....	84
5.4	A case study and evaluation results .....	86
5.4.1	A case study .....	86
5.4.2	Evaluation results .....	87
6.	Conclusions .....	91

## List of Figures

Figure 1. The California Connected Vehicle Testbed .....	16
Figure 2. Typical Tuesday traffic at 10:30AM on the ECR along SR 82 (from Google Maps) .....	19
Figure 3. Example of TSP with/without HAWK signals.....	23
Figure 4. Example of connection paths inside an intersection conflict area.....	24
Figure 5. Example of one MAP/SPaT message for each HAWK signal.....	25
Figure 6. Example of two MAP/SPaT messages for each HAWK signal .....	26
Figure 7. TSP Application Reside on Transit On-Board Unit.....	30
Figure 8. TSP Application Reside on a Separate Application Processor than Transit On-Board Unit.....	30
Figure 9. System Architecture.....	32
Figure 10. Previous OBU Architecture. ....	32
Figure 11. Message Transmitting Direction. ....	33
Figure 12. tcpdump Captured Inbound Packets.....	34
Figure 13. Analysis framework of the arterial performance measurement system.....	36
Figure 14. System architecture of the arterial performance measurement system.....	37
Figure 15. Example of raw detector data from the California CV Testbed. ....	40
Figure 16. Example of aggregated data from Detector 5 at Intersection 1001 on 2022-08-31.....	40
Figure 17. Example of health metrics for the detectors at Intersection 1001 on 2022-08-31.....	42
Figure 18. Example of data filtering for Detector 3 at Intersection 1008 on 2022-08-31.....	43
Figure 19. Example of ring-barrier-phase settings for different timing plans at Intersection 1002.....	44
Figure 20. Example of raw event-based signal phase data from Intersection 1002 on 2022-08-31. ....	45
Figure 21. Example of reconstructed signal cycles at Intersection 1002 on 2022-08-31. ....	46
Figure 22. Trapezoidal fundamental diagram for signalized arterial road links.....	47
Figure 23. Example of vehicle platoons without stopping. ....	48
Figure 24. Example of vehicle platoons with a short waiting time.....	48
Figure 25. Example of vehicle platoons with a long waiting time .....	48
Figure 26. Example of flow-occupancy plots from the advance detectors in the SB and NB directions at Intersection 1002 (Embarcadero/Galvez @ El Camino Real).....	49
Figure 27. Snapshot of real-time detector data availability in the California CV Testbed .....	50
Figure 28. Snapshot of real-time intersection signal status in the California CV Testbed .....	51
Figure 29. Example of detector layout at Intersection 1002.....	52
Figure 30. Example of detector inventory at Intersection 1002.....	53
Figure 31. Example of aggregated data from and advance detector (Detector 3 at Intersection 1002).....	54
Figure 32. Example of aggregated data from a stopbar detector (Detector 1 at Intersection 1002) .....	55
Figure 33. Example of data filtering for Detector 24 at Intersection 1006 on 2022-06-11.....	55
Figure 34. Example of health analysis report for Detector 3 at Intersection 1002 between 2022-06-05 and 2022-06-11.....	56
Figure 35. Example of bad detectors reporting long periods of zero values.....	57
Figure 36. Example of bad detectors reporting high percentages of inconsistent values .....	57
Figure 37. Example of bad detectors reporting high missing rates.....	57
Figure 38. Example of intersection-level health metrics for Intersection 1002.....	58
Figure 39. Example of corridor-level health metrics for all detectors in the California CV Testbed .....	58
Figure 40. Example of ring-barrier-phase settings for different timing plans at Intersection 1013.....	59

Figure 41. Example of coordination plans for Intersection 1013. ....	60
Figure 42. Example of phase settings at Intersection 1013.....	60
Figure 43. Temporal distribution of phase durations for coordination plan 2 at Intersection 1013 between 9AM and 10AM on 2022-06-07.....	61
Figure 44. Table view of phase durations for coordination plan 2 at Intersection 1013 between 10AM and 11AM on 2022-06-07.....	62
Figure 45. Table view of phase Gap-Out/Max-Out/Forced-Off for coordination plan 2 at Intersection 1013 between 10AM and 11AM on 2022-06-07.....	63
Figure 46. Plot view of phase Gap-Out/Max-Out/Forced-Off for coordination plan 2 at Intersection 1013 between 10AM and 11AM on 2022-06-07.....	64
Figure 47. Table view of pedestrian phase durations for coordination plan 2 at Intersection 1013 between 10AM and 11AM on 2022-06-07.....	65
Figure 48. Impacts of different coordination levels on the flow-occupancy plots at advance detectors.....	66
Figure 49. Selection of three coordinated intersection approaches in the NB direction.....	67
Figure 50. Progression of traffic measurements at the three selected intersection approaches on 2022-08-31 between 5PM and 6PM.....	68
Figure 51. Estimated traffic states at the three selected intersection approaches on 2022-08-31 between 5PM and 6PM.....	70
Figure 52. Estimated traffic states at 5:30PM on 2022-12-06 and the identified traffic bottlenecks.....	70
Figure 53. Estimated traffic states, signal timing plans, and detector layouts at Embarcadero Rd @ ECR. ....	71
Figure 54. Table & Plot views of phase gap-out/max-out statistics at Embarcadero Rd @ ECR between 3PM and 4PM on 2022-12-06.....	72
Figure 55. Histogram of phase gap-out/max-out statistics at Embarcadero Rd @ ECR between 3PM and 4PM on 2022-12-06.....	72
Figure 56. Detector measurements, phase gap-out/max-out statistics, pedestrian calls at the intersection Embarcadero Rd @ ECR between 3PM and 4PM on 2022-12-06.....	73
Figure 57. Flow and occupancy measurements at Detector 1002-03 in the SB direction of Embarcadero Rd @ ECR on 2022-12-06.....	74
Figure 58. Traffic state representation in the flow-occupancy plot.....	77
Figure 59. State transition diagram at an intersection approach.....	78
Figure 60. Example of offset determination in Path B.....	79
Figure 61. Example of offset determination in Path C.....	80
Figure 62. The California CV Testbed model in Aimsun.....	82
Figure 63. Illustration of attributes (timing plans, detectors, and centroids) in the Aimsun model.....	82
Figure 64. Example of GEH statistics on the simulated traffic flows at an intersection.....	84
Figure 65. GEH statistics between 3PM and 7PM in the calibrated Aimsun model for the testbed.....	85
Figure 66. Regression results between the observed and the simulated flows in the PM peak (3PM—7PM).....	85
Figure 67. Bottlenecks observed from the field vs. those identified from simulation.....	86
Figure 68. Four intersections selected in the case study.....	87
Figure 69. Before-and-after comparison of detector measurements at the intersection @Curtner Ave in Replication #5.....	88

## List of Tables

Table 1. Intersection Name and Intersection ID in the California CV Testbed.....	17
Table 2 Recommended Interface Specification for OBU to Exchange Messages with a Separate Application Processor.....	31
Table 3 Tested SAE J2375 Messages.....	33
Table 4. Network-level delay reduction under the active control strategy between 4PM and 7PM.....	88
Table 5. Offset changes at the four intersections in Replication #5 .....	89

## Acronyms

AI	Artificial Intelligence
A-PeMS	Arterial Performance Measurement System
API	Application Programming Interface
BSM	Basic Safety Message
CAV	Connected and Automated Vehicle
CSW	Curve Speed Warning
CV	Connected Vehicle
C-V2X	Cellular-V2X
DSRC	Dedicated Short-Range Communications
ECR	El Camino Real
EVA	Emergency Vehicle Alert
FCC	Federal Communications Commission
GNSS	Global Navigation Satellite System
HAWK	High Intensity Activated CrossWalk
IF	Immediate Forward
MAP	Map Data Message
MF	Message Forward
MMITSS	Multimodal Intelligent Traffic Signal System
OBU	On-Board Unit
OD	Origin-Destination
PDM	Probe Data Management
PSM	Personal Safety Messages
PVD	Probe Vehicle Data
RLVW	Red-Light Violation Warning
RSA	Roadside Alert
RSU	Roadside Unit
RTCM	Radio Technical Commission for Maritime Services
RTK	Real-Time Kinematics
SDK	Software Development Kit
SPaT	Signal Phase and Timing Message
SRM	Signal Request Message
SSM	Signal Status Message
TMDD	Traffic Management Data Dictionary
TOD	Time Of Day
TSP	Transit Signal Priority
V2X	Vehicle to Everything
VRU	Vulnerable Road User
WAAS	Wide Area Augmentation System

## Executive Summary

In the California Connected Vehicle (CV) Testbed, four intersections have been instrumented with NoTraffic sensors for more accurate detection of multi-modal traffic within the intersection conflict area, and six operational High Intensity Activated CrossWalk (HAWK) signals have been installed to enhance the safety for pedestrians and cyclists while crossing the major arterial, El Camino Real. In this project, efforts have been devoted to enhancing the Multimodal Intelligent Traffic Signal System (MMITSS) to support these infrastructure upgrades. To ensure the Transit Signal Priority application can function properly after the installation of HAWK signals, functions in the MAP Engine Library have been revised to allow the identification of multiple downstream intersections and the calculation of the corresponding distances and travel times. To incorporate the more accurate detection data from the NoTraffic sensors into Vehicle-to-Everything (V2X) messages, new functions have been added to the MAP Engine Library to determine the lane-of-travel for vulnerable road users and track road user movements inside an intersection conflict area. In addition, new schemes have been proposed to construct appropriate MAP and Signal Phase and Timing (SPaT) messages for the HAWK signals with different road geometry settings.

As regulated by the Federal Communications Commission (FCC), Dedicated Short-Range Communications (DSRC) is going to phase out and is being replaced by Cellular V2X (C-V2X). As a result, communications standards have been updated to facilitate flexibility and adaptability in developing, testing, and deploying C-V2X safety and mobility applications. However, application's system requirement and specifications are usually specified in separate documents. There is no one-fit-all solution that an On-Board Unit (OBU) could provide service for all envisioned safety and mobility applications as V2X technology and V2X communications are still evolving and different C-V2X use cases would have different system requirements. Therefore, efforts have been devoted to developing an application programming interface (API) specification for exchanging V2X messages between an OBU and a local device (e.g., an application processor) so that the vehicle-resident CV applications running on the local device can be device-independent and work seamlessly with OBUs from different vendors. These implemented API functions have been tested using the devices (e.g., Roadside Units - RSUs and OBUs) in the PATH laboratory.

To monitor the traffic performance in the California CV Testbed, an Arterial Performance Measurement System (A-PeMS) has been developed to collect, aggregate, and analyze the raw detector and signal phase data from the field. In the A-PeMS, functions are available to monitor real-time data availability from the detectors and the traffic controllers in the field. To better analyze the data, algorithms have been developed to aggregate the raw detector data into fixed intervals and the event-based signal phase data into cycles. A set of health criteria has been proposed to check the quality of the detector data, and algorithms have been developed to filter out bad detector measurements. For the signal phase data, metrics like phase duration statistics, phase gap-out/max-out statistics, and pedestrian phase duration statistics have been developed to measure the intersection signal performance. Leveraging both the detector and the signal phase data, functions have been developed to estimate the traffic states and visualize the coordination performance in the testbed. Furthermore, procedures on how to leverage the A-PeMS to assess arterial traffic performance, especially identification of traffic bottlenecks and the corresponding causes, are provided.

To support the testing of new control strategies and CV/CAV – Connected and Automated Vehicle – applications, a microsimulation model in Aimsun has been created and calibrated for the California CV Testbed. The FHWA microsimulation calibration guideline was adopted in the model calibration, and the GEH statistics were used to measure the match between the simulated detector measurements and those

observed from the field. Results have demonstrated that the Aimsun model for the California CV Testbed was well calibrated for the weekday PM period between 3PM and 7PM.

To improve the coordination performance in the California CV Testbed, a novel active control strategy has been developed that recommends new offsets according to the changing traffic conditions measured from the advance detectors located at the coordinated intersection approaches. In the active control strategy, traffic at an intersection only consists of two states, uncongested and congested, and different actions will be applied to different state transition processes, for example, from uncongested to congested or vice versa. For performance evaluations, a case study was provided in which the active control strategy was applied to four bottleneck intersections in the testbed Aimsun model. Simulation results demonstrated that the proposed active control strategy is effective and can achieve about 2% reduction in vehicle delay for the whole network of 16 intersections by applying only a few changes to the offsets at the four bottleneck intersections.

In the future, efforts will be devoted to: (i) developing new performance metrics from the more accurate detection data provided by the Artificial Intelligence (AI) powered video and radar sensors, e.g., the NoTraffic Sensors, and incorporating them into the A-PeMS; (ii) improving the active control strategy with additional considerations of traffic conditions from the cross streets, and assessing its performance in the well-calibrated Aimsun model for the I-210 Corridor network; (iii) conducting field tests of the active control strategy in the California CV Testbed, and assessing the before-and-after impacts through the A-PeMS.

This page left blank  
intentionally

# 1. Introduction

The California Connected Vehicle (CV) Testbed is located in the heart of the Silicon Valley in Palo Alto, California. As shown in Figure 1, the testbed spans 16 consecutive intersections equipped with DSRC RSUs (from Medical Foundation Dr to Dinah's Ct) and another 15 intersections equipped with C-V2X RSUs (from Los Altos Ave to Grant Rd), about a seven-mile stretch of State Route 82 (a.k.a., El Camino Real - ECR). This project includes the 16 operational DSRC intersections. The other 15 C-V2X intersections were not operational during the execution period of this project and are not included in this project.

The name and id of these 31 intersections are provided in Table 1 for reference.

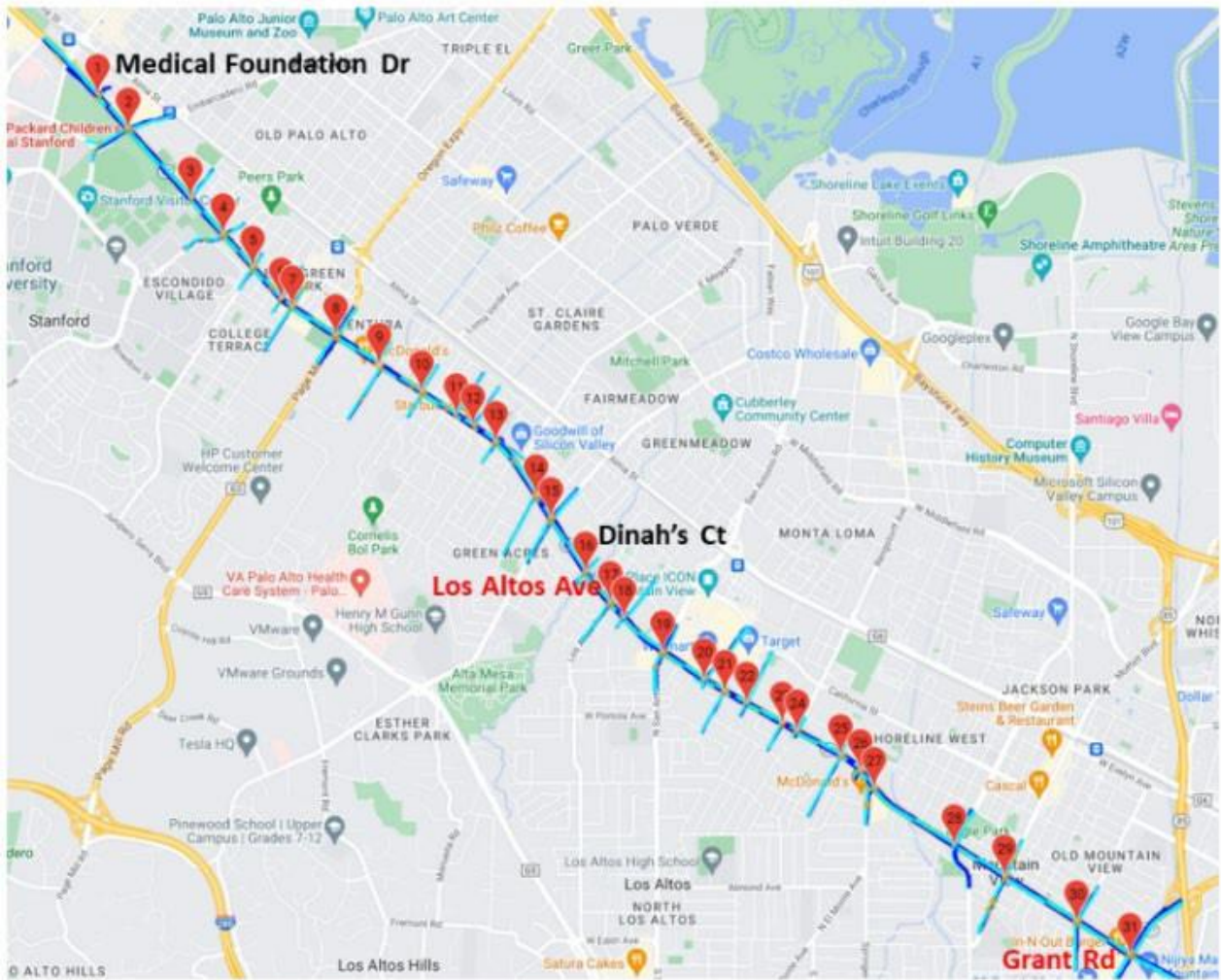


Figure 1. The California Connected Vehicle Testbed.

Table 1. Intersection Name and Intersection ID in the California CV Testbed

Intersection ID	Cross Street Name
1001	Medical Foundation Dr
1002	Embarcadero Rd
1003	Churchill Ave
1004	Serra/Park
1005	Stanford Ave
1006	Cambridge Ave
1007	S California Ave
1008	Page Mill Rd
1009	Portage/Hansen
1010	Matadero Ave
1011	Curtner Ave
1012	Ventura Ave
1013	Los Robles Ave
1014	Maybell Ave
1015	W Charleston Rd
1016	Dinahs Ct
1017	Los Altos Ave
1018	Del Medio Ave
1019	San Antonio Rd
1020	Showers Dr
1021	Jordan Ave
1022	Ortega Ave
1023	Distel Circle
1024	S Rengstorff Ave
1025	Clark Ave
1026	Escuela Ave
1027	El Monte Ave
1028	S Shoreline Blvd
1029	Castro St
1030	Calderon Ave
1031	Grant Rd

During the project period, there have been some infrastructure upgrades to the California CV Testbed, which include the following:

- AI-powered NoTraffic<sup>1</sup> sensors have been installed at four intersections to provide more accurate detection of traffic.
  - @Medical Foundation Dr
  - @Embarcadero Rd
  - @Churchill Ave
  - @Serra/Park Blvd
- HAWK (High Intensity Activated CrossWalk) signals have been installed at six intersections to enhance the safety for pedestrians and cyclists while crossing the ECR.
  - @College Ave (between Stanford Ave and Cambridge Ave)
  - @Fernando Ave (between Portage/Hansen and Matadero Ave)
  - @Wilton/Barron Ave (between Matadero Ave and Curtner Ave)
  - @Vista Ave (between Los Robles Ave and Maybell Ave)
  - @Monroe Dr (between Dinah's Ct and Los Altos Ave)
  - @Distel Circle (between Ortega Ave and Distel Dr)

To support these infrastructure upgrades, additional enhancements to the MMITSS (Multimodal Intelligent Traffic Signal System) are required:

- To guarantee the Transit Signal Priority (TSP) application function properly, existing functions in the MAP Engine Library need to be revised to allow the identification of multiple downstream intersections and the calculation of the corresponding distances and travel times.
- To incorporate the more accurate traffic detection data from the NoTraffic Sensors into the V2X messages, new functions are needed in the MAP Engine Library to: (i) determinate the lane-of-travel for vulnerable road users (VRUs), and (ii) track road user movements inside an intersection conflict area.
- Depending on where the HAWK signals are installed, different schemes are required to construct appropriate MAP and SPaT messages to consider the differences in road geometries.

As regulated by the Federal Communications Commission (FCC)<sup>2</sup>, DSRC is going to phase out and is being replaced by C-V2X. As a result, communications standards have been updated to facilitate the flexibility and adaptability in developing, testing, and deploying C-V2X safety and mobility applications. However, application's system requirement and specifications are usually specified in separate documents. There is no one-fit-all solution that an OBU could provide service for all envisioned safety and mobility applications as V2X technology and V2X communications are still evolving and different C-V2X use cases would have different system requirements. To address this issue, this project proposes a solution of developing an application programming interface (API) specification for exchanging V2X messages between an OBU and a local device (e.g., an application processor). Adding this local device interface to OBU will allow a

---

<sup>1</sup> <https://notraffic.tech>.

<sup>2</sup> <https://www.fcc.gov/wireless/bureau-divisions/mobility-division/dedicated-short-range-communications-dsrc-service>

hardware-agnostic solution, that the vehicle-resident CV applications running on a separate application processor can be device-independent and work seamlessly with OBUs from different vendors.

Furthermore, as shown in Figure 2, the major arterial in the testbed, i.e., El Camino Real, is a busy commuter route and suffers from heavy traffic congestion during busy hours<sup>3</sup>. In order to improve traffic performance in the testbed, it is needed as a first step to identify key traffic bottlenecks and potential causes before making any changes to existing signal control settings. However, currently there is a lack of a tool that collects and analyzes traffic data (e.g., detector and signal phase data) from the detectors and controllers in the field. In this project, efforts will be devoted to developing an Arterial Performance Measurement System (A-PeMS)<sup>4</sup> with functions to aggregate the raw detector and signal phase data from the field, analyze the data quality and signal performance, and estimate the traffic states in the testbed.

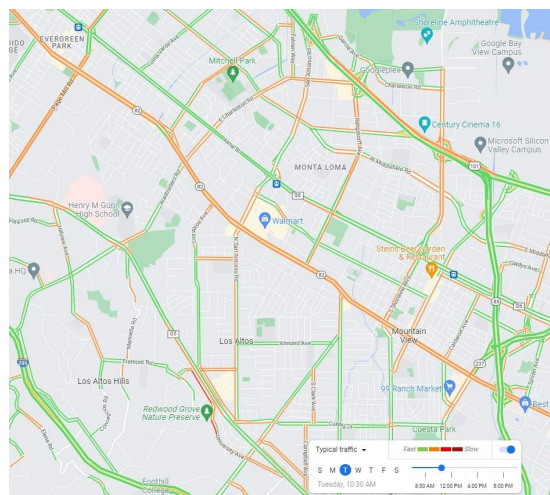


Figure 2. Typical Tuesday traffic at 10:30AM on the ECR along SR 82 (from Google Maps).

Due to the variations in traffic demands, coordination at certain bottleneck intersections may be degraded as the offsets predefined in the Time-Of-Day (TOD) coordination plan are no longer able to accommodate the platoon arrivals from upstream intersections. Therefore, it is necessary to develop novel control strategies that can recommend new control settings based on the newly collected data to better accommodate the upstream platoon arrivals with fewer stops. Although there are new advanced sensors, like AI powered video and radar sensors<sup>5</sup> and LiDAR sensors<sup>6</sup>, available in the market to support high resolution detection of traffic, the most common traffic control at signalized intersections is coordinated actuated control with data support from loop detectors. While it is too costly to upgrade all signalized intersections with these new advanced sensors to help with traffic control, a more cost-effective and scalable approach would be developing new control strategies or adding more adaptive features into existing control systems by leveraging the loop detector and signal phase data available from the field. Instead of making

<sup>3</sup> According to Google Maps' typical traffic, traffic at this location is congested between 10AM and 7PM on weekdays.

<sup>4</sup> <https://caconnectedvehicletestbed.org/apems/index.php>

<sup>5</sup> NoTraffic: <https://notraffic.tech/>, Miovision: <https://miovision.com/>, Street Simplified: <https://www.streetsimplified.com/>, and BOSCH: <https://www.boschsecurity.com/xc/en/>.

<sup>6</sup> <https://velodynelidar.com/products/bluecity/>

significant changes to the signal control settings, this report will introduce a novel active control strategy that only adjusts the offsets according to the changing traffic conditions observed from the detectors. To support the testing of the proposed active control strategy as well as future testing of CV/CAV applications, a microsimulation model in Aimsun will be developed and calibrated for the California CV Testbed.

The rest of the report is organized as follows. In Section 2, we will describe the enhancements to intersection safety and transit signal priority performance to support the new infrastructure upgrades in the California CV Testbed. In Section 3, we will describe the enhancements to the deployability of MMITSS vehicle-resident applications to allow the vehicle-resident CV applications running on a separate application processor and working seamlessly with OBUs from different vendors during the transition to C-V2X. In Section 4, we introduce the development of an Arterial Performance Measurement System (A-PeMS) that manages the detector and signal phase data retrieved from the field, monitors the sensor network performance, and provides functions to identify traffic bottlenecks and potential causes. In Section 5, we provide the development of an active control strategy that recommends new offsets based on the newly collected detector data at bottleneck intersections so as to improve the coordination along the major arterial. In Section 6, we draw our final conclusions with some future research directions.

This page left blank  
intentionally

## 2. Enhancements to Intersection Safety and Transit Signal Priority Performance

Although conventional traffic controllers have detectors (e.g., push buttons) and phases (e.g., pedestrian phases) to allow pedestrians and bicyclists to cross the intersections, there is still a lot of work to be done to enhance intersection efficiency and safety for pedestrians and bicyclists. For example, below are some common situations that need to be addressed:

- There is no pedestrian crossing the street when a pedestrian phase is activated.
- There are pedestrians and bicyclists crossing the street, but the corresponding pedestrian phase is not activated.
- There are pedestrians (e.g., elderly people) on the crosswalks, but the pedestrian phase is ending soon.
- There are bicyclists (e.g., making a left turn) inside the intersection conflict area, but the corresponding vehicle phase (e.g., left-turn phase) is ending soon.

Therefore, in the California CV Testbed the following four intersections are instrumented with NoTraffic sensors (<https://notraffic.tech/>):

- @Medical Foundation Dr,
- @Embarcadero Rd,
- @Churchill Ave,
- @Serra/Park Blvd

With the newly installed NoTraffic sensors, we are able to detect the presence of pedestrians and bicyclists inside the intersection conflict area in a more accurate and timely manner. This new source of information, together with the pedestrian phase activation information obtained from conventional traffic controllers, can be incorporated into the SPaT messages, which will increase the intersection visibility for connected vehicles and other road users with communication capabilities, e.g., those equipped with OBUs. However, this enriched pedestrian and bicyclist information also requires some software enhancements to the existing MAP engine library.

Besides NoTraffic sensors, six operational HAWK (High Intensity Activated CrossWalk) signals have been installed at the following intersections:

- @College Ave (between Stanford Ave and Cambridge Ave)
- @Fernando Ave (between Portage/Hansen and Matadero Ave)
- @Wilton/Barron Ave (between Matadero Ave and Curtner Ave)
- @Vista Ave (between Los Robles Ave and Maybell Ave)
- @Monroe Dr (between Dinah's Ct and Los Altos Ave)
- @Distel Circle (between Ortega Ave and Distel Dr)

Caltrans is currently working on installing RSUs at the above intersections. While these new HAWK signals provide pedestrians and bicyclists protection to cross El Camino Real, they create new issues that require further software enhancements: (i) it is difficult to construct appropriate MAP and SPaT messages for some road geometry layouts where the HAWK signals are located; and (ii) it creates uncertainty in predicting transit's arrival time and degrades the performance of the existing application of Transit Signal Priority (TSP) in the MMITSS system.

## 2.1 Enhancements to the MAP Engine Library

In the current version of MAP Engine Library, there have been functions to:

- (i) Identify current approaching intersection and estimate the corresponding distance and travel time to the stopbar;
- (ii) Determine lane-of-travel for vehicles for the Basic Safety Message (BSM).

However, due to more accurate detection of the presence of pedestrians and bicyclists inside the intersection conflict area and the newly installed HAWK signals, new functions are needed to incorporate these changes into the MAP/SPaT messages.

### 2.1.1 Functions to identify downstream intersections and estimate the corresponding distances and travel times

As shown in Figure 3, for the application of Transit Signal Priority (TSP), the current MAP Engine Library supports the functions to identify current approaching intersection and estimate the corresponding distance and travel time ( $\Delta d_{Int}, \Delta t_{Int}$ ) to the stopbar when there is no HAWK signal ahead. However, these functions become inappropriate when there exists a HAWK signal between a transit vehicle and its next downstream signalized intersection. When the HAWK signal is not activated (e.g., in the dark mode), the transit vehicle can cross freely and thus it can calculate its distance and travel time to the stopbar the same as the case when there is no HAWK signal ahead. However, when the HAWK signal is activated, the travel time to the downstream signalized intersection becomes uncertain, which depends on the current status (e.g., flashing yellow, red, or flashing red) at the HAWK signal.

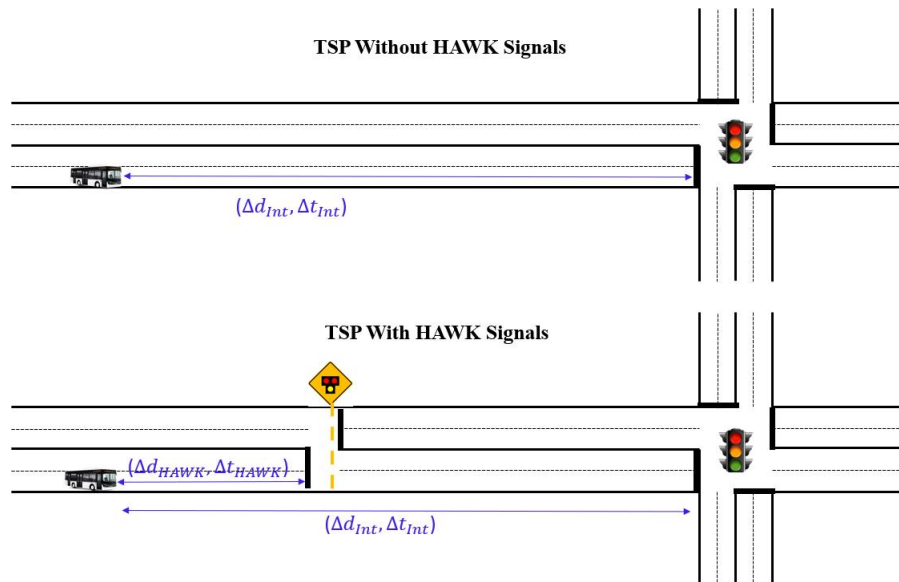


Figure 3. Example of TSP with/without HAWK signals.

To maintain the functionality of the TSP application, we have applied the following enhancements to the MAP Engine Library:

- (i) Improved functions to identify both current approaching intersection and next downstream intersection;
- (ii) Improved functions to estimate the distance and travel time to the stopbar of a downstream intersection.

With these improved functions, a transit vehicle can estimate not only its distance and travel time ( $\Delta d_{\text{HAWK}}$ ,  $\Delta t_{\text{HAWK}}$ ) to the HAWK signal when it is activated but also the distance and travel time ( $\Delta d_{\text{next}}$ ,  $\Delta t_{\text{next}}$ ) to the next downstream signalized intersection in order to request signal priority.

### 2.1.2 Functions to determine lane-of-travel for vulnerable road users

With the newly installed NoTraffic sensors, we are able to detect the movements (e.g., location and speed) of bicyclists approaching or departing from the intersection. Since bicyclists are allowed to share arterial roads like El Camino Real with motorists, we have further developed functions to map the lane-of-travel for the detected bicyclists according to their location information. This lane-of-travel information can be incorporated into BSMs (Basic Safety Messages) or PSMs (Personal Safety Messages) to notify nearby intersections equipped with RSUs, connected vehicles, or other road users with communication capabilities.

### 2.1.3 Functions to track road user movements inside an intersection conflict area

The SAE J2735 standard<sup>9</sup> – V2X Communications Message Set Dictionary – specifies a message set, and its data frames and data elements, for use by applications that use V2X communications systems. At a road intersection, SAE J2735 MAP does not specify travel paths between ingress and egress links inside the intersection conflict area. However, through NoTraffic sensors, positions (or trajectories) of road users (e.g., vehicles, pedestrians, and bicyclists) inside the intersection conflict area can be identified and tracked. Therefore, there is a need to create travel paths inside the intersection conflict area and develop functions to map the positions of road users onto the corresponding paths.

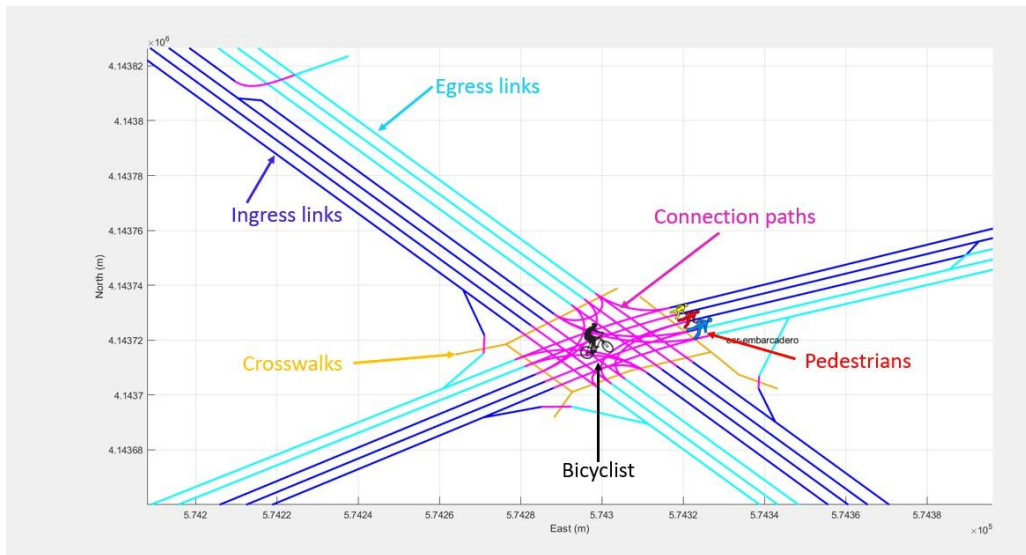


Figure 4. Example of connection paths inside an intersection conflict area.

The solution we have implemented in the California CV Testbed is to use Bezier Curve to model connection paths inside an intersection conflict area. This solution has been widely used in microsimulation software like Aimsun (<https://www.aimsun.com/>) to create connections between lanes at road intersections. In Figure 4, we provide an example of connection paths inside an intersection conflict area. In the figure, the purple lines stand for the connection paths, while the orange lines stand for crosswalks. If there is presence of bicyclists and pedestrians inside the intersection conflict area, their locations will be identified and mapped to the corresponding connection paths or crosswalks. Then this information will be broadcasted to nearby

connected vehicles and other road users with communication capabilities to avoid potential conflicts. Besides that, according to the identified locations on the connection paths, we can predict the remaining time for pedestrians and bicyclists to safely exit the intersection conflict area and then extend the corresponding phase's green times in the traffic controller. Through this approach, visibility inside the intersection conflict area will be increased and thus safety for vulnerable road users like pedestrians and bicyclists will be improved.

## 2.2 New schemes in constructing MAP and SPaT messages for HAWK signals

Currently, there are six new HAWK signals installed in the California CV Testbed. Depending on their specific road geometries and control settings, we have applied two different schemes to construct their MAP and SPaT messages.

### 2.2.1 One MAP/SPaT message per signal

As shown in Figure 5, there is a HAWK signal with only one crosswalk for pedestrians and bicyclists to cross the street. Therefore, there are only one stopbar for each direction of the major arterial road, e.g., stopbars A and B shown in the figure. When the HAWK signal is activated, vehicles need to stop at the stopbars A and B. Then as shown in the figure, it is easy to identify the ingress and egress links in the MAP/SPaT messages for the HAWK signal. In this case, it is sufficient to have only one MAP/SPaT message for this type of HAWK signals.

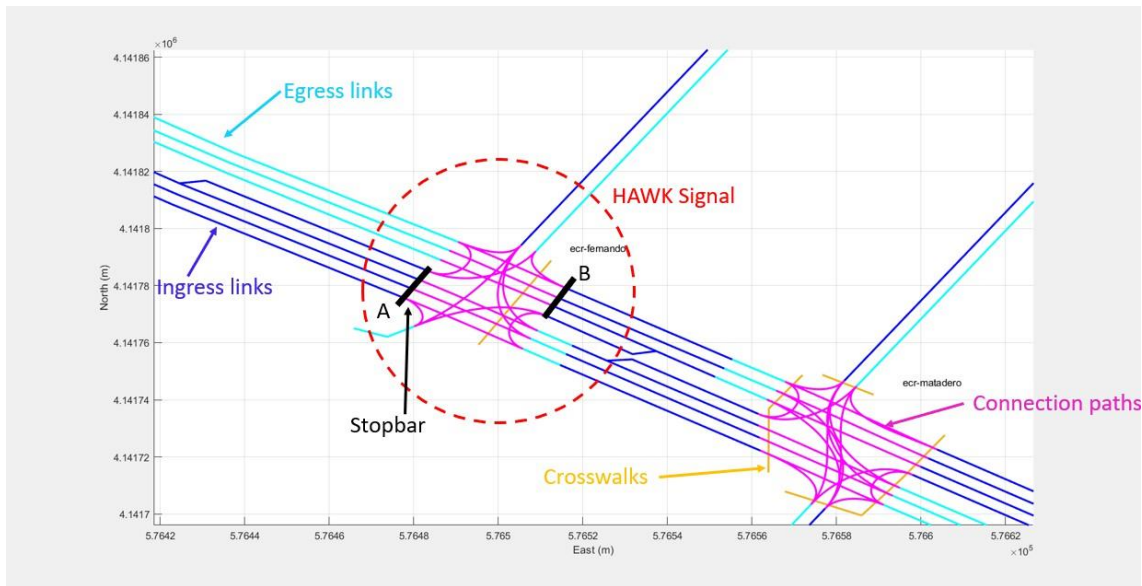


Figure 5. Example of one MAP/SPaT message for each HAWK signal.

### 2.2.2 Two MAP/SPaT per signal

Different from the setting shown in Figure 5, it is possible to have another setting of HAWK signals, which is shown in Figure 6. In this case, there are two crosswalks because the two side streets are connected to the major arterial with two separate road junctions. As indicated in the figure, there are internal links between these two junctions with two additional stopbars. Depending on the activation of the crosswalks, the actual stopbar for vehicles on the major arterial is changeable: it can be either A or B for the vehicles

traveling from left to right (i.e., southbound), and either C or D for the vehicles traveling from right to left (i.e., northbound). When southbound vehicles stop at A, the road segment AB is an egress approach from A, while when vehicles stop at B, the road segment AB is an ingress approach to B. This dynamic egress/ingress is not currently supported by the MAP message. Our solution to this is to construct two MAP/SPaT messages for each HAWK signal. As shown in the figure, each internal link is divided into two sub-links: one sub-link becomes the egress link of one MAP/SPaT message, while the other sub-link becomes the ingress link of the other MAP/SPaT message. Through this approach, no matter which crosswalk is activated, the appropriate stopbar location can be identified for vehicles along the major arterials based on the information from the two MAP/SPaT messages.

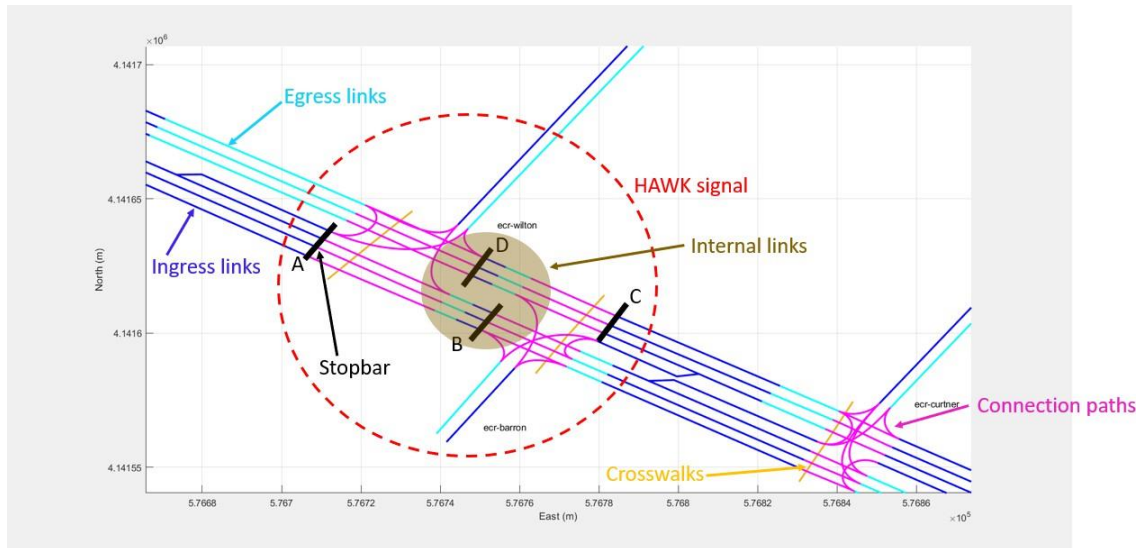


Figure 6. Example of two MAP/SPaT messages for each HAWK signal.

## 2.3 Discussion

In the California CV Testbed, four intersections have been instrumented with NoTraffic sensors to provide timely and accurate detection of pedestrians and bicyclists inside the intersection conflict area. Furthermore, six operational HAWK signals have been installed to provide additional protection for pedestrians and bicyclists to cross the major arterial, El Camino Real.

Because of the above infrastructure upgrades, we have applied some enhancements to the current version of MAP Engine Library. For example, to address the uncertainty caused by the HAWK signals in estimating the travel time to the downstream intersection in the application of Transit Signal Priority, new functions have been developed to identify multiple downstream intersections and estimate the corresponding distances and travel times. To support the enriched pedestrian and bicyclist detection data from the NoTraffic sensor, new functions have been developed to determine lane-of-travel for vulnerable road users and to track road user movements inside an intersection conflict area. Then this new information can be incorporated into and broadcasted through messages like MAP, SPaT, BSM, and PSM to inform nearby road users about traffic conditions.

Depending on the settings of HAWK signals, we have implemented two different schemes in constructing the corresponding MAP and SPaT messages. When there is only one crosswalk with two stopbars in the HAWK signal, we only need to construct one MAP/SPaT message. However, when there are two crosswalks with four stopbars in the HAWK signal, we need to separate each internal link into two sub-

links and construct two MAP/SPaT messages. Through this approach, regardless of the activation status of the two crosswalks in the HAWK signal, we can provide accurate information to the connected vehicles on the major arterial regarding where they should stop.

This page left blank  
intentionally

## **3. Enhancements to the Deployability of MMITSS Vehicle-Resident Applications**

### **3.1 Needs for an interface specification on exchange of SAE J2735 V2X messages between an OBU and a local device**

A Vehicle-to-Everything (V2X) On-Board Unit (OBU) is a vehicle mounted device used to wirelessly communicate with other devices within the Connected Vehicle (CV) environment, including human-driven vehicles and connected and automated vehicles (CAVs), for safety and mobility purposes<sup>7</sup>. To ensure the desired interoperability and data integrity to support the performance of the envisioned safety and mobility applications, the SAE J3161/1 Standard<sup>8</sup> specifies the interface requirements between OBU subsystems and the minimum functional requirements for transmitting and receiving the SAE J2735<sup>9</sup>- defined Basic Safety Message (BSM) over Cellular-V2X (C-V2X). SAE J3161/1 is an updated version of the SAE J2945/1 Standard<sup>10</sup>, which specifies requirements on transmitting and receiving BSM over Dedicated Short-Range Communications (DSRC). The Federal Communications Commission (FCC) issued a Report and Order<sup>2</sup> to phase out DSRC and replace it with C-V2X. SAE J3161/1 adopts the on-board system requirements defined in SAE J2945/1 and replaced V2X DSRC communications interface requirements with C-V2X.

The V2X technology and V2X communications have expanded to include all types of travelers including pedestrians, cyclists, multimodal travelers, and other vulnerable road users (VRUs). The SAE J3161(/0) Standard<sup>11</sup> describes deployment profile and unique features of C-V2X that can be used by current and future application standards. C-V2X supports broadcasting of wider variety of J2735 messages in addition to BSM, including MAP, Signal Phasing and Timing (SPaT), Signal Request Message (SRM), Signal Status Message (SSM), Emergency Vehicle Alert (EVA), Roadside Alert (RSA), Radio Technical Commission for Maritime Services (RTCM) corrections, etc.

To facilitate the flexibility and adaptability in developing, testing, and deploying C-V2X safety and mobility applications, SAE J3161/1 and SAE J2945/1 specify minimum requirements on BSM data frames and data elements that can support various safety and mobility applications. SAE J3161/1 and SAE J2945/1 do not include application's system requirement and application specifications, such as Concept of Operations document<sup>12</sup> and System Requirements Document<sup>13</sup> for Red-Light Violation Warning (RLVW) and Curve Speed Warning (CSW) applications. These are specified in separate documents. C-V2X use cases include, but are not limited to, data exchanges using J2735 messages. There is no one-fit-all solution that an OBU could provide service for all envisioned safety and mobility applications as V2X technology

---

<sup>7</sup> Institute of Transportation Engineers (2021). Roadside Unit (RSU) Standard. CTI 4001 v01.00, September 2021.

<sup>8</sup> SAE J3161/1 (2022). On-Board System Requirements for LTE-V2X V2V Safety Communications. March 2022.

<sup>9</sup> SAE J2735 (2020). V2X Communications Message Set Dictionary. July 2020.

<sup>10</sup> SAE J2945/1 (2020). On-Board System Requirements for V2V Safety Communications. April 2020.

<sup>11</sup> SAE J3161 (2022). LTE Vehicle-to-Everything (LTE-V2X) Deployment Profiles and Radio Parameters for Single Radio Channel Multi-Service Coexistence. April 2022.

<sup>12</sup> FHWA (2012). Accelerated Vehicle-to-Infrastructure (V2I) Safety Applications – Concept of Operations Document. May 2012.

<sup>13</sup> FHWA (2012). Accelerated Vehicle-to-Infrastructure (V2I) Safety Applications – System Requirements Document. July 2012.

and V2X communications are still evolving and different C-V2X use cases would have different system requirements.

Take transit signal priority (TSP) application as an example, the OBU installed on bus needs to determine its eligibility for priority based on business rules and parameters, for example, in service vs. out of service status, service type (rapid vs. local), type of bus stop (near-side vs. far-side), door status (open vs. closed), and headway/schedule adherence (late by x minutes), etc. If eligible for priority, the bus generates and sends SRM to the approaching RSU-equipped intersection. The bus processes SSM received from the RSU and sends updated SRM to the RSU if needed. The OBU will need to connect with bus on-board computer system to get bus operational status data (Figure 7). For agencies with even more complex business rules and parameters for priority, the TSP application residing on the OBU needs to be customized to meet user's needs - either by the OBU vendor or by the user using OBU vendor's software development kit (SDK) and would need continuous support to maintain its functionality.

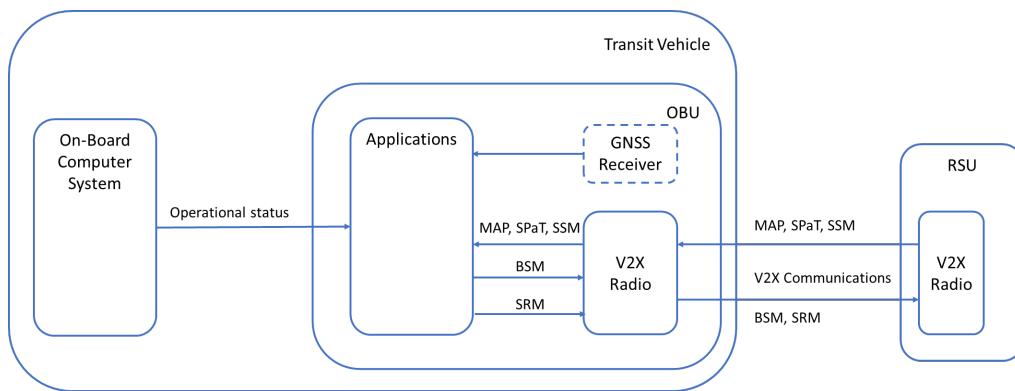


Figure 7. TSP Application Reside on Transit On-Board Unit.

Another approach is to have the TSP application reside on the bus computer system or a separate application processor and exchange J2735 messages between the application processor and OBU (Figure 8). This option provides more flexibility, allowing users to develop their own applications on the application processor. SAE J3161/1 and SAE J2945/1 specify requirements on the V2X radio interface for exchanging J2735 messages between the OBU and other C-V2X devices (OBU, RSU). There is a need to develop an application programming interface (API) specification for exchanging J2735 messages between an OBU and a local device (e.g., the application processor). Adding this interface to OBU allows a hardware-agnostic solution, that the vehicle-resident CV applications running on a separate application processor can be device-independent and work seamlessly with OBUs from different vendors.

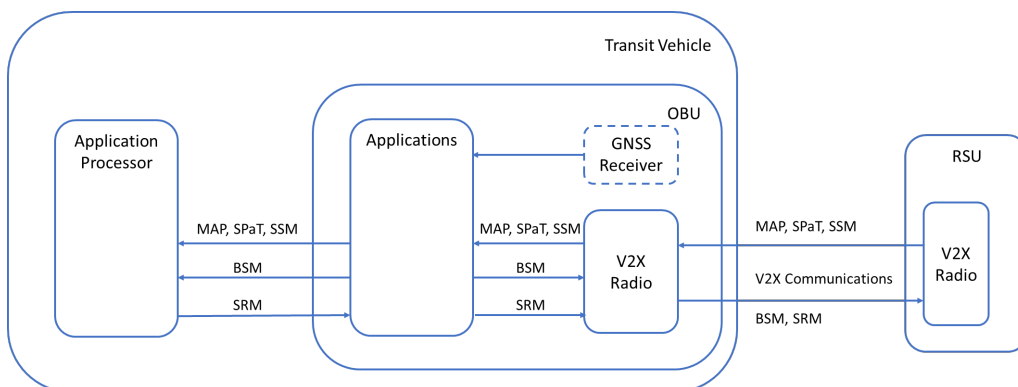


Figure 8. TSP Application Reside on a Separate Application Processor than Transit On-Board Unit.

### 3.2 Interface Specification on Exchange of SAE J2735 Messages between an OBU and a Local Device

USDOT's DSRC Roadside Unit Specifications<sup>14</sup> (also referred as RSU Specifications 4.1) define interface specifications on exchange of J2735 messages between a RSU and a local device. The Roadside Unit Standard<sup>7</sup> supersedes RSU Specifications 4.1 and adopts the interface specifications to C-V2X RSUs, including:

- *Immediate Forward (IF)* API to transmit messages received from the local device on the V2X radio interface (e.g., SPaT messages), and
- *V2X Message Forward (MF)* API to forward messages received on the V2X radio interface to the local device.

Analogous to RSU, an OBU also needs the *Immediate Forward* API and *V2X Message Forward* API to exchange messages with the application processor. Since the OBU moves with the vehicle, the interface should also support OBU forwarding its own BSM to the application processor.

SAE J3161/1 and SAE J2945/1 require the OBU's positioning subsystem (i.e., Global Navigation Satellite System - GNSS) to use Wide Area Augmentation System (WAAS) corrections when available. In area with Radio Technical Commission for Maritime Services (RTCM) corrections service available, the use of a real-time kinematics (RTK) enabled GNSS receiver can significantly improve position accuracy thereby improving reliability in detecting correct lane-of-travel. Although OBU's embedded WASS-enabled GNSS receiver cannot take advantage of RTCM position corrections, all OBUs allow the use of an external RTK-enabled GNSS receiver to bypass its embedded WASS GNSS receiver.

The recommended interface specification for message exchange between an OBU and a local device is summarized in Table 2. Figure 9 illustrates the system architecture with the envisioned interface functions.

Table 2 Recommended Interface Specification for OBU to Exchange Messages with a Separate Application Processor

User Need	Interface Requirement
<b>Immediate Forwarding of Messages Sent by the Local Application Processor</b>	The OBU needs to forward messages received from the local device to the V2X radio interface
<b>Forwarding Messages Received by the OBU on the V2X radio interface</b>	The OBU needs to forward messages received on the V2X radio interface to the local device
<b>Forwarding OBU's own BSM</b>	The OBU needs to forward its own BSM to the local device
<b>Utilizing RTCM Position Corrections</b>	The OBU needs to support the use of an extender RTK-enabled GNSS receiver

<sup>14</sup> USDOT, Saxton Transportation Operations Laboratory (2017). Dedicated Short-Range Communications Roadside Unit Specifications. FHWA-JPO-17-589. April 2017.



The lab test did not include a C-V2X OBU as it is not available at the time of lab testing. Since both RSU and OBU have the same interface for transmitting and receiving V2X messages over DSRC and over C-V2X, the test results apply to both C-V2X and DSRC devices.

Table 3 lists the SAE J2375 messages included in the lab tests. Message transmitting and receiving directions are illustrated in Figure 11.

Table 3 Tested SAE J2375 Messages

SAE J2735 Message	From	To
Map SPaT RTCM Signal Status Message (SSM) Roadside Safety Message (RSM) Personal Safety Message (PSM) Probe Data Management (PDM)	RSU	OBU
BSM Signal Request Message (SRM) Probe Vehicle Data (PVD)	OBU	RSU



Figure 11. Message Transmitting Direction.

To verify the reception of messages received by RSU and OBU and message frequency, packets transmitted on outbound (uplink) and inbound (downlink) were captured using the *tcpdump* tool. Figure 12 shows an example of inbound packets captured by the Siemens dual-mode RSU.

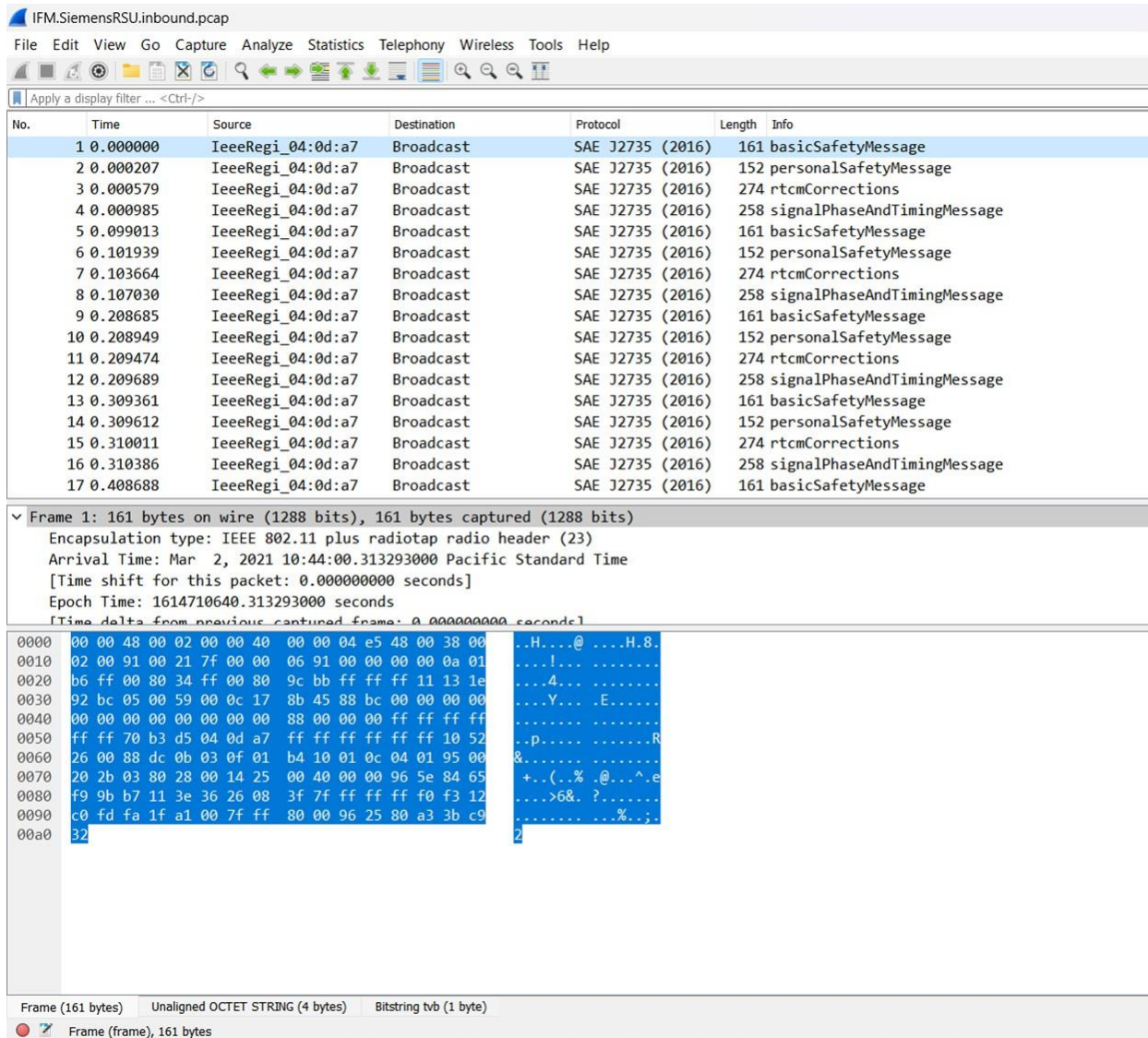


Figure 12. tcpdump Captured Inbound Packets.

Captured inbound and outbound packets on each device were postprocessed to compare message sending frequency and receiving frequency by message type. Lab tests were successful and RSU and OBU received message type and frequency matched with the sending message type and frequency.

This page left blank  
intentionally

## 4. Development of an Arterial Performance Measurement System (A-PeMS)

In this section, we introduce the development of an Arterial Performance Measurement System (A-PeMS) that manages the detector and signal phase data retrieved from the field, monitors the sensor network performance, and provides functions to identify traffic bottlenecks and potential causes. More details on the architecture design, methodologies and algorithms, performance measurement functions, and steps to assess arterial traffic performance are provided in the following subsections.

### 4.1 Architecture design

The Arterial Performance Measurement System (A-PeMS) consists of three different analysis levels, which is shown in Figure 13.

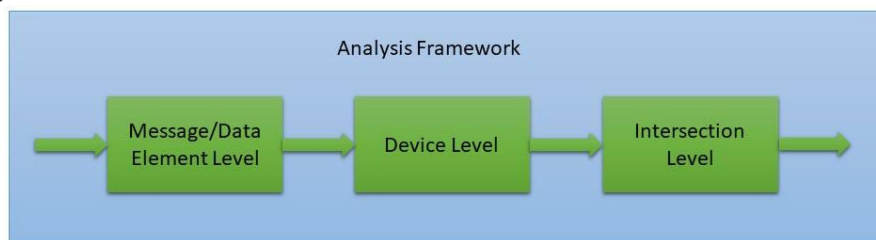


Figure 13. Analysis framework of the arterial performance measurement system.

- **Message/Data Element Level**  
As a first step, the system will check the data availability from the devices (e.g., loop detectors and traffic controllers) in the California CV Testbed. In particular, we focus on the real-time data availability for the loop detectors and intersection signals.
- **Device Level**  
With stable data feeds from the field, the system further aggregates the raw detector and signal phase data into fixed time intervals or cycles. For the detector data, the system analyzes the quality of the data and help identify bad detectors in the testbed. For the signal phase data, the system provides various statistics (e.g., phase duration, gap-out/max-out, and pedestrian activities) to assess the signal performance.
- **Intersection Level**  
At the intersection level, there are two options to assess the traffic performance in the testbed. For the first option, the system provides functions to visualize the coordination performance along El Camino Real under different time periods (e.g., AM peak vs. PM peak). For the second option, with the inputs of detector and signal phase data, the system conducts traffic state estimation and provides functions to visualize the formation and dissipation of traffic congestion at bottleneck intersections.

The architecture of the Arterial Performance Measurement System is shown in Figure 14, which consists of the following key components:

- MySQL Database
  - It is used to store both raw and processed detector and signal phase data.
- Mongo Database
  - It is used to store the arterial network and traffic estimation results.
- Data Aggregation
  - This component is used to aggregate raw detector and signal phase data into fixed time intervals or cycles.
- Detector Health
  - This component is used to analyze the quality of the detector data.
- Data Filtering
  - This component is used to filter out outliers in the detector data.
- Aimsun Microsimulation Model
  - This model is used to host the static network and signal control information (e.g., timing sheets) and for offline traffic analysis.
- Network Builder
  - This component is used to provide Traffic Management Data Dictionary (TMDD) input files for traffic state estimation.
- Arterial Traffic State Estimation
  - This component is used to generate estimates of traffic states at each intersection approach.
- Result Analysis and Visualization
  - This component is used to provide an interactive visualization tool (website) for performance evaluation.

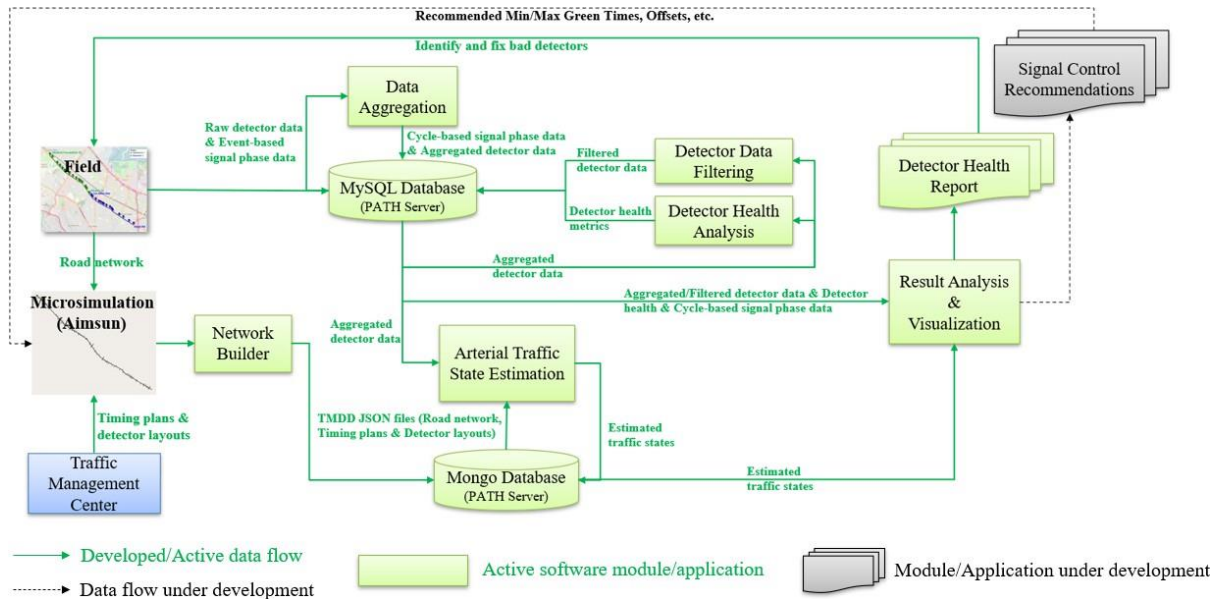


Figure 14. System architecture of the arterial performance measurement system.

As shown in Figure 14, the following data flows among the key components have been implemented:

- Real-time raw detector data and event-based signal phase data → MySQL Database (PATH Server).
- MySQL Database (Raw detector data) → Data Aggregation → MySQL Database (Aggregated detector data)
- MySQL Database (Event-based signal phase data) → Data Aggregation → MySQL Database (Cycle-based signal phase data)
- MySQL Database (Aggregated detector data) → Data Filtering → MySQL Database (Filtered detector data)
- MySQL Database (Aggregated detector data) → Detector Health Analysis → MySQL Database (Detector health metrics)
- Field intersection layouts → A microsimulation model in Aimsun (Road network; Manually created)
- Detector layouts and timing plans from TMC → A microsimulation model in Aimsun (detectors and timing plans; Manually created)
- The microsimulation model in Aimsun → Network Builder → Mongo Database (PATH Server; TMDD JSON files of the road network, detectors, and timing plans)
- Mongo Database (TMDD JSON files of the road network, detectors, and timing plans) and MySQL Database (Aggregated detector data) → Arterial Traffic State Estimation → Mongo Database (Estimated traffic states)
- MySQL Database (Aggregated/Filtered detector data, detector health metrics, and cycle-based signal phase data) → Result Analysis and Visualization → Website (<https://caconnectedvehicletestbed.org/apems/>)
- Mongo Database (Estimated traffic states) → Result Analysis and Visualization → Website (<https://caconnectedvehicletestbed.org/apems/>)

With the help from the Result Analysis and Visualization component, users can:

- Extract a Detector Health Report, identify and fix bad detectors;
- Identify bottleneck intersections and recommend new signal control settings of Min/Max Green Times, Offsets, etc.

## 4.2 Methodologies and algorithms

In this subsection, we introduce the methodologies and algorithms implemented in the Arterial Performance Measurement System. More details are provided below.

### 4.2.1 Detector data Aggregation

In Figure 15, we provide an example of raw detector data from the California CV Testbed. In the figure, “id” is the Intersection Id, “tm” is the date, “msec” is the millisecond since midnight, “indx” is the Detector System Index, “seq” is the sequence number of the data sample, “vol” is the number of detected vehicles since the last reported timestamp, and “occ” is the integer number of occupancy in 0.5% increments that is measured since the last reported timestamp.

As shown in Figure 15, the raw detector measurements are not in fixed time intervals, which is difficult to use to support common applications like traffic performance analysis and traffic modeling, simulation and calibration. Therefore, we apply simple algorithms to aggregate the raw detector data into fixed time intervals. Here, we chose 5 minutes as the time interval because we think it is an appropriate interval to smooth oscillations caused by transient congestion while retaining key traffic information (e.g., onset/dissipation of traffic congestion) inside the aggregated data.

For each day we expect to have 288 aggregated measurements of flow rate and occupancy for each detector. For a given detector  $dd$ , at the  $i^{\text{th}}$  ( $ii = 1, 2, \dots, 288$ ) interval of 5 mins (i.e.,  $tt \in [(ii - 1) * 300\text{ss}, ii * 300\text{ss})$ ), we assume there are  $MM$  raw data measurements of volume and occupancy. If there is no data measurement at the  $i^{\text{th}}$  interval with  $MM = 0$ , there will be no aggregated measurement for that interval. When  $MM \geq 1$ , we will use the following equations to aggregate the raw data measurements:

$$FFFFF_{ii}^{dd} = 12 * \sum_{jj=1}^{MM} WFFF_{jj}^{dd} \quad (1)$$

$$OOOO_{ii}^{dd} = \frac{\sum_{jj=1}^{MM} OOOO_{jj}^{dd} (tt_{jj} - tt_{jj-1})}{5 * 60} \quad (2)$$

where

$FFFFF_{ii}^{dd}$ : aggregated hourly flow rate for detector  $dd$  at the  $i^{\text{th}}$  interval;

$OOOO_{ii}^{dd}$ : averaged occupancy for detector  $dd$  at the  $i^{\text{th}}$  interval;

$WFFF_{jj}^{dd}$ : the  $j^{\text{th}}$  measured vehicle volume for detector  $dd$  within the  $i^{\text{th}}$  interval;

$OOOO_{jj}^{dd}$ : the  $j^{\text{th}}$  measured vehicle occupancy for detector  $dd$  within the  $i^{\text{th}}$  interval;

$tt_{jj}$ : timestamp when the  $j^{\text{th}}$  detector measurement is reported;

$tt_{jj-1}$ : timestamp when the  $(j-1)^{\text{th}}$  detector measurement is reported ( $tt_{jj-1} < tt_{jj}$ );

$tt_{jj=0}$  is the beginning time of the  $i^{\text{th}}$  interval.

id	tm	msec	indx	seq	vol	occ
1001	2022-08-31	36109428	1	122	0	0
1001	2022-08-31	36109428	2	122	26	22
1001	2022-08-31	36109428	3	122	7	90
1001	2022-08-31	36109428	4	122	0	0
1001	2022-08-31	36109428	5	122	7	2
1001	2022-08-31	36109428	6	122	2	112
1001	2022-08-31	36109428	7	122	4	12
1001	2022-08-31	36109428	8	122	10	118
1001	2022-08-31	36109428	9	122	2	126
1001	2022-08-31	36109428	10	122	19	8
1001	2022-08-31	36109428	11	122	18	14
1001	2022-08-31	36109428	12	122	18	6
1001	2022-08-31	36109428	13	122	0	0
1001	2022-08-31	36109428	14	122	0	0
1001	2022-08-31	36109428	15	122	0	0
1001	2022-08-31	36109428	16	122	0	0
1001	2022-08-31	36314431	1	123	0	0
1001	2022-08-31	36314431	2	123	11	84
1001	2022-08-31	36314431	3	123	5	112
1001	2022-08-31	36314431	4	123	0	0
1001	2022-08-31	36314431	5	123	7	2
1001	2022-08-31	36314431	6	123	1	180
1001	2022-08-31	36314431	7	123	3	94
1001	2022-08-31	36314431	8	123	8	116
1001	2022-08-31	36314431	9	123	1	196
1001	2022-08-31	36314431	10	123	26	16

Figure 15. Example of raw detector data from the California CV Testbed.

We apply the above aggregation method to all available detectors in the California CV Testbed. In Figure 16, we provide an example of aggregated data from Detector 5 at Intersection 1001 on 2022-08-31. As shown in the figure, this aggregated data is smoother than the raw data and is easier to support various transportation needs with a fixed time interval, e.g., traffic model calibration and detector data quality analysis.

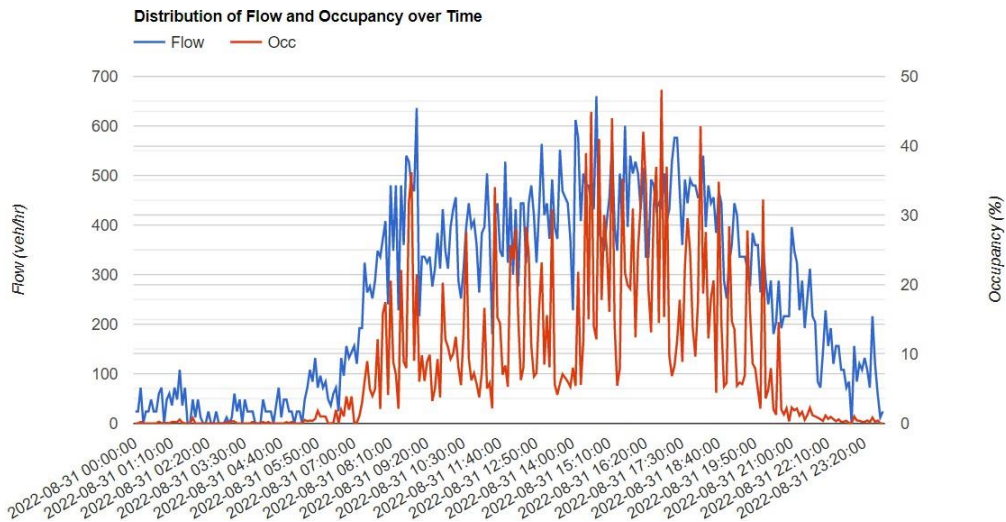


Figure 16. Example of aggregated data from Detector 5 at Intersection 1001 on 2022-08-31.

## 4.2.2 Detector Health Analysis

In practice the reported data from a detector may be incomplete or even too bad to use if the network connection or the detector is in a bad state. Therefore, it is of great importance to monitor the health of detectors and help traffic engineers identify and fix potential issues in a timely manner.

In the California CV Testbed, once we calculate the aggregated detector measurements from the raw data, we will check their quality in the following five aspects:

- **Missing data.**  
Due to unstable network connection, maintenance work, or other unknown issues, it is possible to miss a large number of data samples for a set of detectors on a certain day. If the data missing rate for a given detector is high on a particular day, we will consider the detector is bad (with poor data quality) on that day.
- **High values.**  
Due to the presence of traffic signals and potential queue spillback, it is possible for a loop detector to report data samples with high occupancy. Therefore, we only check high values for the flow measurements (i.e., flow rate  $ff$ ). In our current setting, we apply the same flow threshold  $ff_{\text{min}}$  to all detectors. If a detector keeps reporting high values on a certain day (i.e.,  $ff > ff_{\text{min}}$ ), which is over a certain percentage, e.g., 10%, we will consider the detector is bad (with poor data quality) on that day. In the future, this can be improved with multiple flow thresholds to consider the differences in detector types and allocated green times.
- **Zero values.**  
For arterial detectors, it is normal to report zero values of flow and occupancy if there is no traffic during the measured time period. This is particularly true for minor streets and during midnight. However, during daytime it is abnormal for a detector to report zero values of flow and occupancy for a long time period, e.g., several hours. Therefore, if this happens, we will consider this detector is bad (with poor data quality) on that day.
- **Non-zero constant values.**  
In practice, a detector may be stuck at a faulty state so it keeps reporting non-zero constant values, for example, zero flow but 100% occupancy. If this happens for a whole day, we will consider the detector is bad (with poor data quality) on that day.
- **Inconsistent data.**  
Sometimes we do find the reported measurements of flow and occupancy do not follow fundamental laws of traffic flow. For example, in the raw detector data, we do see measurements with zero occupancy but non-zero vehicle count. If this happens a lot during a day, e.g., over a certain percentage, we will consider the detector is bad (with poor data quality) on that day.

In our current system design, we consider a detector is in a good state (with good data quality) on a given day only when the aggregated data meets the following requirements:

- The daily missing rate is less than a user-defined threshold  $\epsilon_{\text{min}}$
- The daily high value rate ( $ff > ff_{\text{min}}$ ) is less than a user-defined threshold  $\epsilon_{\text{high}}$
- The daily flow and occupancy measurements are not non-zero constant values.
- Between morning hour  $tt_1$  and evening hour  $tt_2$ , the maximum period of zero flow and occupancy is less than a user-defined threshold  $\epsilon_{\text{zero}}$

- The daily rate of inconsistent data is less than a user-defined threshold  $\epsilon_{\text{inconsistent}}$ .

For the detectors in the California CV Testbed, we apply the following values to the parameters mentioned above:

- $\epsilon_{\text{missing}} = 10\%$
- $f_{\text{high}} = 150 \text{ veh/hr}$
- $\epsilon_{\text{inconsistent}} = 10\%$
- $tt_1 = 6\text{AM}$
- $tt_2 = 10\text{PM}$
- $\epsilon_{\text{zero}} = 4\text{h}$
- $\epsilon_{\text{inconsistent}} = 10\%$

We apply the above health criteria to all the detectors in the California CV Testbed. In Figure 17, we provide an example of health metrics for the detectors at Intersection 1001 on 2022-08-31. As shown in the figure, four detectors (Detectors 4, 8, 27, and 28) at Intersection 1001 reported long periods of zero values on 2022-08-31, so they were categorized as bad detectors on that day. Though Detector 25 reported 3.4% inconsistent values during the day, it was categorized as a good detector because the inconsistent rate is not over the defined threshold.

Detector Health								
Intersection ID	Detector ID	Selected Date	Missing Rate(%)	High Value(%)	Constant Value(Y/N)	Max Period of Zero Values(hr)	Rate of Inconsistent Values(%)	Health (Good/Bad)
1001	3	2022-08-31	0	0	N	0.083	0.347	Good
1001	4	2022-08-31	0	0	N	16	0	Bad
1001	5	2022-08-31	0	0	N	0	0.694	Good
1001	6	2022-08-31	0	0	N	0	0	Good
1001	7	2022-08-31	0	0	N	0	0	Good
1001	8	2022-08-31	0	0	N	16	0	Bad
1001	11	2022-08-31	0	0	N	0.417	0	Good
1001	12	2022-08-31	0	0	N	0.417	0	Good
1001	21	2022-08-31	0	0	N	0.083	0	Good
1001	23	2022-08-31	0	0	N	0	0.347	Good
1001	24	2022-08-31	0	0	N	0	1.736	Good
1001	25	2022-08-31	0	0	N	0	3.472	Good
1001	27	2022-08-31	0	0	N	16	0	Bad
1001	28	2022-08-31	0	0	N	16	0	Bad

Figure 17. Example of health metrics for the detectors at Intersection 1001 on 2022-08-31.

### 4.2.3 Detector data Filtering

In the current system design, we only apply simple moving averages to: (i) fill in missing data; and (ii) replace data measurements if they contain high values or inconsistent values. Currently, we use the span of 3 for the moving average. That means if the  $i^{\text{th}}$  aggregated detector measurement is problematic, we will

replace it with the averages from the  $(ii - 3)^{th}$ ,  $(ii - 2)^{th}$ ,  $(ii - 1)^{th}$  aggregated detector measurements. In the future, we can improve it with more advanced data filtering algorithms proposed in the literature.

In Figure 18, we provide an example of data filtering for Detector 3 at Intersection 1008 on 2022-08-31. As shown in Figure 18(a), there was an outlier with a high flow rate at 13:40 before data filtering. But after data filtering, the outlier was replaced by the moving average from the previous 3 detector measurements (i.e., the previous 15 minutes), which is shown in Figure 18(b).

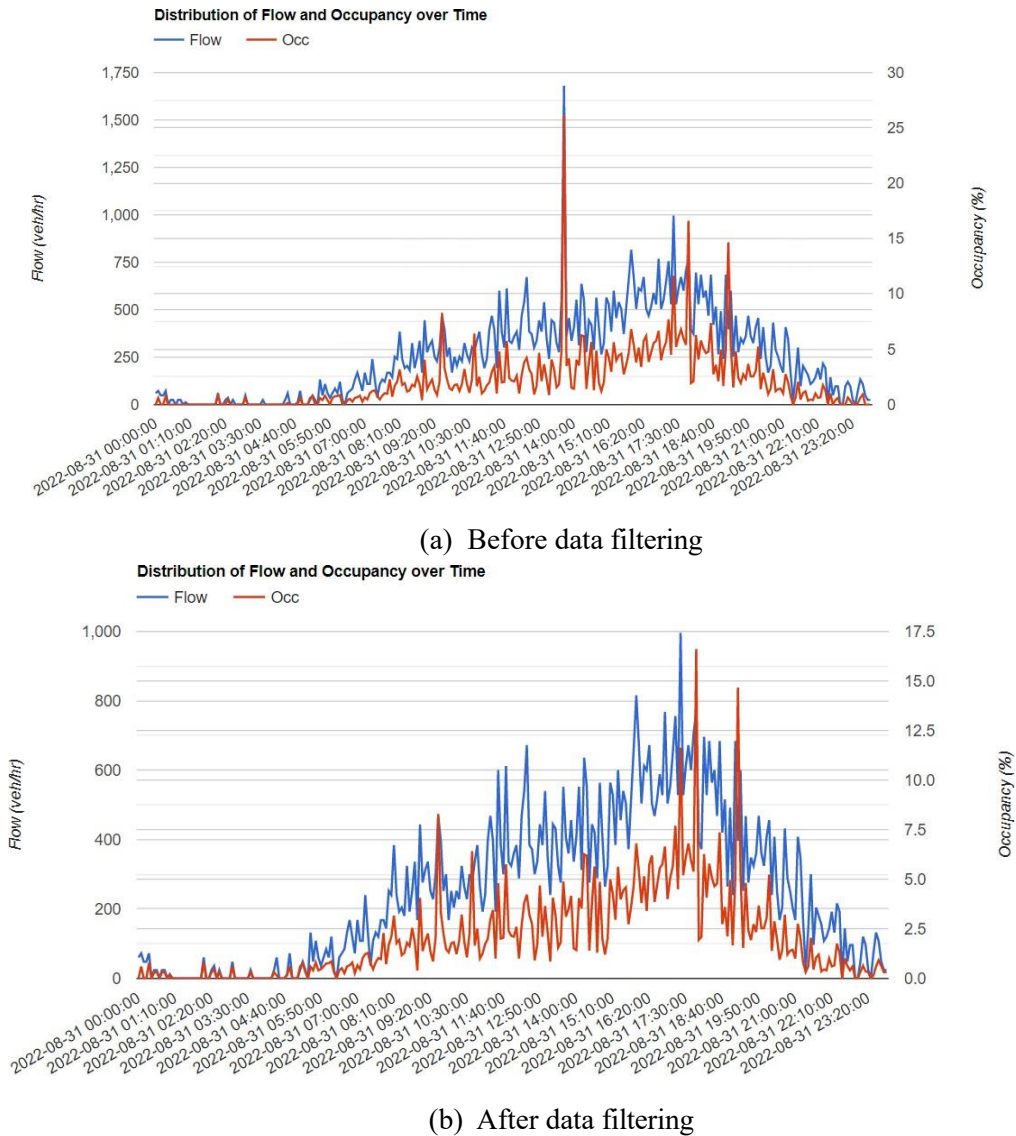


Figure 18. Example of data filtering for Detector 3 at Intersection 1008 on 2022-08-31.

#### 4.2.4 Signal phase data aggregation

Currently, we are receiving real-time raw signal phase data from the 16 operational intersections in the California CV Testbed. The raw signal phase data we received is event-based as the field controllers will send out updates whenever there is a change to the phases, e.g., switching from green to yellow. This kind of event-based data is not easy to analyze, and therefore, we have developed algorithms to aggregate it into

cycle-based. For each cycle, its length and phase green times are closely related to the timing plan being used as well as detector actuation activities in the field.

In Figure 19, we provide an example of ring-barrier-phase settings for different timing plans at Intersection 1002 (Embarcadero/Galvez @ El Camino Real). As shown in the figure, there are four timing plans implemented at this intersection: (i) free mode with plan id 255, and (ii) coordinated plans 1 to 3. For plans 1 to 3, phases 2 and 6 are assigned as the coordinated phases. Also there exist lead-lag phasing settings for the left turns in plans 1 and 3: (i) phase 1 (leading), phase 3 (lagging), phase 5 (lagging), and phase 7 (leading) for plan 1; (ii) phase 1 (leading), phase 3 (leading), phase 5 (lagging), and phase 7 (leading) for plan 3. In addition, for the coordinated timing plans, the reference point is the end of green of the coordinated phases, i.e., phase 2 at Intersection 1002 as shown in Figure 19.

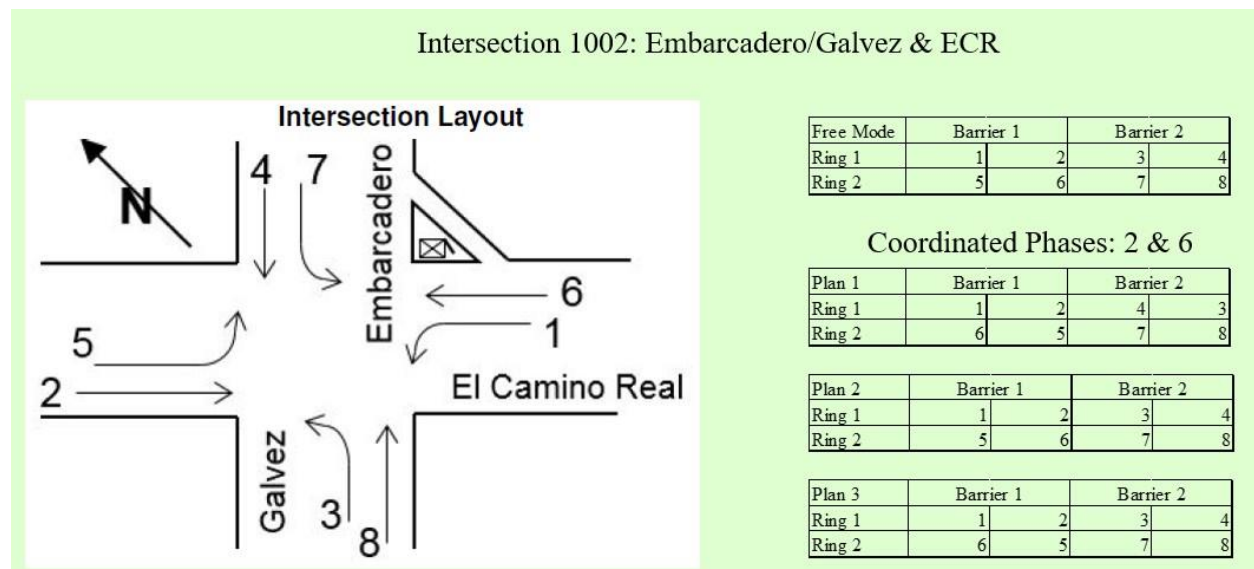


Figure 19. Example of ring-barrier-phase settings for different timing plans at Intersection 1002.

In Figure 20, we provide an example of raw event-based signal phase data from Intersection 1002 on 2022-08-31. As shown in the figure, each row represents an event of signal status update sent from field controllers. The available columns are described below:

- “id” is the intersection id;
- “tm” is the date;
- “msec” is the time in milliseconds measured from midnight;
- “ph” is the phase id (1 to 8 for vehicle phases, and 9 to 16 for pedestrian phases);
- “status” is the phase status (0: dark; 1: green or walk; 2: yellow or flashing don’t walk; 3: red or solid don’t walk; 4: flashing red);
- “term\_type” is the termination type (0: NA; 12: gap out; 13: max out; 14: forced off);
- “plan\_num” is the current plan number;
- “of\_indx” is the offset index in the timing sheet (1 ~ 3 = Offset A ~ C, respectively);
- “mclock” is the master cycle clock in seconds;
- “lclock” is the local cycle clock in seconds.

To identify a sequence of signal status updates belonging to the same cycle, the first step is to find out the corresponding starting time and ending time. According to the signal control settings shown in Figure 19, we use the following criteria to identify the time stamp (e.g.,  $tt_1$  and  $tt_2$  in Figure 20) that indicates the beginning of a cycle (or in other words, the end of the previous cycle):

- (i) At that time stamp (e.g., “msec”=36281105 in Figure 20), at least one of the coordinated phases (e.g., phases 2 and 6 in Figure 20) shows the end of green indicator (e.g., “status”=2 in Figure 20).
- (ii) Meanwhile, the next available time stamp (e.g., “msec”=36286107 in Figure 20), there is an indicator of a barrier change (e.g., “status”=1 for phase 3 in Figure 20).

With the above criteria, we can find out a sequence of signal status updates belonging to the same cycle, e.g., those updates (i.e., rows) between  $tt_1$  and  $tt_2$  in Figure 20. Once we get this list, it is very straightforward to calculate the corresponding green times for the available vehicle phases as well as pedestrian phases. When the intersection is in the coordination mode, we use the following method to calculate the actual offset at the beginning of the cycle (e.g., “msec”=36281105 in Figure 20):

- (i) If “mclock”  $\geq$  “lclock”, actual offset = “mclock” - “lclock”;
- (ii) Else, actual offset = default cycle length - “mclock” + “lclock”.

Then a whole signal cycle (i.e., cycle length, offset and phase green times) can be reconstructed.

id	tm	msec	ph	status	term_type	plan_num	of_idx	mclock	lclock
1002	2022-08-31	36203111	10	2	0	2	1	136	89
1002	2022-08-31	36212111	14	3	0	2	1	5	95
1002	2022-08-31	36222111	10	3	0	2	1	15	101
1002	2022-08-31	36281105	2	2	14	2	1	74	1
1002	2022-08-31	36281105	6	2	14	2	1	74	1
1002	2022-08-31	36286107	2	3	0	2	1	79	4
1002	2022-08-31	36286107	3	1	0	2	1	79	4
1002	2022-08-31	36286107	6	3	0	2	1	79	4
1002	2022-08-31	36286107	7	1	0	2	1	79	4
1002	2022-08-31	36297109	3	2	12	2	1	90	13
1002	2022-08-31	36300109	3	3	0	2	1	93	16
1002	2022-08-31	36301109	4	1	0	2	1	94	17
1002	2022-08-31	36306109	7	2	13	2	1	99	22
1002	2022-08-31	36309110	7	3	0	2	1	102	25
1002	2022-08-31	36310110	8	1	0	2	1	103	26
1002	2022-08-31	36310110	16	1	0	2	1	103	26
1002	2022-08-31	36327112	16	2	0	2	1	120	43
1002	2022-08-31	36359112	4	2	14	2	1	12	75
1002	2022-08-31	36359112	8	2	14	2	1	12	75
1002	2022-08-31	36359112	16	3	0	2	1	12	75
1002	2022-08-31	36363112	4	3	0	2	1	16	79
1002	2022-08-31	36363112	8	3	0	2	1	16	79
1002	2022-08-31	36364112	1	1	0	2	1	17	80
1002	2022-08-31	36364112	5	1	0	2	1	17	80
1002	2022-08-31	36385119	1	2	14	2	1	38	101
1002	2022-08-31	36386119	5	2	12	2	1	39	102
1002	2022-08-31	36389120	1	3	0	2	1	42	105
1002	2022-08-31	36389120	2	1	0	2	1	42	105
1002	2022-08-31	36390121	5	3	0	2	1	43	106
1002	2022-08-31	36390121	6	1	0	2	1	43	106
1002	2022-08-31	36425130	2	2	14	2	1	78	1
1002	2022-08-31	36425130	6	2	14	2	1	78	1
1002	2022-08-31	36430132	2	3	0	2	1	83	6
1002	2022-08-31	36430132	4	1	0	2	1	83	6
1002	2022-08-31	36430132	6	3	0	2	1	83	6
1002	2022-08-31	36430132	7	1	0	2	1	83	6

Figure 20. Example of raw event-based signal phase data from Intersection 1002 on 2022-08-31.

In Figure 21, we provide an example of reconstructed signal cycles at Intersection 1002 on 2022-08-31. As shown in the figure, the reconstructed signal cycles are very consistent with the default settings. Sometimes we do notice a tiny difference of 1 or 2 seconds in the cycle length and offset, which may be caused by the

delay when the controller logs the event times and the error when we round up/down the decimals and thus can be ignored.

Intersection ID	Cycle End Datetime	Plan Id	Cycle Length(s)	Ph1(s)	Ph2(s)	Ph3(s)	Ph4(s)	Ph5(s)	Ph6(s)	Ph7(s)	Ph8(s)
1002	2022-08-31 10:30:24	2	140	17	36	11	58	22	31	20	49
1002	2022-08-31 10:32:44	2	140	14	80	11	18	22	72	33	0
1002	2022-08-31 10:35:04	2	140	13	50	13	46	22	41	20	40
1002	2022-08-31 10:37:24	2	140	25	63	0	40	22	65	20	16
1002	2022-08-31 10:39:44	2	140	17	36	12	56	22	31	20	49
1002	2022-08-31 10:42:04	2	140	12	78	12	19	22	68	20	12
1002	2022-08-31 10:44:24	2	140	16	37	0	73	22	31	20	49
1002	2022-08-31 10:46:43	2	139	17	55	11	40	22	49	20	32
1002	2022-08-31 10:49:03	2	140	23	58	0	47	22	58	20	23
1002	2022-08-31 10:51:23	2	140	22	63	11	27	22	63	20	18
1002	2022-08-31 10:53:43	2	140	27	36	18	40	22	41	20	39
1002	2022-08-31 10:56:04	2	141	14	40	12	56	22	32	20	49
1002	2022-08-31 10:58:24	2	140	12	59	11	40	22	49	23	28
1002	2022-08-31 11:00:43	2	139	17	46	12	47	22	40	20	39

Intersection ID	Cycle End Datetime	Plan Id	Default Offset	Actual Offset
1002	2022-08-31 10:30:24	2	77	77
1002	2022-08-31 10:32:44	2	77	77
1002	2022-08-31 10:35:04	2	77	77
1002	2022-08-31 10:37:24	2	77	77
1002	2022-08-31 10:39:44	2	77	77
1002	2022-08-31 10:42:04	2	77	77
1002	2022-08-31 10:44:24	2	77	78
1002	2022-08-31 10:46:43	2	77	77
1002	2022-08-31 10:49:03	2	77	77
1002	2022-08-31 10:51:23	2	77	77
1002	2022-08-31 10:53:43	2	77	77
1002	2022-08-31 10:56:04	2	77	77
1002	2022-08-31 10:58:24	2	77	78
1002	2022-08-31 11:00:43	2	77	78

Figure 21. Example of reconstructed signal cycles at Intersection 1002 on 2022-08-31.

#### 4.2.5 Arterial traffic state estimation

At arterial intersections, loop detectors are installed at various locations to help with actuated traffic control. The flow-occupancy plots obtained from these detectors, which are known as traffic flow fundamental diagrams, are one of the approaches to identify traffic states, e.g., free-flow or congested. However, different from the commonly-used triangular fundamental diagram for freeway road links, the fundamental diagram for arterial road links becomes trapezoidal due to the presence of traffic signals.

As shown in Figure 22, the actual capacity  $qq_{II}$  is determined by the saturation flow rate  $qq_{MM}$  as well as the green ratio  $\frac{GG}{CC}$ , where  $GG$  is the effective green time and  $CC$  is the cycle length. When arterial intersections are narrowly spaced, vehicles from upstream intersections normally arrive in platoons with no or little dispersion. According to different traffic coordination levels, we categorize the trapezoidal fundamental diagram into three different regimes:

- R1: Uncongested regime with  $0 \leq \theta \leq \theta_{c1}$
- R2: Congested regime with  $\theta_{c1} < \theta \leq \theta_{c2}$
- R3: Downstream spillback regime with  $\theta_{c2} < \theta \leq 1$

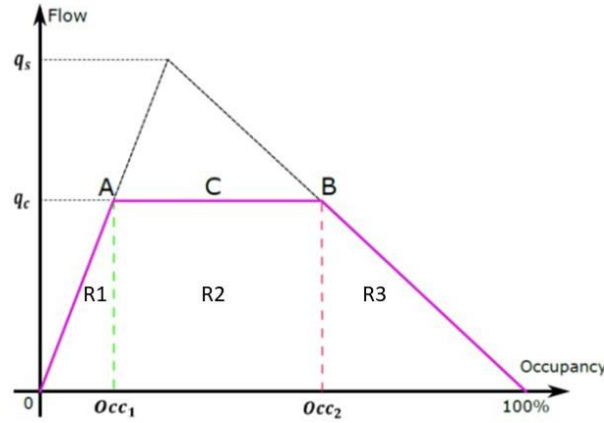


Figure 22. Trapezoidal fundamental diagram for signalized arterial road links.

The two critical thresholds  $\theta_{c1}$  and  $\theta_{c2}$  that are used to divide the trapezoidal fundamental diagram into the above three regimes can be calculated using the following equations:

$$\theta_{c1} = \frac{(LL + DD)q_{MM}GG}{5280v_{MM}CC} \quad (3)$$

$$\theta_{c2} = 1 - \frac{GG}{CC} \frac{(LL + DD)q_{MM}GG}{5280v_{MM}CC} \quad (4)$$

where

$GG$ : effective green time (sec);

$CC$ : cycle length (sec);

$q_{MM}$ : saturation flow rate (veh/hr);

$v_{MM}$ : saturation speed (mph);

$LL$ : average vehicle length (feet);

$DD$ : detector length (feet).

For more details, refer to the SB1 Report “Arterial Traffic Estimation Using Field Detector and Signal Phasing Data”<sup>15</sup>.

Note that the purple line (i.e., the trapezoidal fundamental diagram) in Figure 22 is the optimal solution for signalized arterial road links. For the actual flow-occupancy plots from advance detectors, we expect there will be a lot of points below the purple line.

- As shown in Figure 23, when the coordination level is good, upstream vehicle platoons can cross the intersection without stopping. Therefore, the corresponding flow-occupancy measurement will be at point D.

<sup>15</sup> <https://escholarship.org/content/qt7g5532jh/qt7g5532jh.pdf>

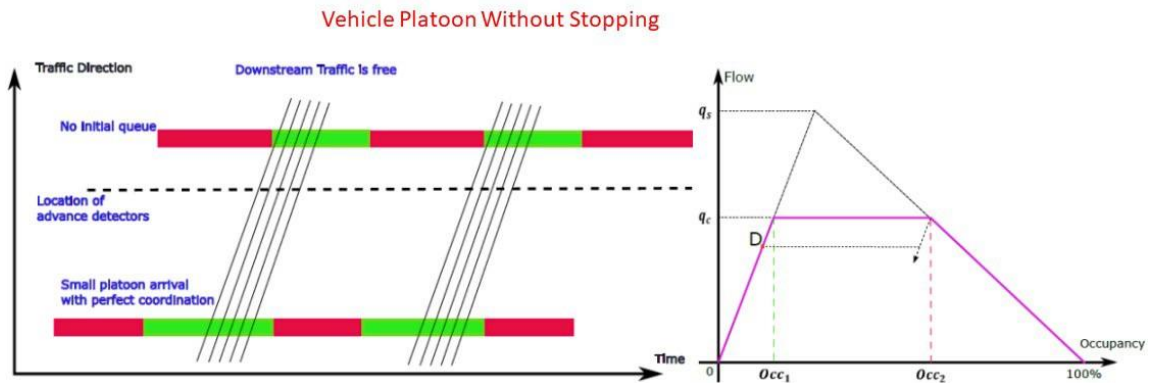


Figure 23. Example of vehicle platoons without stopping.

- As the coordination level degrades, upstream vehicle platoons may need to stop at the intersection and wait for a certain period of red time. In this case, the corresponding flow-occupancy measurement will shift to the right, e.g., at point E in Figure 24. The position of E depends on the platoon waiting time at the intersection: it will shift more to the right if the waiting time gets longer.

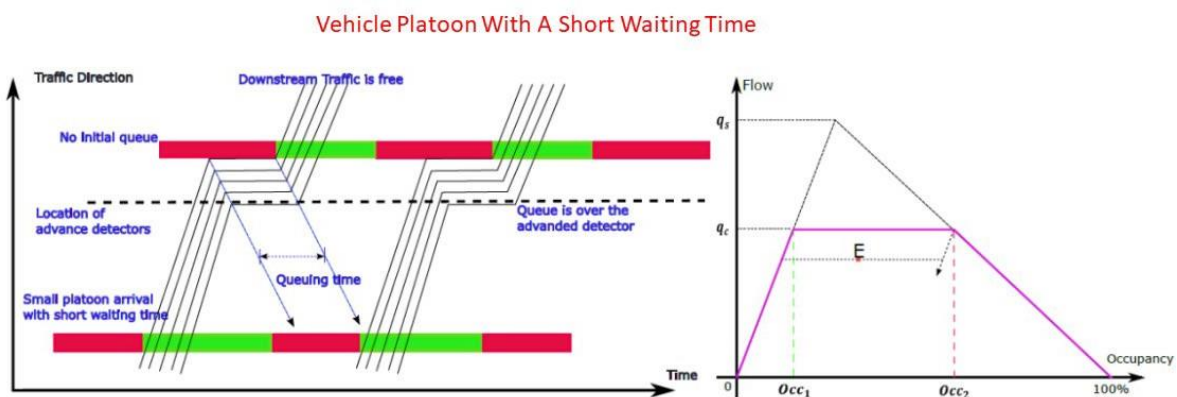


Figure 24. Example of vehicle platoons with a short waiting time.

- The worst case will be that vehicle platoons have to wait for the whole red time period. As a result, the corresponding flow-occupancy measurement will be at point F in Figure 25.

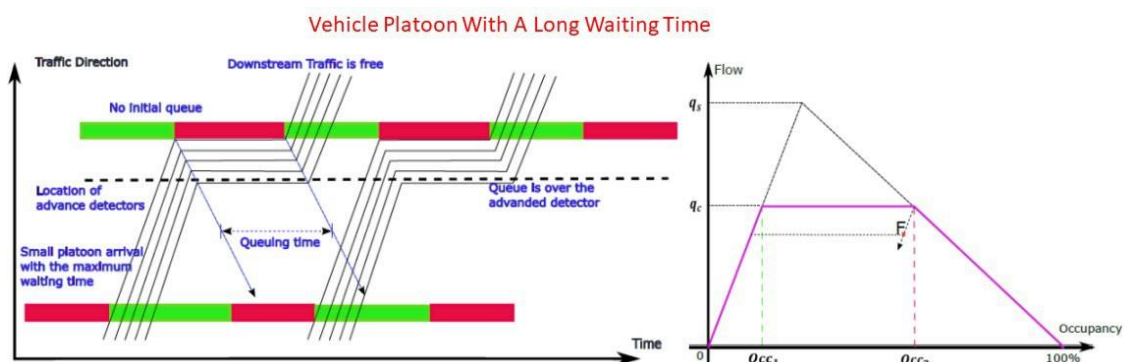


Figure 25. Example of vehicle platoons with a long waiting time.

In Figure 26 we provide two flow-occupancy plots from the advance detectors in the SB and NB directions at Intersection 1002 (Embarcadero/Galvez @ El Camino Real). As shown in the figure, for a given flow rate, there exist infinitely many occupancies in the flow-occupancy plots, which further supports the above arguments from Figure 23 to Figure 25.

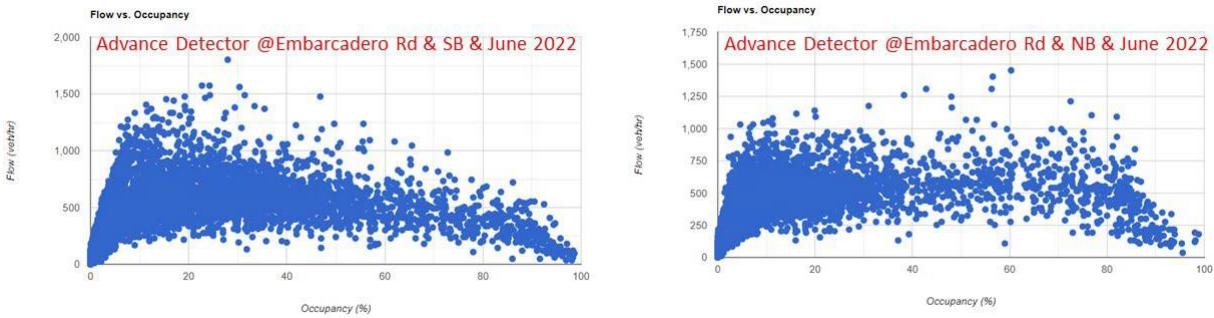


Figure 26. Example of flow-occupancy plots from the advance detectors in the SB and NB directions at Intersection 1002 (Embarcadero/Galvez @ El Camino Real).

## 4.3 Performance measurement functions

In this subsection, we introduce the available performance measurement functions in the Arterial Performance Measurement System.

### 4.3.1 Data availability

As shown in Figure 13, the very first step is to check the raw detector and signal phase data at the message/data element level. Especially, to guarantee enough data for the analysis at the device and intersection levels, we provide functions to monitor the real-time data availability from field detectors and intersection controllers.

#### 4.3.1.1 Real-time detector data availability

As shown in Figure 27, we provide a table view of real-time detector data availability in the California CV Testbed, which was requested at 12:15PM on 2022-08-30. In the Arterial Performance Measurement System, when the request to check the detector data availability is sent, there is a function to query the database and return the information of Intersection Id, Cross-Street Name, Detector Id, and Last Update Time for each detector. The font color of "Last Update Time" indicates different detector data availability: (i) the color is green if the gap between the "Last Update Time" and the current time is less than 15 minutes; (ii) the color changes to purple if the gap is between 15 minutes and 1 hour; (iii) the color is red if the gap is greater than 1 hour. But note that the 'Last Update Time' value may be affected by the quality of backhaul connections.

Real-Time Detector Data Availability

Intersection ID	Cross-Street Name	Detector ID	Last Update Time	2022-08-30 12:15:25
1001	Medical Foundation Dr	4	2022-08-30 12:11:16	
1001	Medical Foundation Dr	5	2022-08-30 12:11:16	
1001	Medical Foundation Dr	7	2022-08-30 12:11:16	
1001	Medical Foundation Dr	8	2022-08-30 12:11:16	
1001	Medical Foundation Dr	3	2022-08-30 12:11:16	
1001	Medical Foundation Dr	11	2022-08-30 12:11:16	
1001	Medical Foundation Dr	12	2022-08-30 12:11:16	
1001	Medical Foundation Dr	6	2022-08-30 12:11:16	
1001	Medical Foundation Dr	21	2022-08-30 12:11:16	
1001	Medical Foundation Dr	23	2022-08-30 12:11:16	
1001	Medical Foundation Dr	24	2022-08-30 12:11:16	
1001	Medical Foundation Dr	25	2022-08-30 12:11:16	
1001	Medical Foundation Dr	27	2022-08-30 12:11:16	
1001	Medical Foundation Dr	28	2022-08-30 12:11:16	
1002	Embarcadero Rd	1	2022-08-30 12:10:44	
1002	Embarcadero Rd	3	2022-08-30 12:10:44	
1002	Embarcadero Rd	9	2022-08-30 12:10:44	
1002	Embarcadero Rd	11	2022-08-30 12:10:44	
1002	Embarcadero Rd	12	2022-08-30 12:10:44	
1002	Embarcadero Rd	21	2022-08-30 12:10:44	
1002	Embarcadero Rd	24	2022-08-30 12:10:44	
1002	Embarcadero Rd	29	2022-08-30 12:10:44	
1002	Embarcadero Rd	31	2022-08-30 12:10:44	
1002	Embarcadero Rd	32	2022-08-30 12:10:44	
1009	Portage/Hansen	1	2022-05-01 18:26:20	
1009	Portage/Hansen	3	2022-05-01 18:26:20	
1009	Portage/Hansen	11	2022-05-01 18:26:20	
1009	Portage/Hansen	21	2022-05-01 18:26:20	
1009	Portage/Hansen	23	2022-05-01 18:26:20	
1009	Portage/Hansen	31	2022-05-01 18:26:20	

Figure 27. Snapshot of real-time detector data availability in the California CV Testbed.

#### 4.3.1.2 Real-time traffic signal status

As shown in Figure 28, we provide a table view of real-time intersection signal status in the California CV Testbed, which was requested at 12:55PM on 2022-08-30. Similar to real-time detector data availability, when the request to check the intersection signal status is sent, there is a function to query the database and return the information of Intersection Id, Cross-Street Name, Current Plan Id, Event Phase Id, Event Phase Status, and Last Update Time for each intersection controller. The font color of "Last Update Time" indicates different signal data availability: (i) the color is green if the gap between the "Last Update Time" and the current time is less than 15 minutes; (ii) the color changes to purple if the gap is between 15 minutes and 1 hour; (iii) the color is red if the gap is greater than 1 hour. But note that the 'Last Update Time' value may be affected by the quality of backhaul connections.

Real-Time Intersection Signal Status

Intersection ID	Cross-Street Name	Current Plan ID	Event Phase ID	Event Phase Status	Event Update Time	2022-08-30 12:59:25
1001	Medical Foundation Dr	2	12	yellow or flashing dont walk	2022-08-30 12:53:27	
1002	Embarcadero Rd	2	16	yellow or flashing dont walk	2022-08-30 12:53:31	
1003	Churchill Ave	2	5	red or solid dont walk	2022-08-30 12:53:42	
1003	Churchill Ave	2	6	green or walk	2022-08-30 12:53:42	
1004	Serra/Park	2	1	red or solid dont walk	2022-08-30 12:53:17	
1004	Serra/Park	2	2	green or walk	2022-08-30 12:53:17	
1005	Stanford Ave	2	1	red or solid dont walk	2022-08-30 12:52:17	
1005	Stanford Ave	2	2	green or walk	2022-08-30 12:52:17	
1006	Cambridge Ave	2	12	yellow or flashing dont walk	2022-08-30 12:53:20	
1006	Cambridge Ave	2	16	yellow or flashing dont walk	2022-08-30 12:53:20	
1007	S California Ave	2	12	yellow or flashing dont walk	2022-08-30 12:53:07	
1008	Page Mill Rd	255	1	green or walk	2022-08-30 12:53:35	
1008	Page Mill Rd	255	4	red or solid dont walk	2022-08-30 12:53:35	
1008	Page Mill Rd	255	5	green or walk	2022-08-30 12:53:35	
1008	Page Mill Rd	255	8	red or solid dont walk	2022-08-30 12:53:35	
1009	Portage/Hansen	2	5	red or solid dont walk	2022-05-01 18:27:11	
1009	Portage/Hansen	2	6	green or walk	2022-05-01 18:27:11	
1010	Matadero Ave	2	2	red or solid dont walk	2022-08-30 12:53:42	
1010	Matadero Ave	2	4	green or walk	2022-08-30 12:53:42	
1010	Matadero Ave	2	6	red or solid dont walk	2022-08-30 12:53:42	
1010	Matadero Ave	2	12	green or walk	2022-08-30 12:53:42	
1011	Curtner Ave	2	1	red or solid dont walk	2022-08-30 12:53:13	
1011	Curtner Ave	2	2	green or walk	2022-08-30 12:53:13	

Figure 28. Snapshot of real-time intersection signal status in the California CV Testbed.

### 4.3.2 Detector data analysis

As shown in Figure 13, the second analysis level is to analyze the aggregated data from the available devices. For loop detectors, we analyze the quality of the aggregated data and help identify bad detectors in the testbed.

### 4.3.2.1 Detector layout and inventory

To better understand the characteristics and quality of the aggregated detector data, we extract the information from the static timing sheet (pdf file) from Caltrans and provide an intuitive way to visualize the detector locations and the corresponding signal control settings (e.g., assigned phases).

In Figure 29, we provide an example of the detector layout at Intersection 1002 (Embarcadero /Galvez @ El Camino Real). The detector locations are identified according to the outdated detector layout (pdf file) from Caltrans, with additional help using the Street Views function in Google Maps. The number inside the green box stands for the assigned detector id. When we see a detector in the field (from the Street Views in Google Maps) but there is no detector id assigned to it, we will use a yellow box with a question mark "?" inside to indicate an unknown detector id. The string next to the green box, e.g., "2I2U" for Detector 3, has special meanings: (i) the first character stands for the assigned phase (e.g., Detector 3 is assigned to phase 2); (ii) the rest of the characters stands for the corresponding slot id in the controller (e.g., Detector 3 is connected to Slot I2U in the controller).

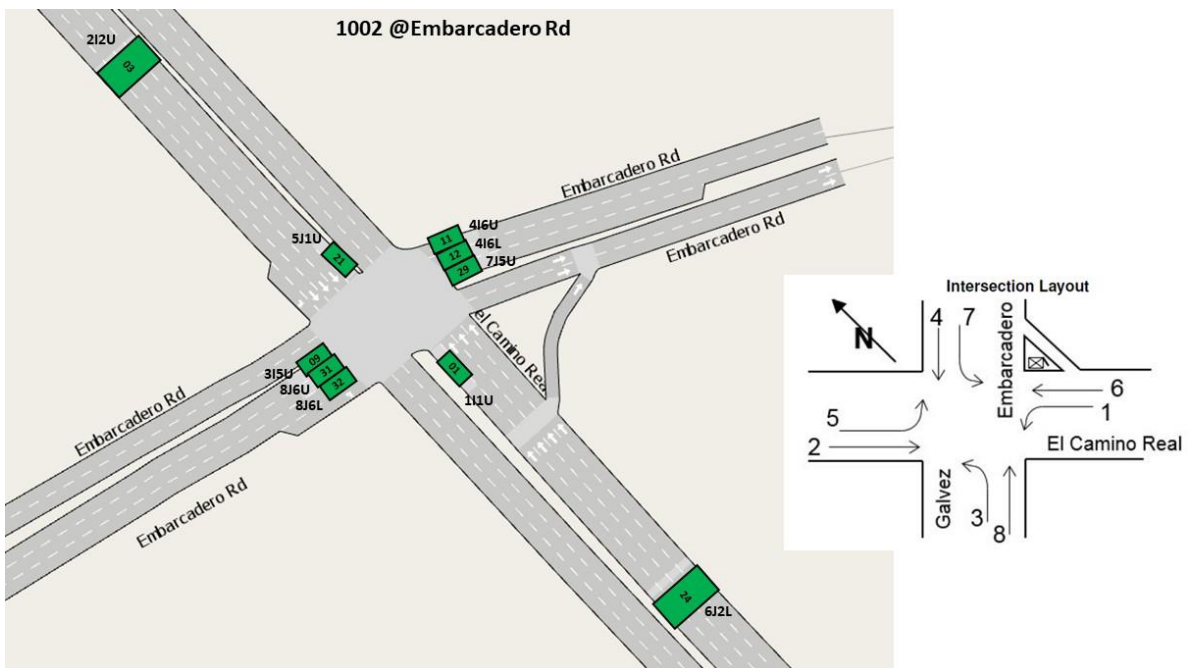


Figure 29. Example of detector layout at Intersection 1002.

Furthermore, we provide a table view of detector inventory at the targeted intersection. As an example, we provide the detector inventory at Intersection 1002 in Figure 30. For each detector, we provide information that includes intersection id, detector id, intersection name, system detector index, detector type, detector description, and assigned signal phase. This information is obtained from field controllers and stored in our database. Therefore, we can validate the information provided in the detailed detector layout and in the detector inventory to make sure they are consistent.

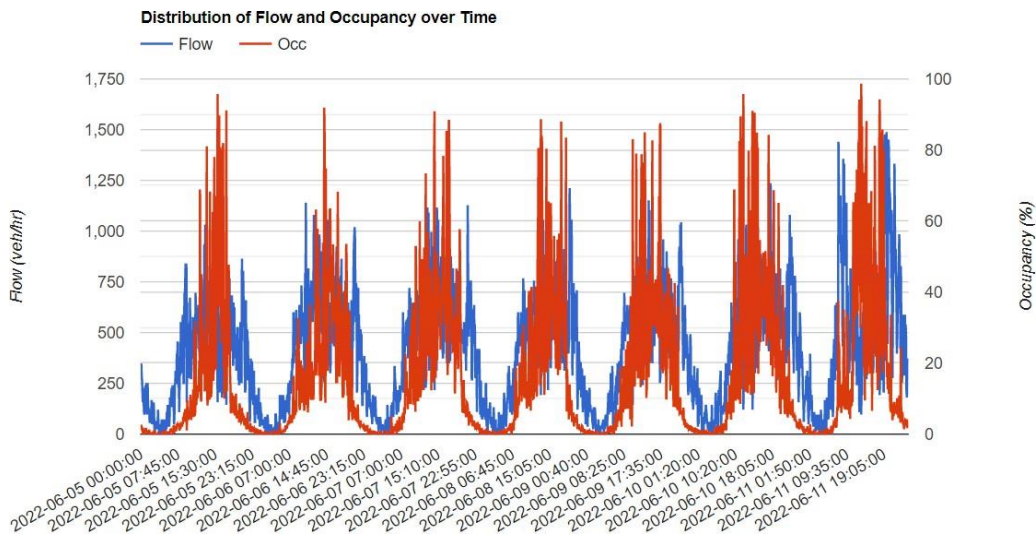
Intersection ID	Detector ID	Intersection Name	System Detector Index	Detector Type	Detector Description	Assigned Phase
1002	1	Embarcadero Rd	1	6	Count + Call + Extend	1
1002	3	Embarcadero Rd	2	6	Count + Call + Extend	2
1002	9	Embarcadero Rd	5	6	Count + Call + Extend	3
1002	11	Embarcadero Rd	6	6	Count + Call + Extend	4
1002	12	Embarcadero Rd	7	6	Count + Call + Extend	4
1002	21	Embarcadero Rd	9	6	Count + Call + Extend	5
1002	24	Embarcadero Rd	10	6	Count + Call + Extend	6
1002	29	Embarcadero Rd	13	6	Count + Call + Extend	7
1002	31	Embarcadero Rd	14	6	Count + Call + Extend	8
1002	32	Embarcadero Rd	15	6	Count + Call + Extend	8

Figure 30. Example of detector inventory at Intersection 1002.

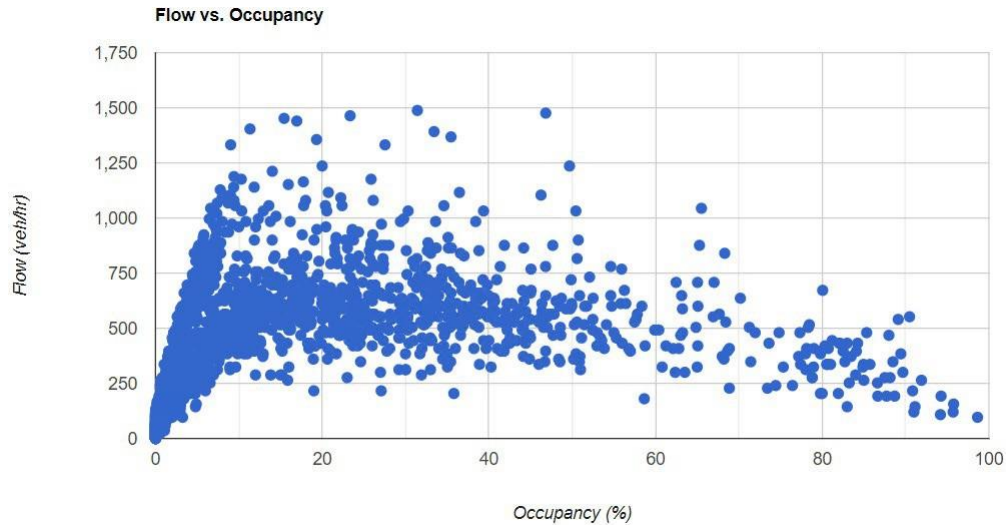
#### 4.3.2.2 Detector aggregated data

As mentioned in previous subsections, we developed algorithms to aggregate the raw detector data into fixed time intervals. We also provided an example in Figure 29 to show different types of detectors (e.g., advance vs. stopbar) are installed at different locations to facilitate with the actuated traffic control.

From the aggregated data, we do find different types of detectors exhibit different characteristics in the flow-occupancy plots. For example, in Figure 31, we provide an example of aggregated data from an advance detector, Detector 3 at Intersection 1002, between 2022-06-05 and 2022-06-11. As shown in the temporal distribution in Figure 31 (a), the flow and occupancy measurements exhibit a very clear day-to-day cyclic pattern. We do see heavy congestion occurring at the corresponding intersection approach where the detector is located as high occupancy values are seen both in the temporal distribution (Figure 31 (a)) and in the flow-occupancy plot (Figure 31 (b)). Also, in Figure 31 (b), it clearly shows a trapezoidal shape between flow and occupancy, which is consistent with the theory in Figure 22.



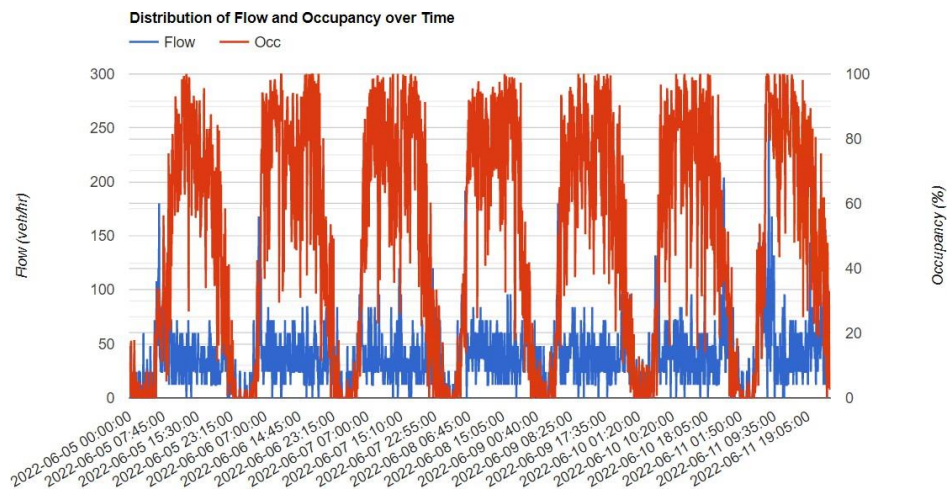
(a) Temporal distribution



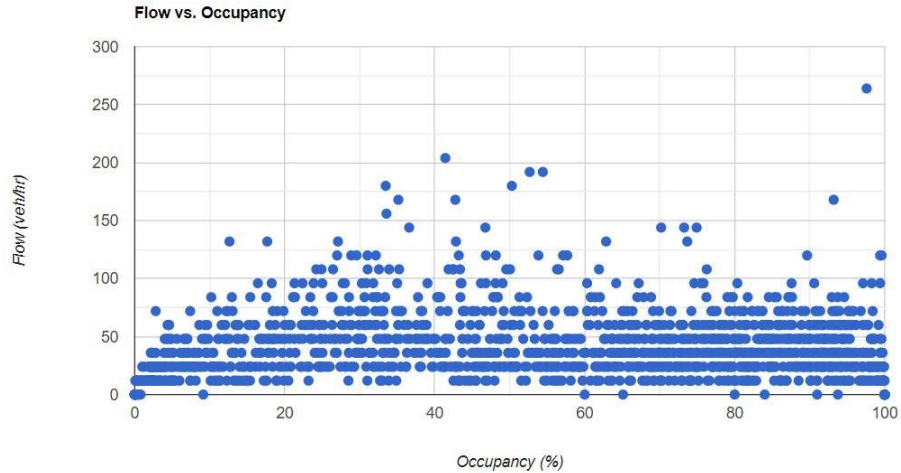
(b) Flow -- occupancy plot

Figure 31. Example of aggregated data from and advance detector (Detector 3 at Intersection 1002).

Different from the advance detector shown in Figure 31, the flow and occupancy data from a stopbar detector exhibits a significantly different pattern. In Figure 32, we provide an example of the aggregated data from a stopbar detector, Detector 1 at Intersection 1002, between 2022-06-05 and 2022-06-11. As shown in the figure, the occupancies measured from the stopbar detector are much higher than those from the advance detector in Figure 31. These high occupancies are caused by the vehicles that have to wait on top of the stopbar detector for the next green time. Unlike the trapezoidal shape of the flow-occupancy plot in Figure 31 (b), the flow-occupancy measurements from the stopbar detector scatter over the whole space below the trapezoidal fundamental diagram in Figure 22. Note that a stopbar detector normally consists of three or more loops, and therefore, its reported flow values are usually undercounted, especially when traffic is congested.



(a) Temporal distribution



(b) Flow – occupancy plot

Figure 32. Example of aggregated data from a stopbar detector (Detector 1 at Intersection 1002).

### 4.3.2.3 Detector filtered data

As mentioned previously, in our current system design we only apply simple moving averages to filter out bad data, e.g., measurements with high flow values or inconsistent values. Besides Figure 18, we provide an additional example of data filtering for Detector 24 at Intersection 1006 on 2022-06-11 in Figure 33.

As shown in the figure, the data filtering algorithm corrected the inconsistent values which occurred in the early morning between 12AM and 6AM. It also corrected the high values which occurred at the morning peak around 9AM.

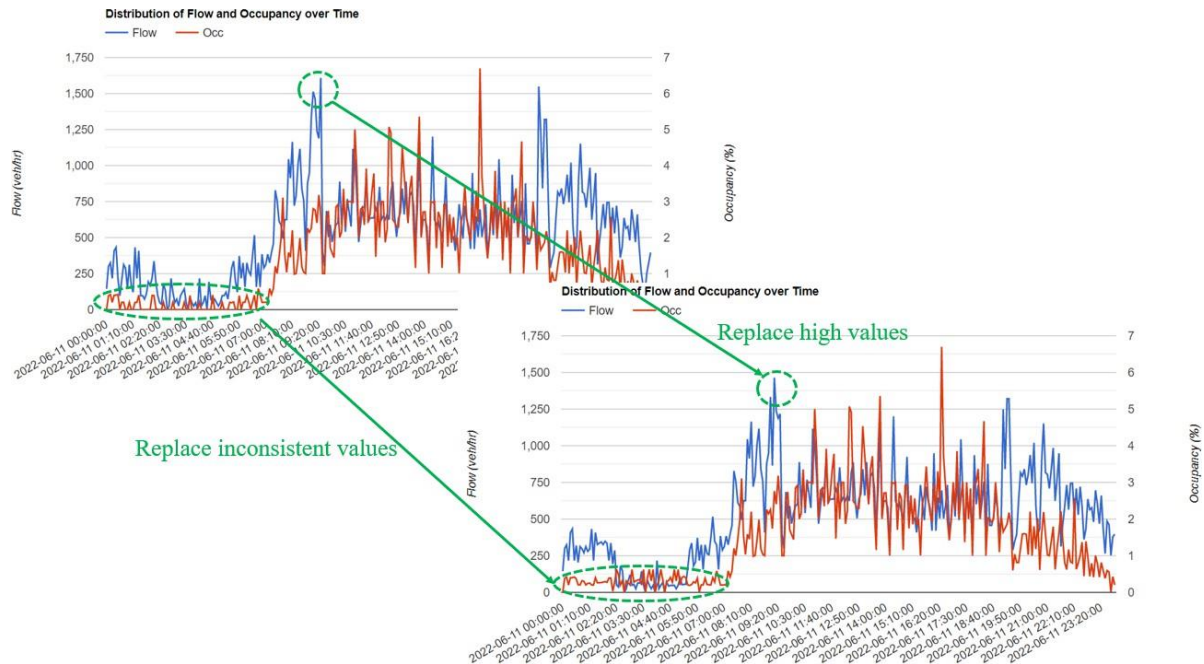


Figure 33. Example of data filtering for Detector 24 at Intersection 1006 on 2022-06-11.

### 4.3.2.4 Detector-level health analysis

As mentioned previously, we applied the following parameter settings to the detector health analysis in the California CV Testbed:

- $\epsilon_{\text{MINIMUM}} = 10\%$
- $f_{\text{MINIMUM}} = 150 \text{ veh/hr}$
- $\epsilon_{\text{HEMMINIMUM}} = 10\%$
- $tt_1 = 6\text{AM}$
- $tt_2 = 10\text{PM}$
- $\epsilon_{\text{ZZZZMINIMUM}} = 4\text{s}$
- $\epsilon_{\text{IIIIZZMINIMUM}} = 10\%$

This analysis is done on a daily basis. As shown in Figure 34, for each detector we provide a detailed report on the missing rate, the high value rate, the max period of zero values, the inconsistent rate, and the existence of non-zero constant values.

Detector Health								
Intersection ID	Detector ID	Selected Date	Missing Rate(%)	High Value(%)	Constant Value(Y/N)	Max Period of Zero Values(hr)	Rate of Inconsistent Values(%)	Health (Good/Bad)
1002	3	2022-06-05	0	0	N	0	1.389	Good
1002	3	2022-06-06	3.125	0	N	0	0.694	Good
1002	3	2022-06-07	1.736	0	N	0	1.042	Good
1002	3	2022-06-08	10.417	0	N	0	0.347	Bad
1002	3	2022-06-09	5.903	0	N	0	0.347	Good
1002	3	2022-06-10	5.208	0	N	0	0	Good
1002	3	2022-06-11	7.292	0	N	0	2.083	Good

Figure 34. Example of health analysis report for Detector 3 at Intersection 1002 between 2022-06-05 and 2022-06-11.

This health analysis report can help identify bad detectors and fix potential issues that lead to poor data quality. In the California CV Testbed, the main issue for most bad detectors is they keep reporting long periods of zero values, for example, Detector 31 at Intersection 1002 in Figure 35. We also find that some detectors keep reporting high percentages of inconsistent values, for example, Detector 4 at Intersection 1006 as shown in Figure 36. In addition, we occasionally find detectors reporting high missing rates, for example, Detector 3 at Intersection 1011 in Figure 37. However, we do not find detectors that keep reporting high percentages of high values and non-zero constant values in the California CV Testbed.

Detector Health								
Intersection ID	Detector ID	Selected Date	Missing Rate(%)	High Value(%)	Constant Value(Y/N)	Max Period of Zero Values(hr)	Rate of Inconsistent Values(%)	Health (Good/Bad)
1002	31	2022-06-05	0	0	N	16	0	Bad
1002	31	2022-06-06	3.125	0	N	15.25	0	Bad
1002	31	2022-06-07	1.736	0	N	15.583	0	Bad
1002	31	2022-06-08	10.417	0	N	13.5	0	Bad
1002	31	2022-06-09	5.903	0	N	14.583	0	Bad
1002	31	2022-06-10	5.208	0	N	14.75	0	Bad
1002	31	2022-06-11	7.292	0	N	14.25	0	Bad

Figure 35. Example of bad detectors reporting long periods of zero values.

Detector Health								
Intersection ID	Detector ID	Selected Date	Missing Rate(%)	High Value(%)	Constant Value(Y/N)	Max Period of Zero Values(hr)	Rate of Inconsistent Values(%)	Health (Good/Bad)
1006	4	2022-06-05	0	0	N	0.083	29.514	Bad
1006	4	2022-06-06	0	0	N	0	12.847	Bad
1006	4	2022-06-07	0	0	N	0	20.833	Bad
1006	4	2022-06-08	0	0	N	0.083	20.139	Bad
1006	4	2022-06-09	0	0	N	0	19.097	Bad
1006	4	2022-06-10	0	0	N	0	17.361	Bad
1006	4	2022-06-11	0	0	N	0	16.667	Bad

Figure 36. Example of bad detectors reporting high percentages of inconsistent values.

Detector Health								
Intersection ID	Detector ID	Selected Date	Missing Rate(%)	High Value(%)	Constant Value(Y/N)	Max Period of Zero Values(hr)	Rate of Inconsistent Values(%)	Health (Good/Bad)
1011	3	2022-06-05	9.375	0.347	N	0	1.042	Good
1011	3	2022-06-06	0	0.347	N	0	3.125	Good
1011	3	2022-06-07	12.847	8.333	N	0	4.514	Bad
1011	3	2022-06-08	0	8.333	N	0	4.861	Good
1011	3	2022-06-09	0	2.431	N	0	1.042	Good
1011	3	2022-06-10	23.264	3.472	N	0	3.125	Bad
1011	3	2022-06-11	22.917	2.431	N	0	2.778	Bad

Figure 37. Example of bad detectors reporting high missing rates.

### 4.3.2.5 Intersection-level health analysis

Besides the detector-level health analysis, we further provide functions to aggregate the detector health metrics into the intersection level. For example, in Figure 38 we provide an example of intersection-level health metrics for Intersection 1002 between 2022-06-05 and 2022-06-11. In the figure, the values from column 3 to column 8 are averaged over all detectors belonging to the same intersection, i.e., Intersection 1002. As shown in the figure, Intersection 1002 had good sensor performance during the analysis period. Two major issues are identified for the detectors at Intersection 1002: (i) high data missing rates; and (ii) some detectors reporting long periods of zero values.

Average Detector Health							
Intersection ID	Selected Date	Avg. Health Rate(%)	Avg. Rate of Missing values (%)	Avg. Rate of High Values (%)	Avg. % of Constant Values	Avg. Max Period of Zero Values (hr)	Avg. Rate of Inconsistent Values (%)
1002	2022-06-05	90	0	0	0	1.683	0.278
1002	2022-06-06	90	3.125	0	0	1.692	0.278
1002	2022-06-07	90	1.736	0	0	1.75	0.174
1002	2022-06-08	0	10.417	0	0	1.375	0.313
1002	2022-06-09	90	5.903	0	0	1.475	0.139
1002	2022-06-10	90	5.208	0	0	1.517	0.139
1002	2022-06-11	90	7.292	0	0	1.467	0.417

Figure 38. Example of intersection-level health metrics for Intersection 1002.

Furthermore, we can aggregate the detector-level health metrics into the corridor level. For example, in Figure 39 we provide an example of the corridor-level health metrics for all detectors in the California CV Testbed. As shown in the figure, the sensor performance in the California CV Testbed was moderate, in which the average health rate was between 60% and 75%. Three issues are identified from the results shown in Figure 39: (i) there were high missing rates on some of the days (e.g., on 2022-06-08) due to an unstable data feed; (ii) there exist a significant portion of detectors reporting long periods of zero values; (iii) there exist some detectors reporting high percentages of inconsistent values.

Average Detector Health							
Intersection ID	Selected Date	Avg. Health Rate(%)	Avg. Rate of Missing values (%)	Avg. Rate of High Values (%)	Avg. % of Constant Values	Avg. Max Period of Zero Values (hr)	Avg. Rate of Inconsistent Values (%)
all	2022-06-05	73.118	0.202	0.011	0	3.835	1.484
all	2022-06-06	74.194	0.168	0.049	0	3.849	1.128
all	2022-06-07	65.054	2.04	0.118	0	3.824	1.148
all	2022-06-08	61.828	4.945	0.138	0	3.778	1.128
all	2022-06-09	72.581	0.317	0.065	0	3.845	1.113
all	2022-06-10	71.505	0.78	0.082	0	3.767	1.042
all	2022-06-11	72.043	0.885	0.054	0	3.815	1.165

Figure 39. Example of corridor-level health metrics for all detectors in the California CV Testbed.

### 4.3.3 Signal phase data analysis

Once we aggregate the event-based signal phase data into cycle-based, we provide the following metrics to help understand the performance of intersection signals: (i) phase duration statistics, (ii) phase gap-out/max-out statistics, and (iii) pedestrian phase duration statistics.

#### 4.3.3.1 Signal timing inventory

To help better understand and analyze the aggregated (cycle-based) signal phase data, we provide the signal timing inventory for each intersection, which includes the ring-barrier-phase settings, the coordination plans, and the phase settings. In Figure 40, we provide an example of ring-barrier-phase settings for different timing plans at Intersection 1013. From the figure, we find that phase 1 is a lagging phase for all coordination plans, and phase 7 is a lagging phase for coordination plan 2. In Figure 41, we provide an example of coordination plans for Intersection 1013. For each coordination plan, the information of synchronized phase, lag phase, green time and forced-off point is provided for each phase. In Figure 42, we provide details settings of Walk, Don't Walk, Min Green, Max Initial, Max Green #1 to #3, Extension, Min Gap, Max Gap, Yellow Time, and All-Red Time for each phase.

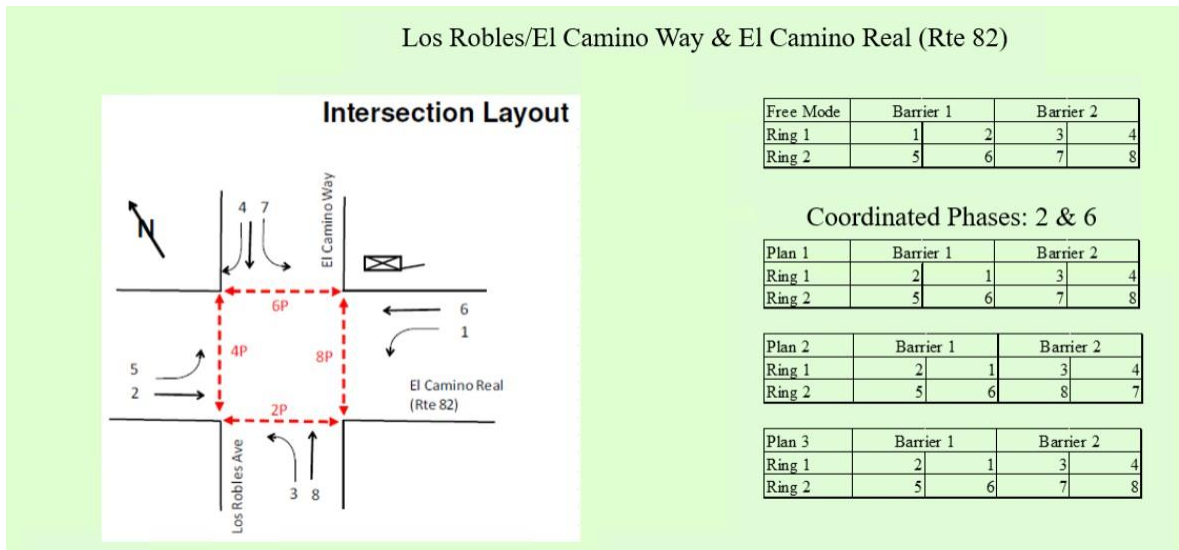


Figure 40. Example of ring-barrier-phase settings for different timing plans at Intersection 1013.

Settings	Phase 1	Phase 2	Phase 3	Phase 4	Phase 5	Phase 6	Phase 7	Phase 8
Sync Phase(Yes:1/No:0)	0	1	0	0	0	1	0	0
Lag Phase(Yes:1/No:0)	1	0	0	1	0	1	0	1
Green Time(s)	20	55	18	42	20	56	18	42
Forced Off Point(s)	25	0	47	92	116	0	47	92

Settings	Phase 1	Phase 2	Phase 3	Phase 4	Phase 5	Phase 6	Phase 7	Phase 8
Sync Phase(Yes:1/No:0)	0	1	0	0	0	1	0	0
Lag Phase(Yes:1/No:0)	1	0	0	1	0	1	1	0
Green Time(s)	17	48	17	42	20	46	17	42
Forced Off Point(s)	22	0	43	88	113	0	89	68

Settings	Phase 1	Phase 2	Phase 3	Phase 4	Phase 5	Phase 6	Phase 7	Phase 8
Sync Phase(Yes:1/No:0)	0	1	0	0	0	1	0	0
Lag Phase(Yes:1/No:0)	1	0	0	1	0	1	0	1
Green Time(s)	22	53	18	42	25	51	18	42
Forced Off Point(s)	27	0	49	94	123	0	49	94

Figure 41. Example of coordination plans for Intersection 1013.

Settings	Phase 1	Phase 2	Phase 3	Phase 4	Phase 5	Phase 6	Phase 7	Phase 8
Walk(s)	0	7	0	5	0	7	0	5
Don't Walk(s)	0	22	0	37	0	22	0	31
Min Green(s)	12	10	12	15	12	10	12	15
Max Initial(s)	0	20	0	0	0	20	0	0
Max Green#1(s)	18	30	2	2	21	30	18	16
Max Green#2(s)	0	0	0	0	0	0	0	0
Max Green#3(s)	0	0	0	0	0	0	0	0
Extension(s)	1	2.5	1	1.5	1	2.5	1	1
Max Gap(s)	2	4	2	2	2	4	2	2
Min Gap(s)	1	2.5	1	1.5	1	2.5	1	1
Yellow Time(s)	4	4	3	3	3	4	3	3
All Red Time(s)	0	0	0	1	0	0	0	1

Figure 42. Example of phase settings at Intersection 1013.

#### 4.3.3.2 Phase duration statistics

Once the signal phase data is aggregated into cycle-based, we can visualize the actual phase green times to get a closer look on how the actual signal control system works. Especially with the information from Figure 40, Figure 41, and Figure 42, we are able to tell what happened to each phase in each cycle. As an example, we provide both the temporal distribution and the table view of phase durations for coordination plan 2 at Intersection 1013 between 9AM and 10AM on 2022-06-07 in Figure 43 and Figure 44, respectively. The Max-Out periods are also highlighted in Figure 44. According to Figure 40, phase 1 in coordination plan 2 is a lagging phase, which will be forced-off for traffic coordination. As a result, we can see in Figure 43 and Figure 44 phase 1 was capped at the max value of 17 seconds, which is the green time shown in Figure 41. Furthermore, we observe there are cycles with a duration of 42 seconds for phase 4 and a duration of 36 seconds for phase 8. These are the max-out periods for phase 4 and phase 8 caused by the pedestrian calls, which can be validated by adding the “Walk” and “Don’t Walk” times together in Figure 42.

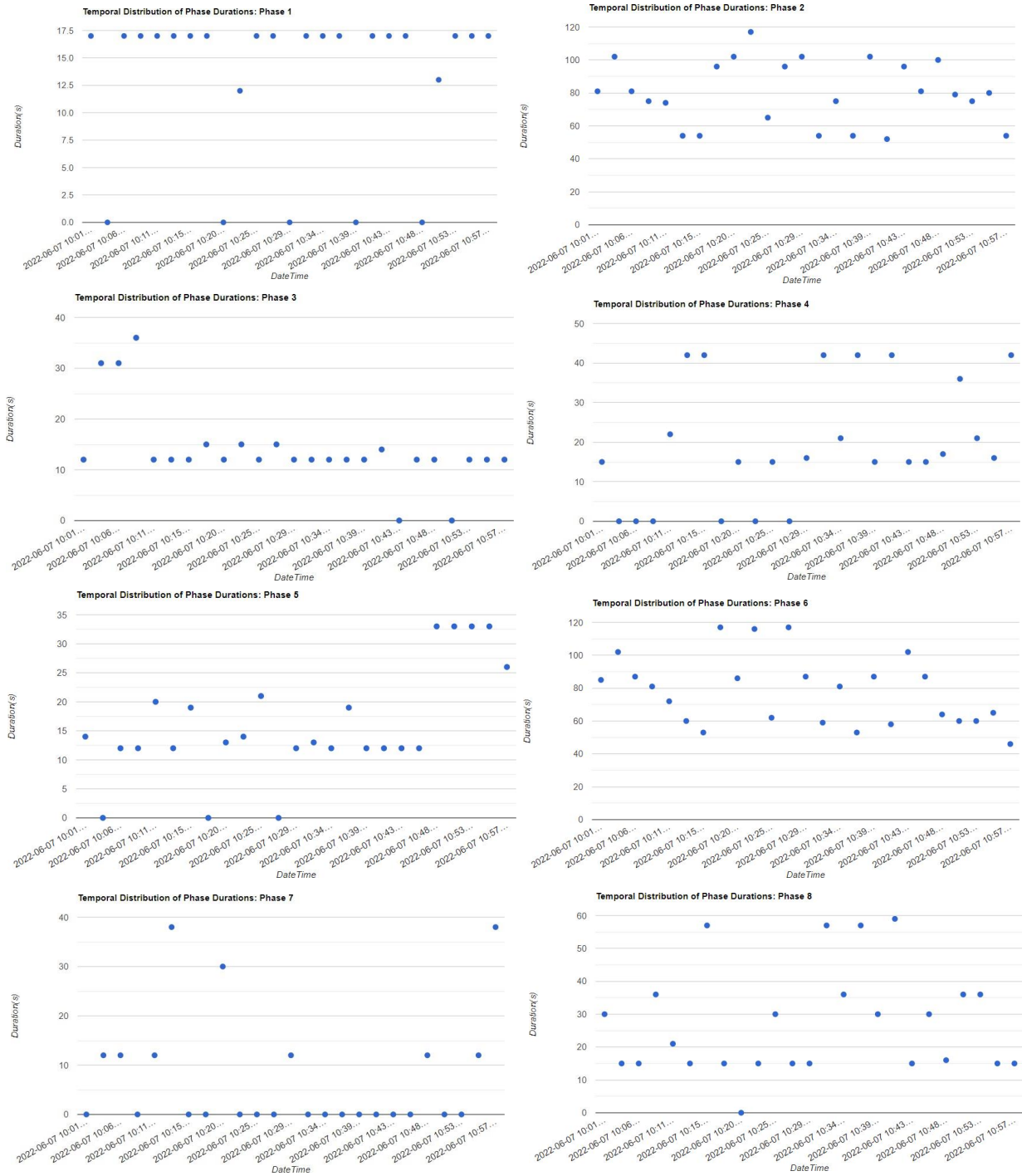


Figure 43. Temporal distribution of phase durations for coordination plan 2 at Intersection 1013 between 9AM and 10AM on 2022-06-07.

Intersection ID	Cycle End Datetime	Plan Id	Cycle Length(s)	Ph1(s)	Ph2(s)	Ph3(s)	Ph4(s)	Ph5(s)	Ph6(s)	Ph7(s)	Ph8(s)
1013	6/7/2022 10:01:41	2	140	17	81	12	15	14	85	0	30
1013	6/7/2022 10:04:01	2	140	0	102	31	0	0	102	12	15
1013	6/7/2022 10:06:21	2	140	17	81	31	0	12	87	12	15
1013	6/7/2022 10:08:41	2	140	17	75	36	0	12	81	0	36
1013	6/7/2022 10:11:01	2	140	17	74	12	22	20	72	12	21
1013	6/7/2022 10:13:21	2	140	17	54	12	42	12	60	38	15
1013	6/7/2022 10:15:41	2	140	17	54	12	42	19	53	0	57
1013	6/7/2022 10:18:01	2	140	17	96	15	0	0	117	0	15
1013	6/7/2022 10:20:21	2	140	0	102	12	15	13	86	30	0
1013	6/7/2022 10:22:57	2	156	12	117	15	0	14	116	0	15
1013	6/7/2022 10:25:01	2	124	17	65	12	15	21	62	0	30
1013	6/7/2022 10:27:21	2	140	17	96	15	0	0	117	0	15
1013	6/7/2022 10:29:42	2	141	0	102	12	16	12	87	12	15
1013	6/7/2022 10:32:02	2	140	17	54	12	42	13	59	0	57
1013	6/7/2022 10:34:22	2	140	17	75	12	21	12	81	0	36
1013	6/7/2022 10:36:42	2	140	17	54	12	42	19	53	0	57
1013	6/7/2022 10:39:02	2	140	0	102	12	15	12	87	0	30
1013	6/7/2022 10:41:22	2	140	17	52	14	42	12	58	0	59
1013	6/7/2022 10:43:42	2	140	17	96	0	15	12	102	0	15
1013	6/7/2022 10:46:02	2	140	17	81	12	15	12	87	0	30
1013	6/7/2022 10:48:22	2	140	0	100	12	17	33	64	12	16
1013	6/7/2022 10:50:42	2	140	13	79	0	36	33	60	0	36
1013	6/7/2022 10:53:02	2	140	17	75	12	21	33	60	0	36
1013	6/7/2022 10:55:22	2	140	17	80	12	16	33	65	12	15
1013	6/7/2022 10:57:42	2	140	17	54	12	42	26	46	38	15

Figure 44. Table view of phase durations for coordination plan 2 at Intersection 1013 between 10AM and 11AM on 2022-06-07.

#### 4.3.3.3 Phase gap-out/max-out statistics

For actuated traffic control, phase gap-out will occur if the corresponding traffic demand is low with large vehicle gaps. However, it is different for phase max-out, which can be caused by two different cases. The first case is the corresponding traffic demand is high and the allocated phase green time is not long enough to clear the vehicle queue and accommodate the upstream vehicle arrivals. The second case is there are pedestrian calls for that phase. For example, as shown in Figure 40, phase 4 will max out if there are pedestrian calls for pedestrian phase 4.

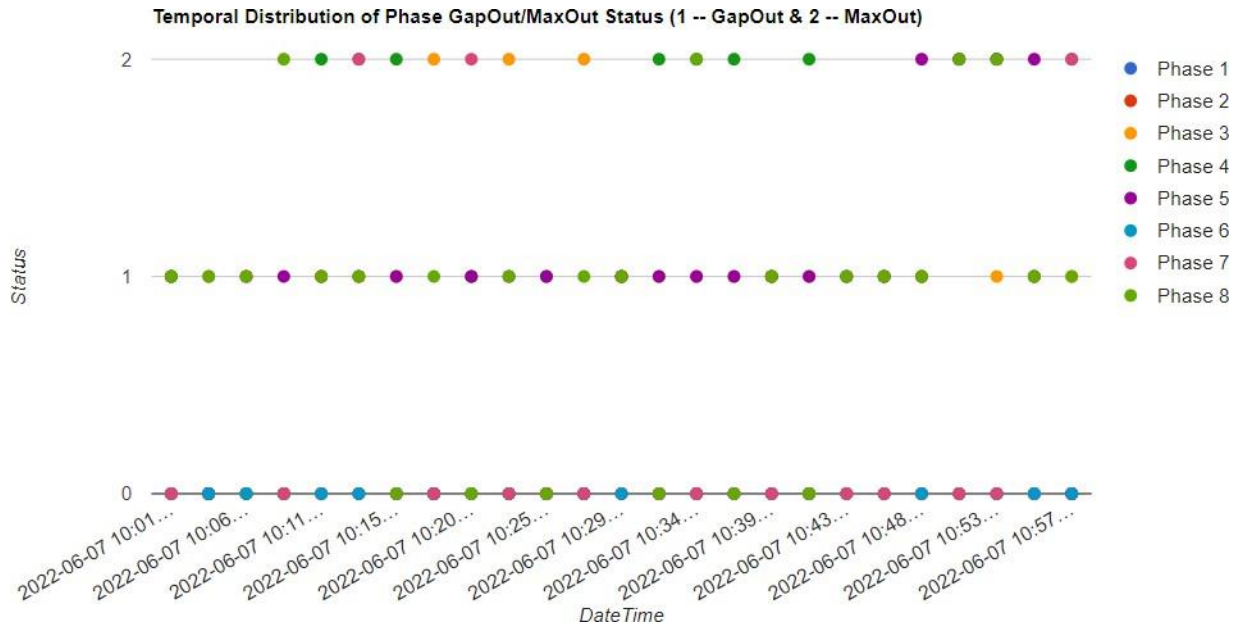
As an example, we further provide a table view and a plot view of phase Gap-Out/Max-Out/Forced-Off for coordination plan 2 at Intersection 1013 between 10AM and 11AM on 2022-06-07, in Figure 45 and Figure 46, respectively. In addition, the same Max-Out periods are highlighted in Figure 44 for reference. As shown in Figure 40, Figure 45 and Figure 46, phases 1, 2 and 6 were forced off because phase 1 is the lagging phase and phases 2 and 6 are the coordinated phases in the coordination plan 2. Phases 4 and 8 were maxed out more often due to the pedestrian calls, which can be validated through the phase green durations listed in Figure 44. But for phases 3, and 7, they were maxed out in some cycles, which may be caused by

high left turn traffic demand and need to be further confirmed with the traffic measurements (e.g., flow count and occupancy) from associated loop detectors.

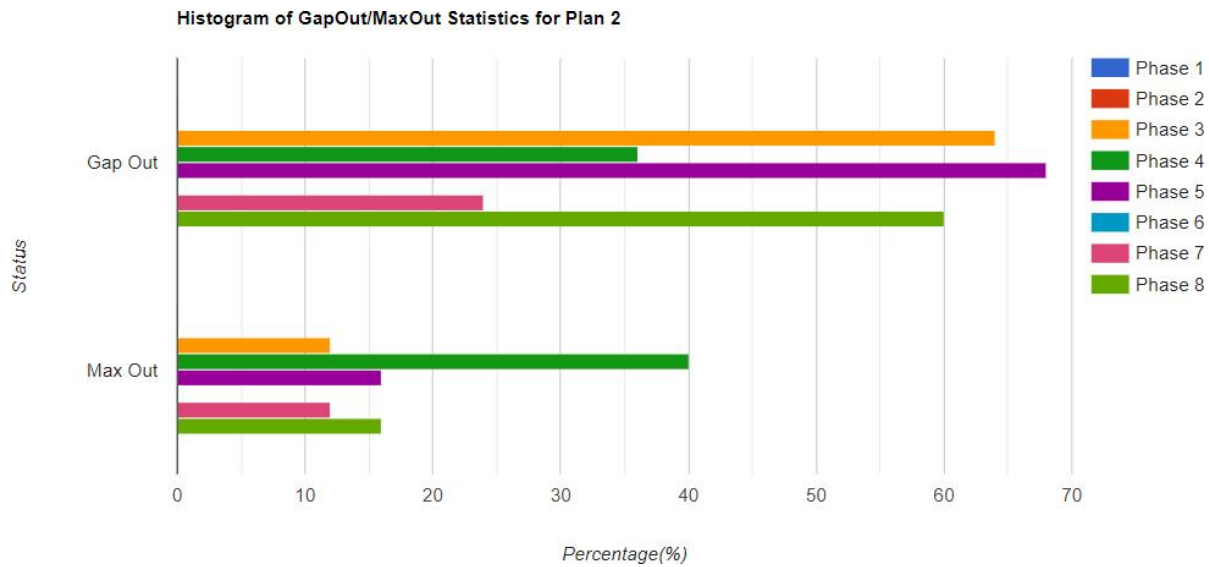
Phase GapOut/MaxOut Statistics  
(GO: GapOut & MO: MaxOut & FO: ForcedOff)

Intersection ID	Cycle End Datetime	Plan Id	Cycle Length(s)	Ph1	Ph2	Ph3	Ph4	Ph5	Ph6	Ph7	Ph8
1013	2022-06-07 10:01:41	2	140	FO	FO	GO	GO	GO	FO	--	GO
1013	2022-06-07 10:04:01	2	140	FO	FO	FO	--	--	FO	GO	GO
1013	2022-06-07 10:06:21	2	140	FO	FO	FO	--	GO	FO	GO	GO
1013	2022-06-07 10:08:41	2	140	FO	FO	FO	--	GO	FO	--	MO
1013	2022-06-07 10:11:01	2	140	FO	FO	GO	MO	GO	FO	GO	GO
1013	2022-06-07 10:13:21	2	140	FO	FO	GO	MO	GO	FO	MO	GO
1013	2022-06-07 10:15:41	2	140	FO	FO	GO	MO	GO	FO	--	FO
1013	2022-06-07 10:18:01	2	140	FO	FO	MO	--	--	FO	--	GO
1013	2022-06-07 10:20:21	2	140	FO	FO	GO	GO	GO	FO	MO	--
1013	2022-06-07 10:22:57	2	156	FO	FO	MO	--	GO	FO	--	GO
1013	2022-06-07 10:25:01	2	124	FO	FO	FO	GO	GO	FO	--	FO
1013	2022-06-07 10:27:21	2	140	FO	FO	MO	--	--	FO	--	GO
1013	2022-06-07 10:29:42	2	141	FO	FO	GO	GO	GO	FO	GO	GO
1013	2022-06-07 10:32:02	2	140	FO	FO	GO	MO	GO	FO	--	FO
1013	2022-06-07 10:34:22	2	140	FO	FO	GO	MO	GO	FO	--	MO
1013	2022-06-07 10:36:42	2	140	FO	FO	GO	MO	GO	FO	--	FO
1013	2022-06-07 10:39:02	2	140	FO	FO	GO	GO	GO	FO	--	GO
1013	2022-06-07 10:41:22	2	140	FO	FO	GO	MO	GO	FO	--	FO
1013	2022-06-07 10:43:42	2	140	FO	FO	--	GO	GO	FO	--	GO
1013	2022-06-07 10:46:02	2	140	FO	FO	GO	GO	GO	FO	--	GO
1013	2022-06-07 10:48:22	2	140	FO	FO	GO	GO	MO	FO	GO	GO
1013	2022-06-07 10:50:42	2	140	FO	FO	--	MO	MO	FO	--	MO
1013	2022-06-07 10:53:02	2	140	FO	FO	GO	MO	MO	FO	--	MO
1013	2022-06-07 10:55:22	2	140	FO	FO	GO	GO	MO	FO	GO	GO
1013	2022-06-07 10:57:42	2	140	FO	FO	GO	MO	FO	FO	MO	GO

Figure 45. Table view of phase Gap-Out/Max-Out/Forced-Off for coordination plan 2 at Intersection 1013 between 10AM and 11AM on 2022-06-07.



(a) Temporal distribution



(b) Histogram distribution

Figure 46. Plot view of phase Gap-Out/Max-Out/Forced-Off for coordination plan 2 at Intersection 1013 between 10AM and 11AM on 2022-06-07

#### 4.3.3.4 Pedestrian phase duration statistics

As shown in previous figures, the activation of a pedestrian phase (e.g., pedestrian phase 4) will cause the corresponding vehicle phase (e.g., phase 4) to max out. In order to identify whether a max-out is caused by heavy traffic demand or by pedestrian calls, it is necessary to provide functions to visualize the pedestrian activities (e.g., pedestrian phase durations) for each signal cycle. As an example, in Figure 47 we provide a table view of pedestrian phase durations for coordination plan 2 at Intersection 1013 between 10AM and

11AM on 2022-06-07. In the figure, the pedestrian phases with a non-zero duration are highlighted in yellow. From the figure, we do notice that there existed high pedestrian demand for pedestrian phase 2 since it was often activated with a maximum duration of 29 seconds (i.e., Walk for 7 seconds and Don't Walk for 22 seconds as shown in Figure 42). We also notice that when pedestrian phase 4 was activated with a maximum duration of 42 seconds (i.e., Walk for 5 seconds and Don't Walk for 37 seconds as shown in Figure 42), the corresponding vehicle phase 4 was maxed out (shown in Figure 45) with a maximum duration of 42 seconds (shown in Figure 44).

Intersection ID	Cycle End Datetime	Plan Id	Cycle Length(s)	Ped Ph1(s)	Ped Ph2(s)	Ped Ph3(s)	Ped Ph4(s)	Ped Ph5(s)	Ped Ph6(s)	Ped Ph7(s)	Ped Ph8(s)
1013	6/7/2022 10:01:41	2	140	0	0	0	0	0	0	0	0
1013	6/7/2022 10:04:01	2	140	0	29	0	0	0	0	0	0
1013	6/7/2022 10:06:21	2	140	0	0	0	0	0	0	0	0
1013	6/7/2022 10:08:41	2	140	0	29	0	0	0	0	0	36
1013	6/7/2022 10:11:01	2	140	0	0	0	0	0	0	0	0
1013	6/7/2022 10:13:21	2	140	0	29	0	42	0	0	0	0
1013	6/7/2022 10:15:41	2	140	0	29	0	42	0	0	0	0
1013	6/7/2022 10:18:01	2	140	0	29	0	0	0	0	0	0
1013	6/7/2022 10:20:21	2	140	0	0	0	0	0	0	0	0
1013	6/7/2022 10:22:57	2	156	0	0	0	0	0	0	0	0
1013	6/7/2022 10:25:01	2	124	0	0	0	0	0	0	0	0
1013	6/7/2022 10:27:21	2	140	0	0	0	0	0	0	0	0
1013	6/7/2022 10:29:42	2	141	0	29	0	0	0	0	0	0
1013	6/7/2022 10:32:02	2	140	0	29	0	42	0	0	0	0
1013	6/7/2022 10:34:22	2	140	0	0	0	0	0	0	0	36
1013	6/7/2022 10:36:42	2	140	0	29	0	42	0	0	0	0
1013	6/7/2022 10:39:02	2	140	0	0	0	0	0	0	0	0
1013	6/7/2022 10:41:22	2	140	0	29	0	42	0	29	0	0
1013	6/7/2022 10:43:42	2	140	0	0	0	0	0	0	0	0
1013	6/7/2022 10:46:02	2	140	0	0	0	0	0	0	0	0
1013	6/7/2022 10:48:22	2	140	0	0	0	0	0	29	0	0
1013	6/7/2022 10:50:42	2	140	0	0	0	0	0	0	0	36
1013	6/7/2022 10:53:02	2	140	0	0	0	0	0	29	0	36
1013	6/7/2022 10:55:22	2	140	0	0	0	0	0	0	0	0
1013	6/7/2022 10:57:42	2	140	0	29	0	42	0	29	0	0

Figure 47. Table view of pedestrian phase durations for coordination plan 2 at Intersection 1013 between 10AM and 11AM on 2022-06-07.

### 4.3.4 Traffic performance

With both detector and signal phase data available, we can better assess the traffic performance at signalized road intersections. In this subsection, we provide options to visualize the coordination performance along an arterial corridor and the estimated traffic states at each intersection approach.

#### 4.3.4.1 Coordination analysis

Along a coordinated arterial corridor, when the coordination is good, we should expect low occupancies from the advance detectors in the upstream of each intersection approach. However, as the coordination starts to degrade, we should expect the occupancies from the advance detectors shift to the right in the flow-occupancy plots, which indicates traffic congestion starts to build up. For example, during an AM peak period, traffic coordination may start to degrade due to the increasing traffic demand, e.g., the offsets between adjacent intersections are no longer appropriate to accommodate vehicle platoons from upstream. In this case, the reflection on the flow-occupancy plot in Figure 48 can be Point A shifting to Point B with a higher occupancy and probably a lower flow rate. In contrast, if the coordination improves as the traffic demand decreases, e.g., the offsets between adjacent intersections are relatively appropriate to accommodate the upstream vehicle platoons, the reflection on the flow-occupancy plot in Figure 48 can be Point A shifting to Point C with a lower occupancy and probably a higher flow rate.

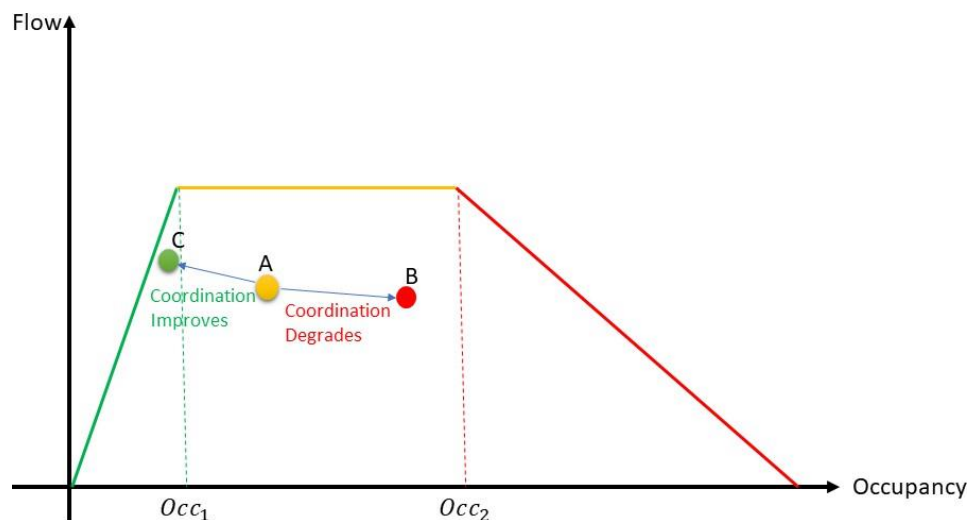


Figure 48. Impacts of different coordination levels on the flow-occupancy plots at advance detectors.

In Figure 49, we select three intersection approaches in the NB direction as an example: 1007 NB @ California Ave, 1008 NB @ PageMill Rd/Oregon Expwy, and 1010 NB @ Matadero Ave/ Margarita Ave. We do not select Intersection 1009 @ Hansen Way/ Portage Ave because the connection between our server and that intersection has been dead for a long time. In addition, we want to point out that Intersection 1008 is running free for most of the time because the cross street PageMill Rd/Oregon Expwy is also under coordination. The only time periods that are under coordination at this intersection are: (i) 07:05AM – 09:15AM for coordination plan 5, and (ii) 04:30PM – 06:00PM for coordination plan 6.

For demonstration purposes, we pick the PM period between 5:00PM and 6:00PM on 2022-08-31, and the corresponding traffic measurements are provided in Figure 50. As shown in the figure, traffic at the downstream intersection (i.e., 1007 NB @ California Ave) and the upstream intersection (i.e., 1010 NB @ Matadero Ave/ Margarita Ave) was not congested during the selected time period since the measured occupancies from the corresponding advance detectors were relatively low, e.g., less than 10%. In contrast, traffic at the middle intersection (i.e., 1008 NB @ PageMill Rd/Oregon Expwy) was very congested during the selected time period. The flow rate was not very high, e.g., below 1200 veh/hr, for a three-lane arterial

road. But the corresponding occupancies were all greater than 40%. As indicated by the time stamps, traffic between 5:00PM and 5:15PM was congested with an average occupancy about 45%. In the next time interval between 5:15PM and 5:30PM, it became even more congested as the average occupancy increased to above 70% and the corresponding flow rate dropped from about 1100 veh/hr to about 400 veh/hr. After that, traffic became less congested between 5:30PM and 5:45PM as the average occupancy reduced to 50% and the flow rate increased to about 800 veh/hr. In the final time stamp between 5:45PM and 6PM, traffic was back to the state similar to the first timestamp (e.g., 5:00PM – 5:15PM). The progression of traffic states in the selected time period formed a hysteresis loop and indicates poor coordination between Intersection 1008 and Intersection 1009 in the NB direction because no obvious congestion was observed both in the upstream (Intersection 1010) and the downstream (Intersection 1007) intersections.



Figure 49. Selection of three coordinated intersection approaches in the NB direction.

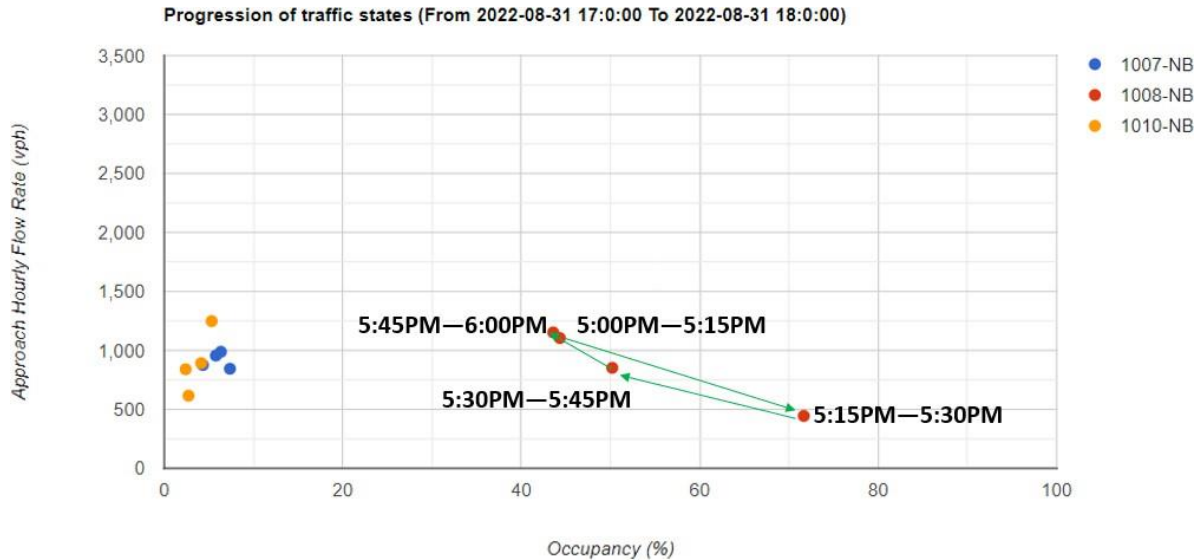


Figure 50. Progression of traffic measurements at the three selected intersection approaches on 2022-08-31 between 5PM and 6PM.

#### 4.3.4.2 Traffic estimation

In the PATH server, the Arterial Estimation Module is triggered every 5 minutes. Once triggered, it retrieves the latest detector data from the testbed, performs estimation, and saves the results into the database. This module produces detailed estimates of traffic states, e.g., uncongested/congested/spillback for the left-turn, through and right-turn movements at each intersection approach. For more details, refer to the SB1 Report “Arterial Traffic Estimation Using Field Detector and Signal Phasing Data”<sup>15</sup>.

But for visualization purposes, we further aggregate these traffic states from the movement level to the approach level. For the displayed results, the color code on a road link is described below:

- When the color is green, it indicates traffic is uncongested with a low traffic density.
- When the color turns yellow, it indicates traffic starts to get saturated with a medium traffic density.
- When the color turns red or even dark red, that means heavy congestion occurs with a high traffic density.
- When the color is gray, it indicates there is no data available for traffic estimation.

As a comparison, in Figure 51 we provide the estimated traffic states at the same coordinated intersection approaches during the same PM peak shown in Figure 49 and Figure 50. As shown in the figure, the estimated traffic states are consistent with the traffic measurements illustrated in Figure 50. For the whole time period from 5PM and 6PM, we do not find traffic congestion at the upstream (Intersection 1010) and the downstream (Intersection 1007) intersections. Therefore, we can identify the NB direction at Intersection 1008 (@PageMill Rd/Oregon Expwy) is the bottleneck location. Traffic congestion occurring at this path is highly related to the poor coordination with the upstream intersection (Intersection 1009) which makes it fail to properly accommodate the upstream platoon arrivals.



(a) Time period: 5:00PM – 5:15PM



(b) Time period: 5:15PM – 5:30PM



(c) Time period: 5:30PM – 5:45PM



(d) Time period: 5:45PM – 6:00PM

Figure 51. Estimated traffic states at the three selected intersection approaches on 2022-08-31 between 5PM and 6PM.

## 4.4 Assessment of arterial traffic performance through A-PeMS

In this subsection, we will discuss how to use the Arterial Performance Measurement System (A-PeMS) to assess the traffic performance in the California CV Testbed. In particular, the analysis will be conducted in the following procedure: (i) use the “Traffic Estimation” function to identify traffic bottlenecks; (ii) use the “Signal Analysis” function to identify potential insufficient signal settings; (iii) use both “Signal Analysis” and “Detector Analysis” functions to identify potential traffic congestion; and (iv) conduct overall assessment and recommend some potential solutions. More details are provided below.

### 4.4.1 Identifying traffic bottlenecks

In the A-PeMS, there is a function called “Traffic Estimation” which allows users to visualize both real-time and historic traffic states on the arterial road links in the testbed. Using this function, users can identify the recurrent traffic bottlenecks in the testbed. For example, Figure 52 provides an example of the estimated traffic states on El Camino Real (ECR) at 5:30PM on 2022-12-06 as well as four identified traffic bottlenecks: @Embarcadero Rd, @Page Mill Rd, @Los Robles Ave/El Camino Way, and @Dinahs Court.



Figure 52. Estimated traffic states at 5:30PM on 2022-12-06 and the identified traffic bottlenecks.

#### 4.4.2 Identifying insufficient signal settings

Once the traffic bottlenecks are identified, users can use the “Signal Analysis” function to further identify any insufficient signal settings that may cause the bottlenecks. Take the intersection Embarcadero Rd @ ECR as an example. As shown in Figure 53, traffic in the SB direction was congested at 5:30PM on 2022-12-06, but traffic in the NB direction was unknown (i.e., in gray color) due to the lack of good detector data. Furthermore, the signal timing plans and the detector layouts at this intersection are also provided in Figure 53 and will be used to support the analysis in the following subsections.

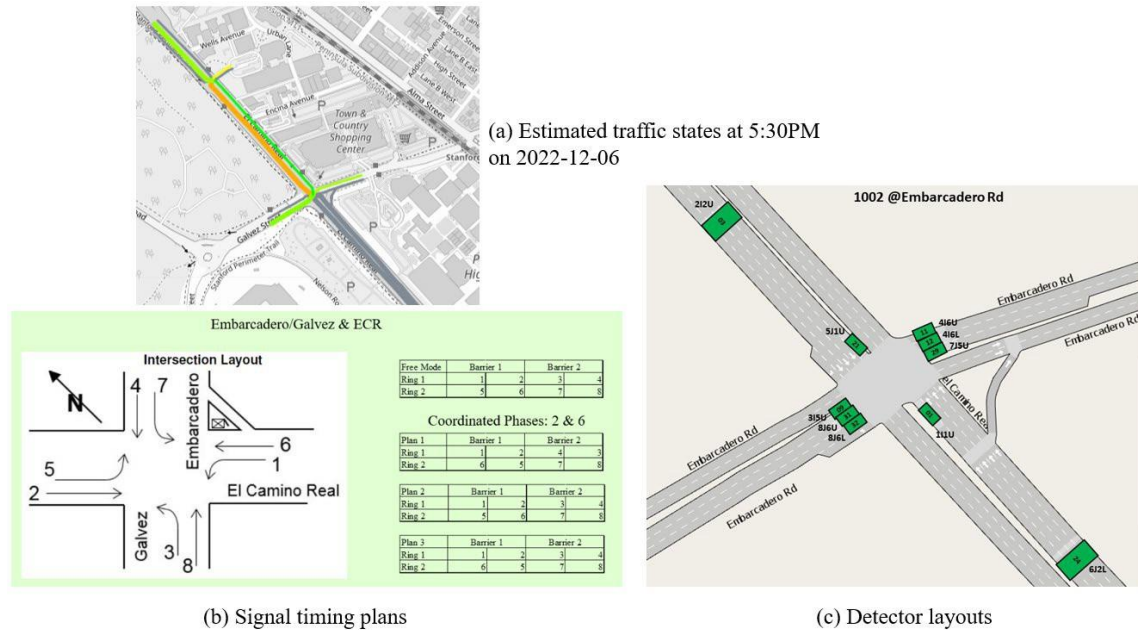


Figure 53. Estimated traffic states, signal timing plans, and detector layouts at Embarcadero Rd @ ECR.

In the “Signal Analysis” function, three performance metrics are provided: (i) phase duration statistics, (ii) phase gap-out/max-out statistics, and (iii) pedestrian phase duration statistics. In particular, the metric of phase gap-out/max-out statistics is a very important indicator to show when a phase is gapped out, maxed out, or forced off, especially for left-turn phases.

For example, Figure 54 provides both table view and plot view of phase gap-out/max-out statistics at Embarcadero Rd @ ECR between 3PM and 4PM on 2022-12-06. In the figure, “FO” stands for “Forced-Off”<sup>16</sup>, “GO” stands for “Gap-Out”<sup>17</sup>, and “MO” stands for “Max-Out”<sup>18</sup>. As shown in the figure, it is easy to identify that Phase 7 (WB left turn as shown in Figure 53) had insufficient green times during that time period since it often maxed out. Furthermore, Figure 55 shows the histogram of phase gap-out/max-out

<sup>16</sup> Forced-Off: A point within a cycle where a phase must end regardless of continued demand. These points in a coordinated cycle ensure that the coordinated phases are provided a minimum amount of green time.

<https://ops.fhwa.dot.gov/publications/fhwahop08024/chapter6.htm>

<sup>17</sup> Gap-Out: A type of actuated operation for a given phase where the phase terminates due to a lack of vehicle calls within a specific period of time (passage time). <https://ops.fhwa.dot.gov/publications/fhwahop08024/chapter5.htm>

<sup>18</sup> Max-Out: A type of actuated operation for a given phase where the phase terminates due to reaching the designated maximum green time for the phase. <https://ops.fhwa.dot.gov/publications/fhwahop08024/chapter5.htm>

statistics at the same time period as in Figure 54. According to the histogram, it is further confirmed that Phase 7 had insufficient green times with a high percentage of max out.

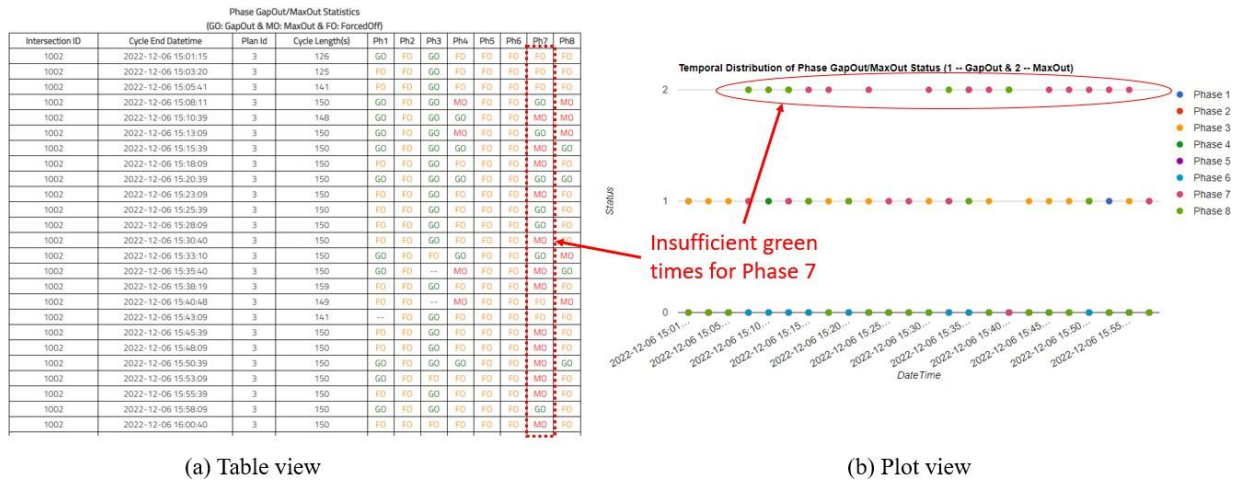


Figure 54. Table & Plot views of phase gap-out/max-out statistics at Embarcadero Rd @ ECR between 3PM and 4PM on 2022-12-06.

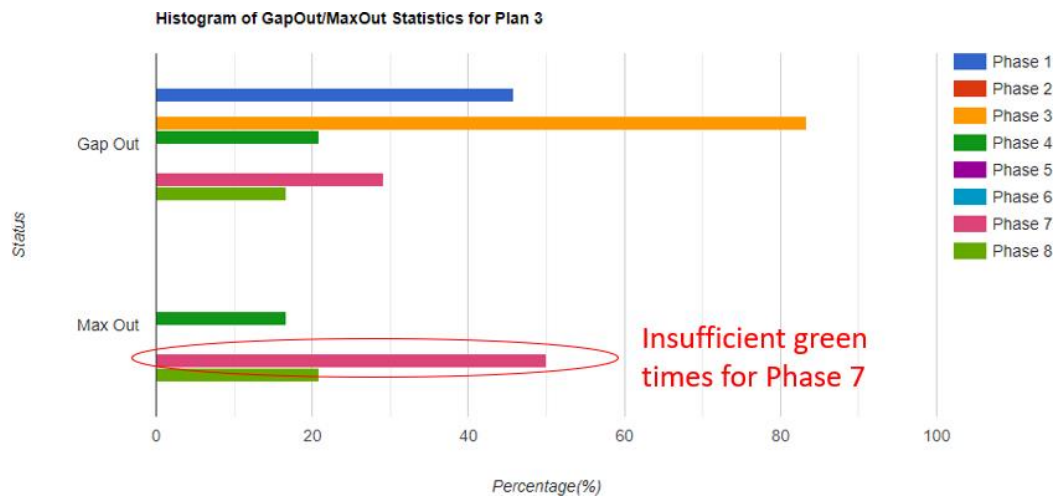


Figure 55. Histogram of phase gap-out/max-out statistics at Embarcadero Rd @ ECR between 3PM and 4PM on 2022-12-06.

In addition, as shown in Figure 54 and Figure 55, Phase 4 and Phase 8 also encountered max-outs, although the frequency is much lower than that of Phase 7. However, as shown in Figure 53, Phase 4 and Phase 8 are the WB and the EB through movements. Different from Phase 7, their max-outs may not be caused by high volumes of through vehicles in these two directions, but instead, by pedestrian calls. Therefore, to further identify the causes of max-outs for Phase 4 and Phase 8, we need to check the corresponding detector and the pedestrian data in the WB and EB directions.

Note that Phase 2, Phase 5, and Phase 6 are often forced off, which is due to the lead-lag left turn settings in Barrier 1 in Plan 3, which is provided in Figure 53. Also, the gap-out rates of Phase 1 and Phase 3 are

high, which indicates the corresponding left-turn demands (i.e., northbound left turn for Phase 1 and eastbound left turn for Phase 3) are low.

### 4.4.3 Identification of traffic congestion

Since there is no advance detector in the WB and EB approaches of Embarcadero Rd @ ECR, it is not intuitive to identify traffic congestion based on the data from the stopbar detectors. Instead, we can combine the detector measurements provided in the “Detector Analysis” function with the phase gap-out/max-out and pedestrian call data provided in the “Signal Analysis” function to get a good sense of traffic congestion at these two approaches. For example, Figure 56 shows the detector measurements, phase gap-out/max-out statistics, pedestrian calls at the intersection Embarcadero Rd @ ECR between 3PM and 4PM on 2022-12-06. According to the figure, we find that:

- Traffic at the EB approach was probably congested during that time period. That is because Phase 8 often maxed out but the pedestrian demand was relatively low. The high occupancies observed from Detector 1002-32 in the EB were probably contributed mostly by the high traffic demand.
- The through and right-turn movements at the WB approach were probably impacted by the high pedestrian demand. Compared to Phase 8, Phase 4 had less max-outs during the same time period. However, the high pedestrian demand may lead to traffic congestion since the right-turn vehicles may have to stop and wait for the pedestrians to cross the streets and thus block the through traffic.

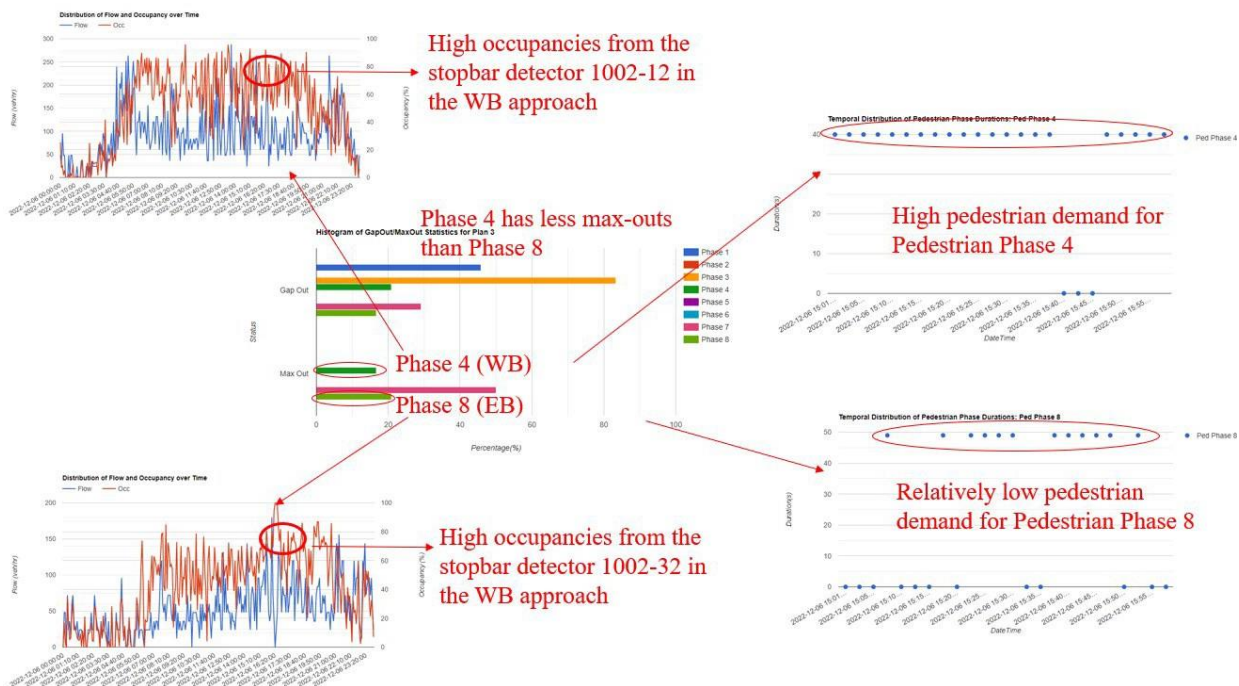


Figure 56. Detector measurements, phase gap-out/max-out statistics, pedestrian calls at the intersection Embarcadero Rd @ ECR between 3PM and 4PM on 2022-12-06.

When advance detector data is available, it is easier to identify traffic congestion at intersection approaches. For example, Figure 57 shows the flow and occupancy measurements at Detector 1002-03 in the SB direction of Embarcadero Rd @ ECR on 2022-12-06. From the figure, it is very straightforward to see traffic at the SB direction was congested during 3PM and 4PM on 2022-12-06 because the corresponding occupancies were very high for advance detectors, greater than 40%.

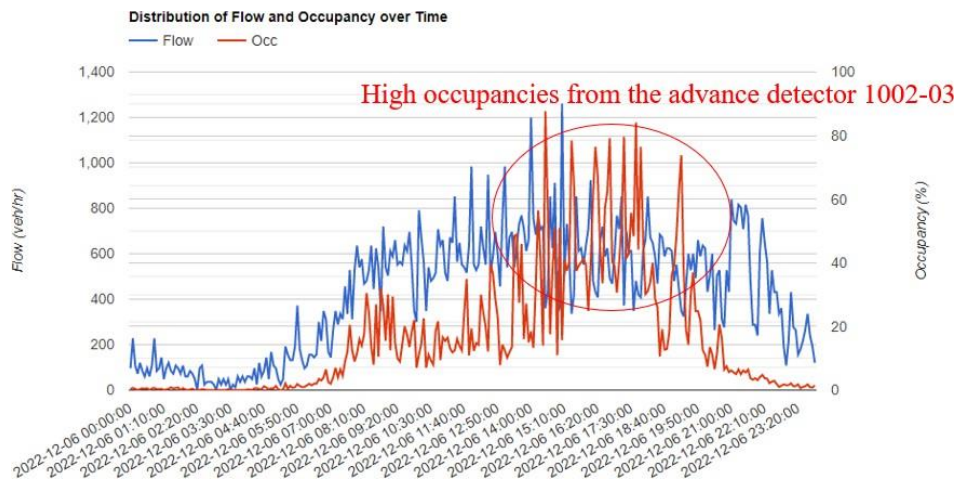


Figure 57. Flow and occupancy measurements at Detector 1002-03 in the SB direction of Embarcadero Rd @ ECR on 2022-12-06.

#### 4.4.4 Overall assessment and potential solutions

According to the above analysis, we have identified that: (i) between 3PM and 4PM on 2022-12-06 traffic in the SB approach was congested; (ii) traffic in the EB approach was probably congested due to a high frequency of max outs but relatively low pedestrian demand; (iii) the through and right-turn traffic in the WB direction was probably impacted by the high pedestrian demand, which may lead to congestion. Even though no data was available for the NB approach, traffic is normally congested according to the historical traffic profiles provided by Google Maps.

Since traffic is congested at the four approaches at Embarcadero Rd @ ECR, there is not much we can do in terms of changing the phase green times in a timing plan. We might be able to slightly allocate more green times for Phase 7, but this may increase the congestion level for the traffic assigned to Phase 8. A better approach would be improving the coordination along the major arterial, ECR, with more adaptive offsets, which will be described in greater detail in Section 5.

This page left blank  
intentionally

## 5. Development of an Active Control Strategy for Dynamic Offsets

In this section, we will introduce an active control strategy that aims to improve coordination and recommends new offsets based on the newly collected detector data at targeted intersections. In the following subsections, we will discuss: (i) the algorithm to change offsets in Aimsun; (ii) the active control strategy; and (iii) simulation settings and evaluation results.

### 5.1 Algorithm to change offsets in Aimsun

According to Chapter 6 (Coordination) in the “Traffic Signal Timing Manual”<sup>19</sup>, when a signal controller needs to change its offset, there are five most common transition modes in the United States, which are Dwell, Max Dwell, Add, Subtract, and Shortway.

- **Dwell.** During the transition, this mode will hold the coordinated phase “Green” until the new local zero point is achieved.
- **Max Dwell.** This mode is a modified version of Dwell, only allowing a limited amount of extra green time to be added to each cycle. Therefore, two or more cycles are required to achieve coordination.
- **Add.** This mode shifts the start of the cycle progressively later, by timing longer cycles during the transition period, which may cause unexpected storage problems like lane blockages and queue spillbacks.
- **Subtract.** Different from Add, this mode shifts the start of the cycle progressively earlier, by subtracting time from one or more phases in the sequence subject to their minimum green time requirements.
- **Shortway.** This mode, sometimes called “Smooth”, chooses either the Add or the Subtract transition logic as the “shortest path” to achieve synchronization. In general, this mode is the default mode in most signal controllers.

In this study, we chose the Shortway transition mode. In Aimsun, there is no API function that can directly change the offset once the simulation is activated. Therefore, we developed an algorithm that leverages existing API functions available in Aimsun to implement the Shortway logic. In the proposed algorithm, the transition period will finish in one cycle. Also, the proposed algorithm is only activated in the case when the timing plan is the same but with a new offset. That is to say, we are not going to change the planned Time-Of-Day coordination, i.e., switching from one timing plan to another, which will be handled by Aimsun internally.

When a new offset is recommended, the actions in the proposed algorithm are described below:

- Determine which transition mode is the shortest path, Add or Subtract, to achieve synchronization according to the difference between the current and the new offsets.
- Calculate a new cycle length and new phase green times for the transition period, according to the transition mode selected, e.g., Add or Subtract, as well as the offset difference (between the current and the new ones). If it is the Add mode, the cycle length will be longer, and the added green time will be proportionally allocated to the phases. If it is the Subtract mode, the cycle length will be

---

<sup>19</sup> <https://ops.fhwa.dot.gov/publications/fhwahop08024/chapter6.htm>

shorter, and the reduced green time will be proportionally subtracted from the phases, subject to their minimum green time constraints.

- At the beginning of a new cycle, stop the automated control by Aimsun and switch to manual control by external commands.
- Activate the phases with new green times in sequence.
- Once done, stop the manual control by external commands and activate the automated control by Aimsun.

## 5.2 Algorithm of the active control strategy for dynamic offsets

In this subsection, we introduce an active control strategy that recommends new offsets based on the newly collected detector data to better accommodate the vehicle platoons at targeted intersections. More detailed description is provided below.

### 5.2.1 Traffic state representation in the flow-occupancy plot

As shown in Figure 58, the flow-occupancy plot from an arterial loop detector (especially the advance detector) normally follows a trapezoidal shape, the capacity of which is capped by the  $g/c$  ratio (i.e., green time / cycle length) of the detected traffic movements (e.g., through movements). Generally, according to different platoon arrival patterns, the flow-occupancy plot can be divided into three different regions with two occupancy thresholds,  $Occ_1$  and  $Occ_2$ :

- Free-flow/uncongested region with  $Occupancy \leq Occ_1$ . In this region, vehicle platoons can cross the intersection without stopping, and thus, the detected occupancy is low.
- Congested region with  $Occ_1 < Occupancy \leq Occ_2$ . In this region, a certain portion of vehicle platoons may have to stop at the stopbar due to the red light and wait for the next green time. In this case, the detected occupancy is relatively high.
- Congested with downstream queue spillback with  $Occupancy > Occ_2$ . In this region, besides potential waiting time at the intersection, the throughput of the vehicle platoons is further restricted by the downstream queue spillback. In this case, the detected occupancy is high but the throughput (i.e., flow-rate) is reduced.

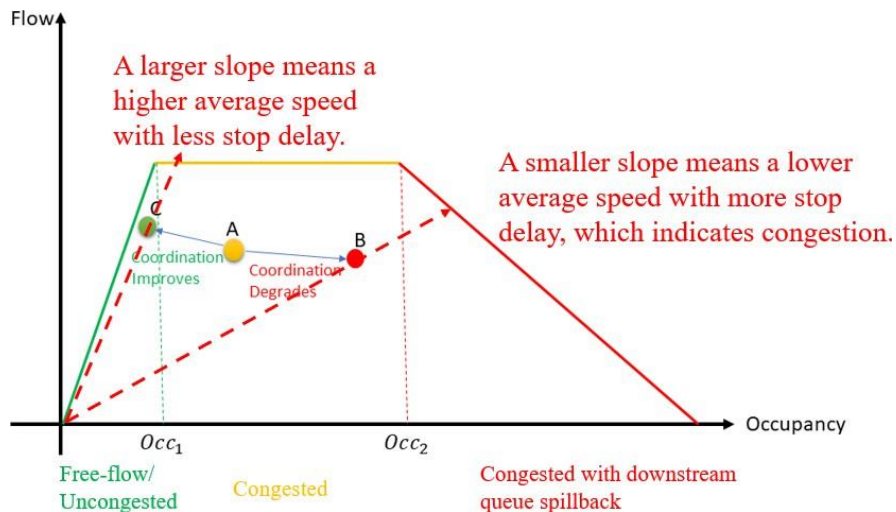


Figure 58. Traffic state representation in the flow-occupancy plot.

Based on the detected traffic states in the flow-occupancy plot, we can tell how traffic condition evolves as time elapses. For example, consider the current traffic state at time step  $tt$  is point A in *Figure 58*. If the detected traffic state in the next time step  $tt + 1$  is at point B, which is shifted to the right with a higher occupancy and potentially a lower flow rate, it indicates coordination degrades and congestion builds up with a lower average speed and more stop delay at the corresponding intersection approach. However, if the detected traffic state in the next time step  $tt + 1$  is at point C, which is shifted to the left with a lower occupancy and potentially a higher flow rate, it indicates coordination improves and congestion dissipates with a higher average speed and less stop delay at the corresponding intersection approach.

In the field, stopbar detectors normally consist of multiple (e.g., three or more) loops and have wider detection regions. As a result, they tend to undercount the volumes (i.e., flows) when vehicles are narrowly spaced while passing the detectors. Therefore, in this study, we use the data from the corresponding advance detectors to represent the traffic states at an intersection approach. When multiple advance detectors exist, the averages among them will be used to represent the overall traffic states. Furthermore, for simplicity, we combine the two congested regions (i.e.,  $000000_1 < 000000 \leq 000000_2$  and  $000000 > 000000_2$ ) as one (i.e.,  $000000 > 000000_1$ ) for our control strategy development in the following subsections. That means, for an intersection approach, there will be only two states: Uncongested and Congested (despite whether the queue spillback exists or not).

### 5.2.2 State transition diagram in the active control strategy

Given the consideration that there are only two states at an intersection approach, i.e., Uncongested and Congested, there will be only four paths in the state transition diagram shown in *Figure 59*, which are listed below:

- Path A: from Uncongested State to Uncongested State.
- Path B: from Uncongested State to Congested State.
- Path C: from Congested State to Congested State.
- Path D: from Congested State to Uncongested State.

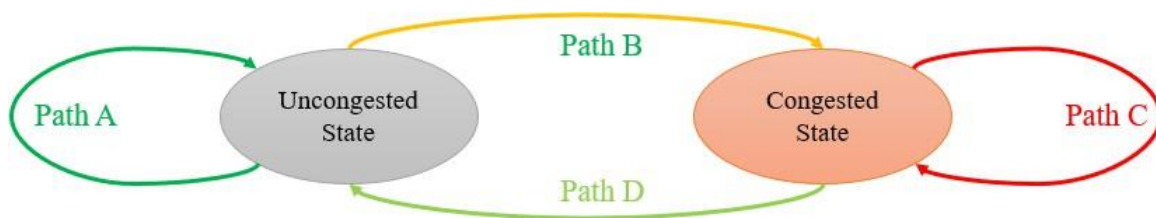


Figure 59. State transition diagram at an intersection approach.

Based on the above state transition diagram, the proposed active control strategy applies different actions in different transition paths, which are described below:

- In Path A: Since traffic is still in the Uncongested State, the active control strategy will take no action and keep the current offset.
- In Path B: This path indicates the first time an intersection becomes congested. The active control strategy will perceive there may be a significant portion of vehicles queuing at the coordinated

intersection approaches. Therefore, it will consider reducing the offset so as to let the coordinated phases start the green time earlier.

- In Path C: This path indicates the traffic state at an intersection is still stuck at the congested states, despite the actions taken in the past action intervals. By comparing the current traffic state and the one observed in the past action interval, the active control strategy applies two different actions. If the congestion is mitigated, which means the previous action provides positive benefits, the active control strategy will continue with the previous action. For example, if the previous action is to reduce the offset, the active control strategy will further reduce the offset. However, if the congestion is increased which means the previous action introduces negative impacts, the active control strategy will revert to the previous action. For example, the active control strategy will increase the offset if the past action was to reduce the offset.
- In Path D: This indicates the intersection is back to the Uncongested State. In this case, the active control strategy will take no action and keep the current offset.

In the following subsections, more details will be provided regarding how to determine the offset changes in Path B and Path C.

### 5.2.3 Determination of offset changes in Path B

Considering the example shown in Figure 60, traffic in the NB and the SB directions is coordinated. Both directions have coverage of advance detectors, e.g., Detector A for the SB and Detector B for the NB. At time  $tt$ , the flow and occupancy measurements are denoted as  $\{ff_{HH}(tt), FF0000_{HH}(tt)\}$  for Detector A, and  $\{ff_{BB}(tt), FF0000_{BB}(tt)\}$  for Detector B

While comparing the traffic states at the current step  $tt_2$  with those at the previous step  $tt_1$ , the traffic at an intersection is considered in Path B when at least one of the following conditions are met:

- Detector A becomes congested, i.e.,  $FF0000_{HH}(tt_1) \leq FF0000_{HH}^1$  but  $FF0000_{HH}(tt_2) > FF0000_{HH}^1$ ;
- Detector B becomes congested, i.e.,  $FF0000_{BB}(tt_1) \leq FF0000_{BB}^1$  but  $FF0000_{BB}(tt_2) > FF0000_{BB}^1$ .

Here,  $FF0000_{HH}^1$  and  $FF0000_{BB}^1$  are the thresholds that divide the flow-occupancy plots into Uncongested and Congested regions at Detector A and Detector B respectively, as shown in Figure 58.

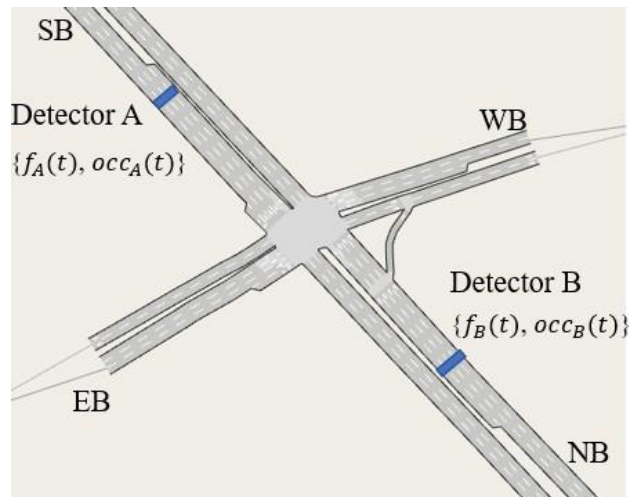


Figure 60. Example of offset determination in Path B.

For practical considerations, two thresholds are applied to regulate the actions of the active control strategy:

- A maximum offset change,  $OOSS_{mmmmm} > 0$ , to avoid too aggressive actions to change the offsets;
- A minimum offset change,  $OOSS_{miiil} > 0$ , to avoid too frequent actions to change the offsets.

Then the recommended offset difference  $\Delta OOSS$  is calculated as follows:

$$\Delta FFOOOO = \frac{FFOOO_H - FFOOO_H(t)}{FFOOO_H} * \frac{ff_{HH}(tt)}{ff_{HH}(tt) + ff_{BB}(tt)} + \frac{FFOOO_B - FFOOO_B(t)}{FFOOO_B} * \frac{ff_{BB}(tt)}{ff_{HH}(tt) + ff_{BB}(tt)} \quad (5)$$

$$\Delta OOSS = \begin{cases} OOSS_{mmmmm} * \text{minimum}(\Delta FFOOOO, 1) & \Delta FFOOOO \geq 0 \\ -OOSS_{miiil} * \text{minimum}(\Delta FFOOOO, 1) & \Delta FFOOOO < 0 \end{cases} \quad (6)$$

In the above equations, the occupancy difference  $\Delta FFOOOO$  is the sum of relative occupancy differences at both coordinated approaches, i.e.,  $\frac{ZZIII^{AA} - ZZIII^{AA}(II)}{ZZIII_1^{AA}}$  and  $\frac{ZZIII^{BB} - ZZIII^{BB}(II)}{ZZIII_1^{BB}}$ , and is further weighted by their observed flow rates, i.e.,  $\frac{ff_{AA}(II)}{ff_{AA}(II) + ff_{BB}(II)}$  and  $\frac{ff_{BB}(II)}{ff_{AA}(II) + ff_{BB}(II)}$ . The recommended offset difference  $\Delta OOSS$  is a linear function of  $\Delta FFOOOO$

but is capped by the threshold of maximum offset change  $OOSS_{mmmmm}$ . Also, this offset difference is capped by the threshold of minimum offset change  $OOSS_{miiil}$ . Therefore, the actual operational regions for the offset difference  $\Delta OOSS$  are  $[-OOSS_{miiil}, -OOSS_{miiil}]$  and  $[OOSS_{miiil}, OOSS_{mmmmm}]$ .

## 5.2.4 Determination of offset changes in Path C

As shown in Figure 61, the flow and occupancy measurements at the previous time step  $tt_1$  and the current time step  $tt_2$  are denoted as  $\{ff_{HH}(tt_1), FFOOOO_{HH}(tt_1)\}$  and  $\{ff_{HH}(tt_2), FFOOOO_{HH}(tt_2)\}$  for Detector A, and  $\{ff_{BB}(tt_1), FFOOOO_{BB}(tt_1)\}$  and  $\{ff_{BB}(tt_2), FFOOOO_{BB}(tt_2)\}$  for Detector B, respectively. Also, the offset difference applied in the previous time step  $tt_1$  is denoted as  $\Delta OOSS(tt_1)$ , and the offset difference to be recommended at the current time step  $tt_2$  is denoted as  $\Delta OOSS(tt_2)$ .

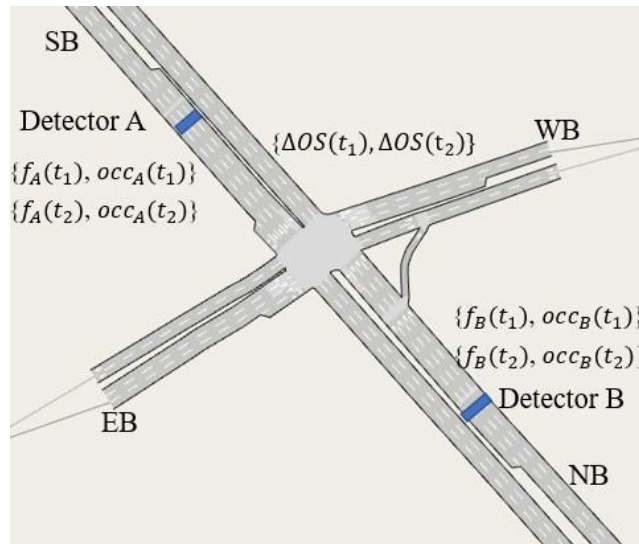


Figure 61. Example of offset determination in Path C.

While comparing the traffic states at the current step  $tt_2$  with those at the previous step  $tt_1$ , the traffic at an intersection is considered in Path C when at least one of the following conditions are met:

- Detector A remains congested, i.e.,  $FFOOO_{HH}(tt_1) > FFOOO_{HH}^{\#}$  but  $FFOOO_{HH}(tt_2) > FFOOO_{HH}^{\#}$ ,

- Detector B remains congested, i.e.,  $FFOOOO_{BB}(tt_1) > FFOOOO_{BB}^1$  but  $FFOOOO_{BB}(tt_2) > FFOOOO_{BB}^1$ .

Also, for practical considerations, thresholds of maximum offset change  $OOSS_{mmmmmm}$  and minimum offset change  $OOSS_{mill}$  are applied to avoid either too aggressive or too frequent actions to change the offsets.

Then the recommended offset  $\Delta OOSS(tt_2)$  is calculated as follows:

$$\Delta sFFFF\Delta\Delta\Delta\Delta(tt_2) = \frac{\frac{ff_{HH}(tt_1)}{FOOOO_H(tt_1)} - \frac{ff_{HH}(tt_2)}{FOOOO_H(tt_2)}}{\frac{ff_{HH}(tt_1)}{FOOOO_H(tt_1)}} * \frac{ff_{HH}(tt_2)}{ff_{HH}(tt_2) + ff_{BB}(tt_2)} + \frac{\frac{ff_{BB}(tt_1)}{FOOOO_{BB}(tt_1)} - \frac{ff_{BB}(tt_2)}{FOOOO_{BB}(tt_2)}}{\frac{ff_{BB}(tt_1)}{FOOOO_{BB}(tt_1)}}} * \frac{ff_{BB}(tt_2)}{ff_{HH}(tt_2) + ff_{BB}(tt_2)} \quad (7)$$

$$\Delta OOSS(tt_2) = \begin{cases} -OOS_{mmmmmm} * \text{miimm}(\Delta sFFFF\Delta\Delta\Delta\Delta(tt_2), 1) & \Delta sFFFF\Delta\Delta\Delta\Delta(tt_2) \geq 0 \text{ and } \Delta OOSS(tt_1) > 0 \\ OOS_{mmmmmm} * \text{miimm}(\Delta sFFFF\Delta\Delta\Delta\Delta(tt_2), 1) & \Delta sFFFF\Delta\Delta\Delta\Delta(tt_2) \geq 0 \text{ and } \Delta OOSS(tt_1) \leq 0 \\ OOS_{mmmmmm} * \text{miimm}(\text{caass}(\Delta sFFFF\Delta\Delta\Delta\Delta(tt_2), 1)) & \Delta sFFFF\Delta\Delta\Delta\Delta(tt_2) < 0 \text{ and } \Delta OOSS(tt_1) > 0 \\ -OOS_{mmmmmm} * \text{miimm}(\text{caass}(\Delta sFFFF\Delta\Delta\Delta\Delta(tt_2), 1)) & \Delta sFFFF\Delta\Delta\Delta\Delta(tt_2) < 0 \text{ and } \Delta OOSS(tt_1) \leq 0 \end{cases} \quad (8)$$

In the above equations, the slope difference  $\Delta sFFFF\Delta\Delta\Delta\Delta(tt_2)$  is the sum of relative slope differences at both coordinated directions, i.e.,  $\left( \frac{\frac{ff_{AA}(I1_1)}{ZZIII_{AA}(I1_1)} - \frac{ff_{AA}(I1_2)}{ZZIII_{AA}(I1_2)}}{\frac{ff_{AA}(I1_1)}{ZZIII_{AA}(I1_1)}}} \right) / \frac{ff_{AA}(I1_1)}{ff_{AA}(I1_2) + ff_{BB}(I1_2)}$  and  $\left( \frac{\frac{ff_{BB}(I1_1)}{ZZIII_{BB}(I1_1)} - \frac{ff_{BB}(I1_2)}{ZZIII_{BB}(I1_2)}}{\frac{ff_{BB}(I1_1)}{ZZIII_{BB}(I1_1)}}} \right) / \frac{ff_{BB}(I1_1)}{ff_{AA}(I1_2) + ff_{BB}(I1_2)}$  but is further weighted by their flow rates, i.e.,  $\frac{ff_{AA}(I1_2)}{ff_{AA}(I1_2) + ff_{BB}(I1_2)}$  and  $\frac{ff_{BB}(I1_2)}{ff_{AA}(I1_2) + ff_{BB}(I1_2)}$ .

The slope  $\frac{ff^{(II)}}{ZZIII^{(II)}}$  is highly related to the average speed at the corresponding intersection approach since occupancy can be converted into density using a so-called g factor<sup>20</sup>. Therefore, the calculation of the recommended offset difference is divided into four different cases:

- When  $\Delta sFFFF\Delta\Delta\Delta\Delta(tt_2) \geq 0$ , that means congestion builds up with lower average speeds at the coordinated approaches. That further indicates the previous action is bad and needs to be reverted. Therefore, depending on the value of the previous offset difference  $\Delta OOSS(tt_1)$ , the recommended offset difference takes the following values:
  - If the previous action is to extend the offset with  $\Delta OOSS(tt_1) > 0$ , the action at the current time step is to shorten the offset with  $\Delta OOSS(tt_2) = -OOS_{mmmmmm} * \text{miimm}(\Delta sFFFF\Delta\Delta\Delta\Delta(tt_2), 1)$ .
  - If the previous action is to shorten the offset with  $\Delta OOSS(tt_1) \leq 0$ , the action at the current time step is to extend the offset with  $\Delta OOSS(tt_2) = OOS_{mmmmmm} * \text{miimm}(\Delta sFFFF\Delta\Delta\Delta\Delta(tt_2), 1)$ .
- When  $\Delta sFFFF\Delta\Delta\Delta\Delta(tt_2) < 0$ , that means congestion is mitigated with higher average speeds at the coordinated approaches. That further indicates the previous action is good and should be kept. Therefore, depending on the value of the previous offset difference  $\Delta OOSS(tt_1)$ , the recommended offset difference takes the following values:
  - If the previous action is to extend the offset with  $\Delta OOSS(tt_1) > 0$ , the action at the current time step is to further extend the offset with  $\Delta OOSS(tt_2) = OOS_{mmmmmm} * \text{miimm}(\text{caass}(\Delta sFFFF\Delta\Delta\Delta\Delta(tt_2), 1))$ .
  - If the previous action is to shorten the offset with  $\Delta OOSS(tt_1) \leq 0$ , the action at the current time step is to further shorten the offset with  $\Delta OOSS(tt_2) = -OOS_{mmmmmm} * \text{miimm}(\text{caass}(\Delta sFFFF\Delta\Delta\Delta\Delta(tt_2), 1))$ .

<sup>20</sup> Jia, Z., Chen, C., Coifman, B., & Varaiya, P. (2001, August). The PeMS algorithms for accurate, real-time estimates of g-factors and speeds from single-loop detectors. In ITSC 2001. 2001 IEEE Intelligent Transportation Systems. Proceedings (Cat. No. 01TH8585) (pp. 536-541). IEEE.

## 5.3 Calibration of a microsimulation model for the California CV Testbed

Before conducting field tests with the proposed algorithm, it is necessary to evaluate its performance in microsimulations. In this subsection, we will discuss the microsimulation network in Aimsun for the California CV Testbed and how we calibrate it to ensure the simulated traffic is consistent with the one in the field.

### 5.3.1 The California CV Testbed model in Aimsun

As shown in Figure 62, a microsimulation model was created in Aimsun for the California CV Testbed. For the 16 operational intersections between Medical Foundation Dr to Dinahs Ct, all Time-Of-Day (TOD) timing plans have been coded into the model. All detectors (both advance and stopbar) have been created and placed at the same locations consistent with those in the field. Centroids, through which simulated vehicles will be assigned into the network, have been created and attached to all the intersection approaches. These attributes like timing plans, detectors, and centroids in Aimsun are illustrated in Figure 63.

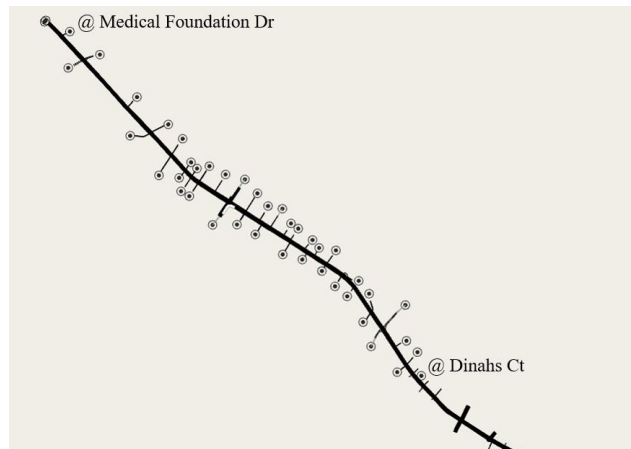


Figure 62. The California CV Testbed model in Aimsun.

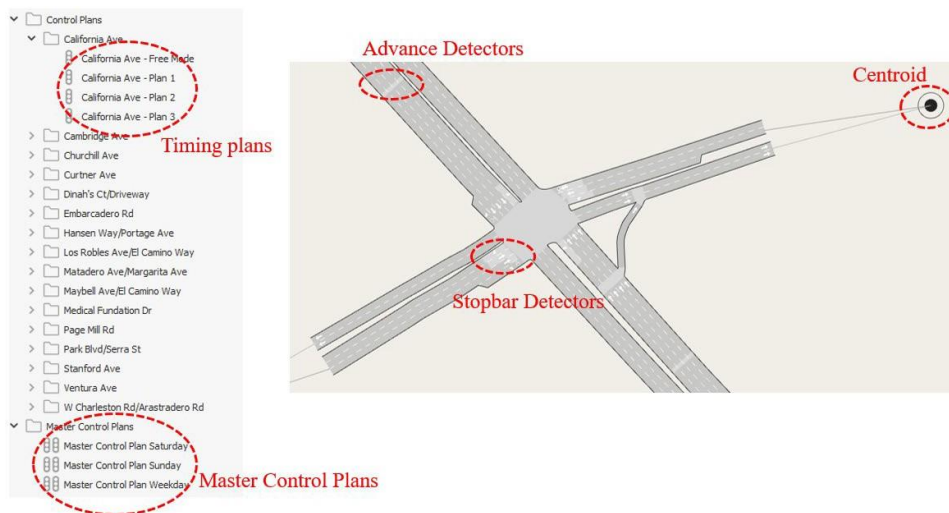


Figure 63. Illustration of attributes (timing plans, detectors, and centroids) in the Aimsun model.

### 5.3.2 Calibration method and criteria

To evaluate the performance of any new control strategies, model calibration is required as the first step to make sure the simulated traffic under the “before” condition (i.e., before making any changes to the traffic system) is consistent with that observed from the field.

In this study, traffic counts from field detectors are used as references to calibrate the model. Parameters like Origin-Destination (OD) demand will be adjusted so as to obtain the best match possible between the simulated traffic counts and the observed ones. To quantify the match between the simulated and the observed traffic counts, the following GEH statistic<sup>21</sup> is used.

$$GEH = \sqrt{\frac{2(GG - W)^2}{GG + W}} \quad (9)$$

where:

$GG$ : model estimated volume;

$W$ : field count.

According to the FHWA (Federal Highway Administration) microsimulation guideline<sup>22</sup>, the following calibration criteria are adopted in this study:

- 85% of individual link flows satisfy the condition: GEH Statistic < 5;
- All bottlenecks and their locations are correctly identified.

To calibrate the Aimsun model for the California CV Testbed, we proceeded with the following steps:

- We obtained the weekday traffic profiles for all available advance and stopbar detectors.
- We constructed the approach-based weekday traffic profiles for the intersection approaches along El Camino Real if individual lane-based advance detector data was available. For example, if there are three advance detectors installed at an approach, approach-based measurements (like a “virtual” approach detector) can be constructed by combining the measurements from these three detectors. In this case, the approach flow takes the sum of flows, and the approach occupancy is the mean of occupancies from these detectors. The reason to use approach-based measurements instead of those from individual advance detectors as the references for calibration is because it is difficult to calibrate vehicle’s lane preference in microsimulation, especially when the routing option is very simple in the network like the California CV testbed network with only one major arterial. It is possible to have bad GEH statistics for individual advance detectors, but a good GEH for the “virtual” approach detector.
- We adjusted the OD demand tables to ensure 85% of detectors with good data have a GEH value < 5. Especially, this criterion was strictly applied to the detectors along El Camino Real.
- However, considering that flows are normally undercounted at stopbar detectors in the field, we allowed higher simulated flow counts at the stopbar detectors.
- We stopped the calibration once the calibration criteria were met.

---

<sup>21</sup> [https://en.wikipedia.org/wiki/GEH\\_statistic](https://en.wikipedia.org/wiki/GEH_statistic)

<sup>22</sup> [https://ops.fhwa.dot.gov/trafficanalysisistools/tat\\_vol3/sect5.htm](https://ops.fhwa.dot.gov/trafficanalysisistools/tat_vol3/sect5.htm)

### 5.3.3 Calibration results

In the Aimsun model for the California CV testbed, hourly OD demands in the PM peak (from 3PM to 7PM) have been calibrated so that the simulated flows from the detectors (including the “virtual” approach detectors) match those observed from the field.

Figure 64 illustrates an example of GEH statistics on the simulated traffic flows at an intersection. The “Green” color stands for good GEH values smaller or equal to 5, the “Orange” color stands for acceptable GEH values between 5 and 10, and the “Red” color stands for bad GEH values that are unacceptable (>10) and need further analysis to identify potential causes<sup>23</sup>. As mentioned, it is difficult to model vehicle’s lane selection preference in microsimulation when there is only one major arterial in the network. Therefore, as shown in the figure, while the GEH values from some advance detectors are bad, the GEH value for the “virtual” approach detector is good.

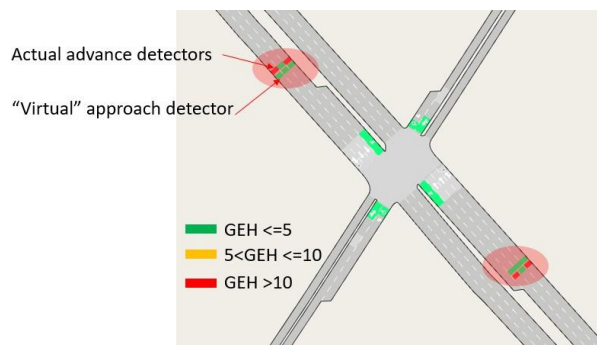


Figure 64. Example of GEH statistics on the simulated traffic flows at an intersection.

Figure 65 further shows the GEH statistics between 3PM and 7PM in the calibrated Aimsun model for the testbed. In the testbed network, 98 detectors (including the “virtual” approach detectors) are used as references to calibrate the Aimsun model. As shown in the figure, the Aimsun model is well calibrated as most of the detectors are “Green”. More specifically, among those 98 detectors, 88 (> 85%) of them report GEH values less than 5, 7 report GEH values between 5 and 10, and only 3 report GEH values greater than 10. We have further verified that the bad GEH values are caused by the inaccurate field measurements from the three advance detectors since they are significantly different from the measurements reported by nearby advance detectors along El Camino Real.

In Figure 66, a linear regression of  $yy = aaaa + aa$  is conducted between the observed flows (x) and the simulated flows (y), where  $aa$  and  $aa$  are the coefficients. Regression results demonstrate a good fit between the simulated flows and the observed ones since the slope  $aa$  of the regression line is close to 1 with an R-Square of 0.9541. In the Regression graphic, the blue line is the regression line, the black lines are the confidence intervals at 95%, and the red line represents the fixed line  $y = x$  (i.e., the perfect match). Note that the intercept  $aa$  of the regression line is greater than zero. That is mainly because we intentionally allowed higher simulated flows at the stopbar detectors in the model calibration, considering the fact that flows at the stopbar detectors are normally undercounted due to their long detection lengths.

<sup>23</sup> Friedrich, M., Pestel, E., Schiller, C., & Simon, R. (2019). Scalable GEH: A quality measure for comparing observed and modeled single values in a travel demand model validation. *Transportation Research Record*, 2673(4), 722-732.

Figure 67 provides a comparison between the bottlenecks observed from the field and those identified from simulations. As shown in the figure, the Aimsun model can replicate the bottlenecks observed in the field, which further demonstrates that the Aimsun model for the California CV testbed is well calibrated.

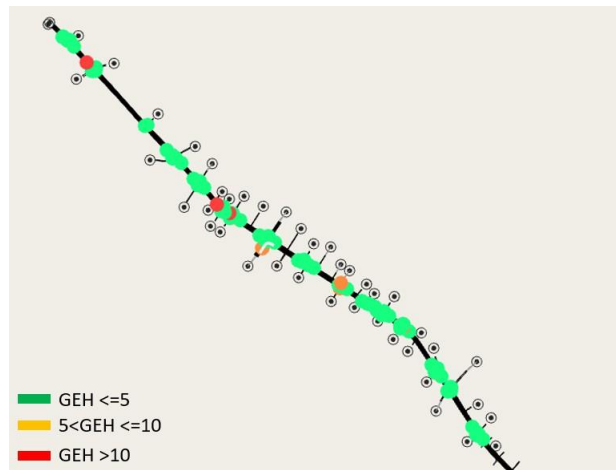


Figure 65. GEH statistics between 3PM and 7PM in the calibrated Aimsun model for the testbed.

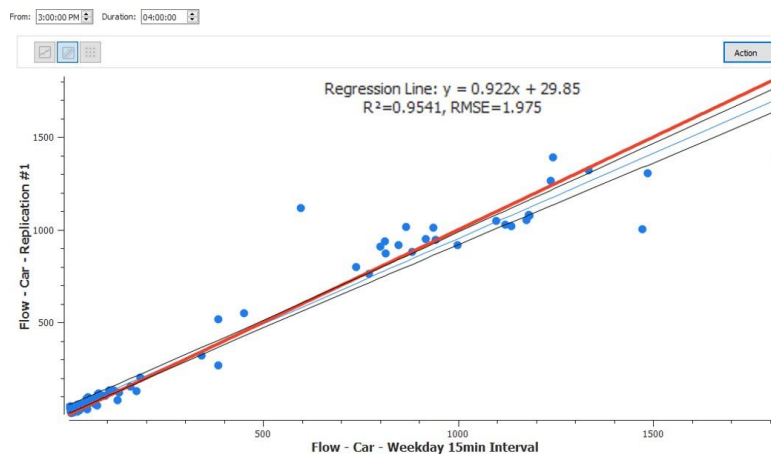


Figure 66. Regression results between the observed and the simulated flows in the PM peak (3PM—7PM).



Figure 67. Bottlenecks observed from the field vs. those identified from simulation.

## 5.4 A case study and evaluation results

In this subsection, we will conduct a case study with selected bottleneck intersections and demonstrate the performance of the proposed active control strategy.

### 5.4.1 A case study

To demonstrate the performance of the proposed active control strategy, the following four intersections are selected based on the observations from a baseline simulation between 4PM and 7PM:

- @Embarcadero Rd
- @Curtner Ave
- @W Charleston Rd/Arastradero Rd
- @Dinahs Ct

The road topologies as well as the congested approach directions in the PM period between 4PM and 7PM are provided in Figure 68. Note that the SB approach between Curtner Ave and Los Robles Ave/El Camino Way is congested during the PM period, and we identified the intersection @Curtner Ave instead of the one @Los Robles Ave/El Camino Way to be a better location to address the coordination. Furthermore, we include the intersection @W Charleston Rd/Arastradero Rd in the analysis since we observe traffic in the NB approach is congested in simulation. The rest two intersections, @Embarcadero Rd and @Dinahs Ct, are the two identified bottlenecks as shown in Figure 67. The intersection @Page Mill Rd is not selected since the coordination interval during the selected PM period is very short. Most of the time this intersection is running free as it is difficult to maintain coordination on both ECR and Page Mill Rd.

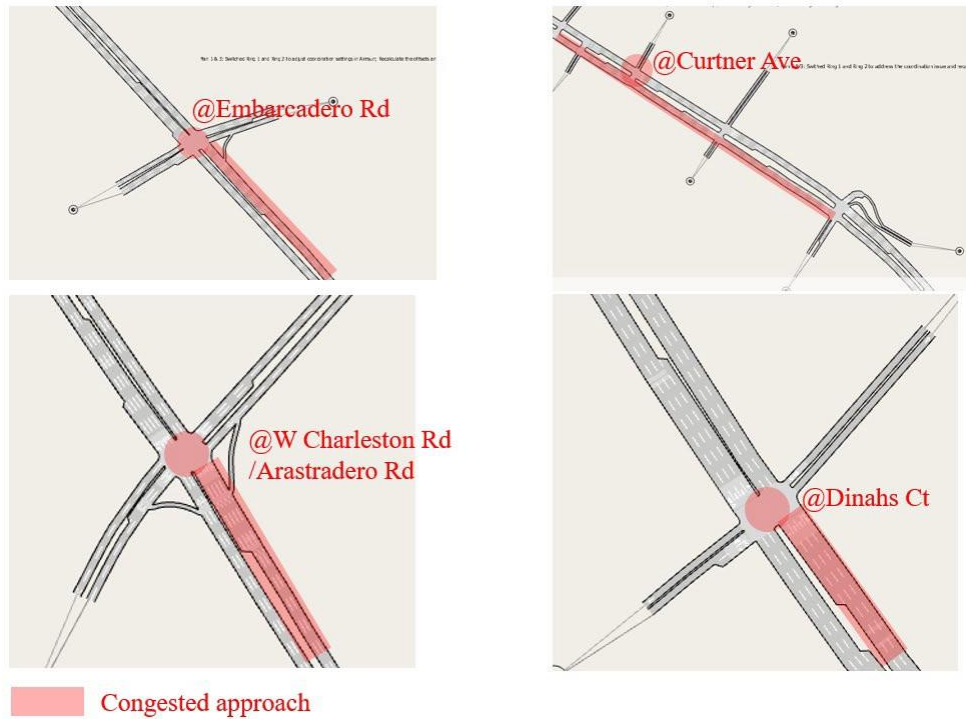


Figure 68. Four intersections selected in the case study.

The following parameter settings are used in the simulation:

- Occupancy thresholds  $FF0000^{HH} = FF0000^{BB} = 12\%$
- Maximum offset change  $OOSS_{mmmmmm} = 10ss/100ss$
- Minimum offset change  $OOSS_{mmill} = 2ss/100ss$
- Action interval = 10mins
- Detector measurement interval = 10mins
- Simulation time period: 4PM – 7PM

The values of occupancy thresholds are determined according to the observations of the aggregated detector data from the field. Since the offset change in the active control strategy is a continuous process, there is no need to set a large value for the maximum offset change. Given the restriction by the minimum offset change, the action interval is set to be a small value, e.g., 10mins, to make the control strategy more adaptive to the changing traffic conditions. A detection interval of 10mins is selected to ensure the changing traffic conditions are captured while the detection noise is suppressed in the detector measurements.

## 5.4.2 Evaluation results

We have conducted 10 simulation replications with the above settings to consider the variations in traffic dynamics. The network-level delays with/without control as well as the delay reductions are provided in Table 4. Despite there is one replication with an increase (-1.08%) in vehicle delay, vehicle delay in all other 9 replications is reduced, with differently magnitudes. In particular, there are 5 replications with delay reductions close to or greater than 2%. This improvement is significant because we only make offset changes at 4 intersections and the delay reduction is calculated at the network level considering the traffic at all 16 intersections.

Table 4. Network-level delay reduction under the active control strategy between 4PM and 7PM.

Simulation Replication	Vehicle Delay (sec/mi) With No Control	Vehicle Delay (sec/mi) With Control	Delay Reduction (%)
#1	161.39	160.98	0.25
#2	162.60	160.31	1.41
#3	162.29	159.08	1.98
#4	164.98	161.26	2.25
#5	165.96	161.69	2.57
#6	162.66	164.41	-1.08
#7	164.55	164.54	0.01
#8	165.64	161.59	2.45
#9	167.95	163.88	2.42
#10	163.26	161.84	0.87

In Figure 69, we further provide the before-and-after comparison of detector measurements at the intersection @Curtner Ave in Replication #5. As shown in the figure, with the adaptive control strategy applied at the intersection @Curtner Ave, measurements at the three advance detectors are shifted to the left with lower occupancies, which indicates traffic coordination in the SB direction is improved.

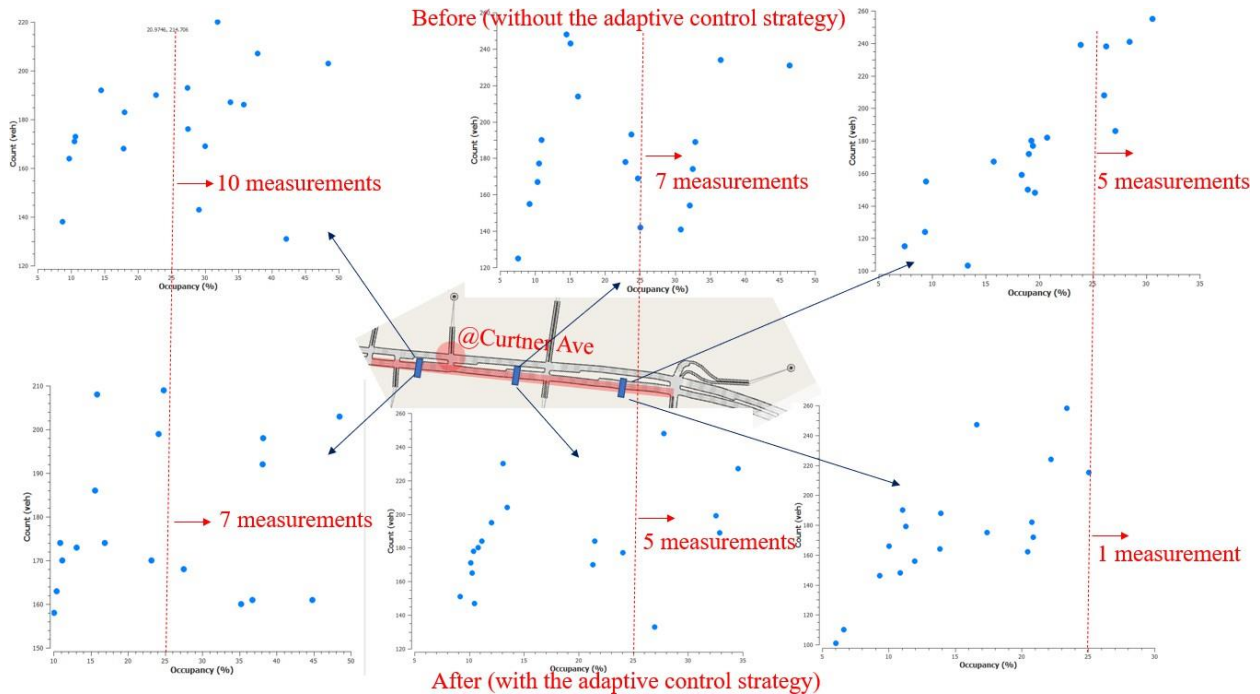


Figure 69. Before-and-after comparison of detector measurements at the intersection @Curtner Ave in Replication #5.

Table 5. Offset changes at the four intersections in Replication #5.

Time	Offset (sec) @Embarcadero Rd	Offset (sec) @Curtner Ave	Offset (sec) @W Charleston Rd /Arastradero Rd	Offset (sec) @Dinahs Ct
4:00PM	141	74	129	95
4:10PM	141	<b>64 (-10)</b>	129	<b>89 (-6)</b>
4:20PM	<b>138 (-3)</b>	<b>58 (-6)</b>	129	89
4:30PM	138	58	<b>122 (-7)</b>	<b>81 (-8)</b>
4:40PM	138	58	<b>118 (-4)</b>	81
4:50PM	138	58	118	81
5:00PM	138	<b>60 (+2)</b>	118	<b>75 (-6)</b>
5:10PM	138	<b>62 (+2)</b>	<b>121 (+3)</b>	75
5:20PM	138	<b>65 (+3)</b>	<b>124 (+3)</b>	75
5:30PM	138	65	124	<b>67 (-8)</b>
5:40PM	138	<b>56 (-9)</b>	124	67
5:50PM	138	<b>46 (-10)</b>	124	<b>70 (+3)</b>
6:00PM	138	46	124	<b>73 (+3)</b>
6:10PM	138	<b>48 (+2)</b>	<b>126 (+2)</b>	<b>76 (+3)</b>
6:20PM	138	48	<b>124 (-2)</b>	76
6:30PM	138	48	124	76
6:40PM	138	48	124	76
6:50PM	138	48	124	76

In Table 5, we provide detailed offset changes at the four intersections at each action interval in Replication #5. From the table, we find that:

- The offset change is not applied at every action interval, which is adapted to the changes in traffic conditions. Traffic in the time period between 5PM and 6PM tends to vary a lot since a majority of offset changes occur in this period.
- Different intersections have different frequencies in offset changes. For example, the intersection @Curtner Ave has a lot of offset changes while the intersection @Embarcadero Rd has only one offset change during the whole simulation period between 4PM and 7PM.

Overall, Table 5 demonstrates that the proposed active control strategy can function well at different intersections and under different traffic conditions.

This page left blank  
intentionally

## 6. Conclusions

In this report, we have made additional enhancements to the MMITSS to support the new infrastructure upgrades (i.e., the installation of NoTraffic sensors and HAWK signals) in the California CV Testbed. To ensure the TSP application can function properly after the installation of HAWK signals, we have improved the functions in the MAP Engine Library to allow the identification of multiple downstream intersections and the calculation of the corresponding distances and travel times. To incorporate the more accurate detection data from the NoTraffic sensors into the V2X messages, we have added new functions in the MAP Engine Library that are able to determinate the lane-of-travel for vulnerable road users (VRUs) and track road user movements inside an intersection conflict area. We also have developed different schemes to construct appropriate MAP and SPaT messages for the HAWK signals with different road geometry settings. Furthermore, we have developed an application programming interface (API) specification for exchanging V2X messages between an OBU and a local device (e.g., an application processor) so that the vehicle-resident CV applications running on the local device can be device-independent and work seamlessly with OBUs from different vendors. These implemented API functions have been tested using the devices (e.g., RSUs and OBUs) in the PATH laboratory.

To monitor the traffic performance in the California CV Testbed, we have developed an Arterial Performance Measurement System (A-PeMS) that is able to collect, aggregate, and analyze the raw detector and signal phase data from the field. In the A-PeMS, there are functions available to check the real-time data availability from the detectors and the traffic controllers in the field. To better analyze the data, algorithms have been developed to aggregate the raw detector data into fixed time intervals and the raw signal phase data into cycles. A set of health criteria has been proposed to check the quality of the detector data, and algorithms have been developed to filter out the bad data measurements. Metrics like phase duration statistics, phase gap-out/max-out statistics, and pedestrian phase duration statistics have been developed to measure the intersection signal performance. Leveraging both the detector and the signal phase data, functions have been developed to estimate the traffic states and visualize the coordination performance in the testbed. In addition, procedures on how to use A-PeMS to assess the arterial traffic performance, especially identification of traffic bottlenecks and the corresponding causes, are provided.

To support the testing of new control strategies and CV/CAV applications, we have created and calibrated a microsimulation model in Aimsun for the California CV Testbed. To calibrate the model, we followed the FHWA microsimulation calibration guideline and used the GEH statistics to measure how good the simulated detector measurements match those observed from the field. Results showed that the Aimsun model for the California CV Testbed was well calibrated for the weekday PM period from 3PM to 7PM.

To improve traffic coordination along major arterials, e.g., the ECR in the California CV Testbed, we developed a novel active control strategy that recommends new offsets according to the changing traffic conditions measured from the advance detectors located at the coordinated intersection approaches. In the proposed active control strategy, traffic at an intersection only has two states: uncongested and congested. The active control strategy applies different actions to different state transition processes, for example, from uncongested to congested and vice versa. For performance evaluations, a case study was provided in which the active control strategies were applied to four bottleneck intersections in the testbed Aimsun model. Simulation results demonstrated that the proposed active control strategy is effective and can achieve about 2% reduction in vehicle delay for the whole network of 16 intersections by applying only a few changes to the offsets at the four bottleneck intersections.

In the future, we are interested in continuing our research in the following directions:

- Improvements to the Arterial Performance Measurement System (A-PeMS). New performance metrics will be developed by using the more accurate detection data from the AI-powered video and radar sensors, e.g., the NoTraffic sensor. New functions will be added to the A-PeMS to visualize these new performance metrics.
- Improvements to the active control strategy. We will refine the strategy by incorporating traffic conditions from the cross streets into the decision process to generate more appropriate offset changes. We will leverage the I-210 Corridor network<sup>24</sup> in Aimsun and conduct a more in-depth analysis to assess its performance under various traffic conditions and its sensitivity to the parameters like action interval, detector measurement interval, and thresholds of maximum/minimum offset changes.
- Field tests in the California CV Testbed. If allowed, we are interested in testing the active control strategy in the California CV Testbed to evaluate its performance with data support from the field. In this case, the A-PeMS will be a very good tool to assess the before-and-after impacts.

---

<sup>24</sup> <https://connected-corridors.berkeley.edu/i-210-pilot-landing-page>.